Guidebook 26

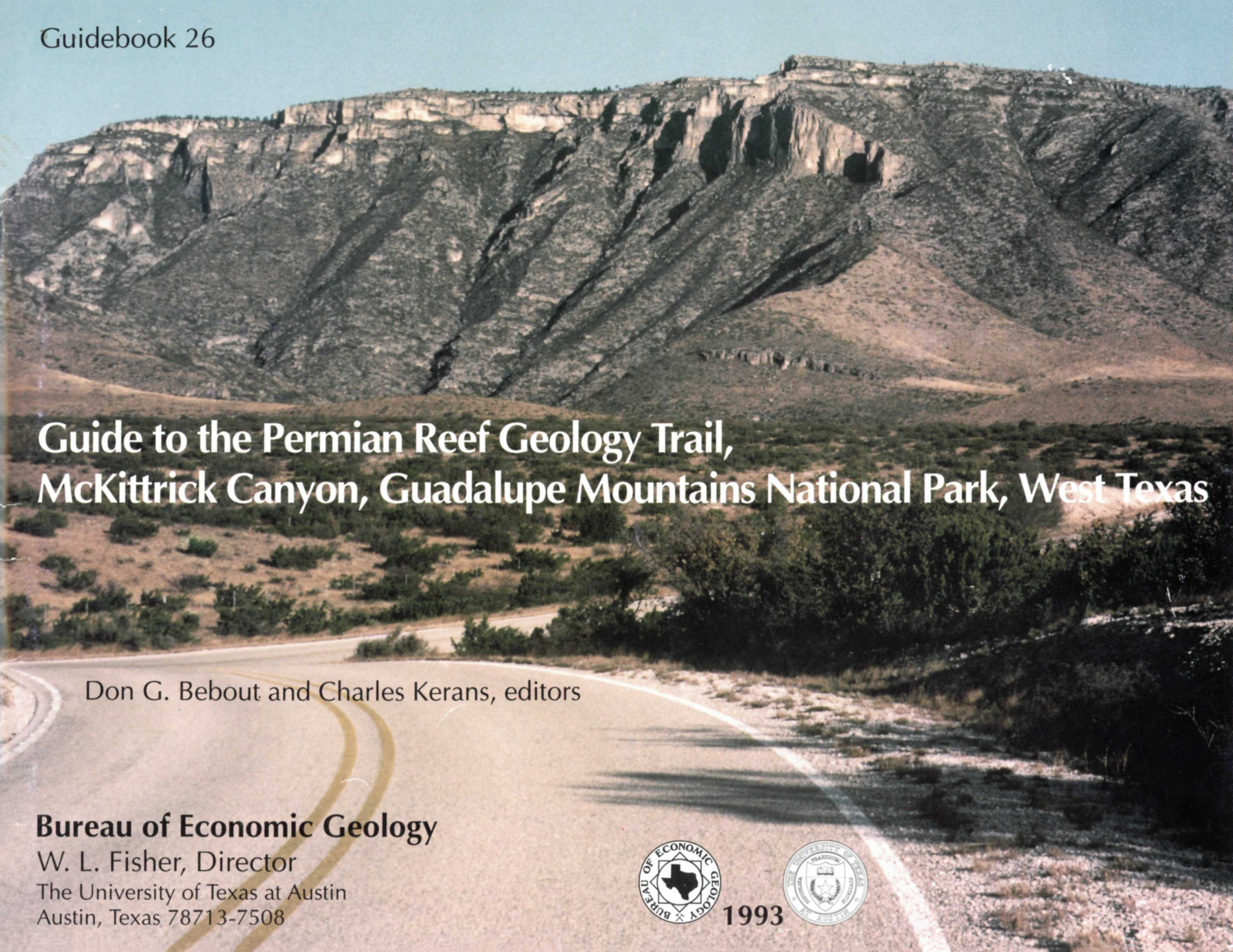

Guide to the Permian Reef Geology Trail, McKittrick Canyon, Guadalupe Mountains National Park, West Texas

Don G. Bebout and Charles Kerans, editors

Bureau of Economic Geology
W. L. Fisher, Director
The University of Texas at Austin
Austin, Texas 78713-7508

1993

Guidebook 26

Guide to the Permian Reef Geology Trail, McKittrick Canyon, Guadalupe Mountains National Park, West Texas

Don G. Bebout and Charles Kerans, editors

Contributing Authors

Toe of Slope and Geology Loop Trail

Alton Brown and Robert G. Loucks
ARCO Oil and Gas Company Research and Technical Services, Plano, Texas

Slope

Denise Mruk
Marathon Oil Company, Midland, Texas
Don G. Bebout
Bureau of Economic Geology, The University of Texas at Austin, Austin, Texas

Reef

Brenda L. Kirkland
Department of Geological Sciences, The University of Texas at Austin, Austin, Texas
Susan A. Longacre and Emily L. Stoudt
Texaco, Inc., Houston Research Center, Houston, Texas

Outer Shelf and Shelf Crest

Charles Kerans
Bureau of Economic Geology, The University of Texas at Austin, Austin, Texas
Paul M. Harris
Chevron Petroleum Technology Company, La Habra, California

Bureau of Economic Geology
W. L. Fisher, Director
The University of Texas at Austin
Austin, Texas 78713-7508

1993

Credits

Financial support for the trail guide was provided by ARCO Resources Technology, Chevron Petroleum Technology Company, Exxon Company, U.S.A., Mobil Research & Development Corporation, Texaco E&P Technology Division, Union Pacific Resources, David E. Eby, and Carlsbad Caverns–Guadalupe Mountains Association.

Contents

Figures

Introduction: Don G. Bebout, Charles Kerans, and Paul M. Harris

The Permian Reef Geology Trail in the mouth of McKittrick Canyon, Guadalupe Mountains National Park (fig. 1), traverses 610 vertical meters (2,000 ft, or 1,520 to 2,130 m [5,000 to 7,000 ft] topographic elevation) of Permian (upper Guadalupian) facies through one of the world's finest exposed examples of a rimmed carbonate platform margin. The present-day topography approximates that formed by the Capitan reef along the edge of the Delaware Basin. Encouraged by geologists from geological societies, universities, the petroleum industry, and the U.S. Geological Survey, the U.S. National Park Service constructed the Permian Reef Geology Trail (fig. 2) in the early 1980's to provide better access to the depositional facies and diagenetic features of this shelf margin.

This trail guide provides detailed documentation of the carbonate facies encountered along the Permian Reef Geology Trail. Carbonate facies descriptions are most useful when they are integrated into the local and regional stratigraphic framework and into a shelf-to-basin depositional model, as was done herein. Assignment of specific depositional environments to many of the facies represented along the trail remains controversial; where this is true, an effort has been made to introduce alternative interpretations.

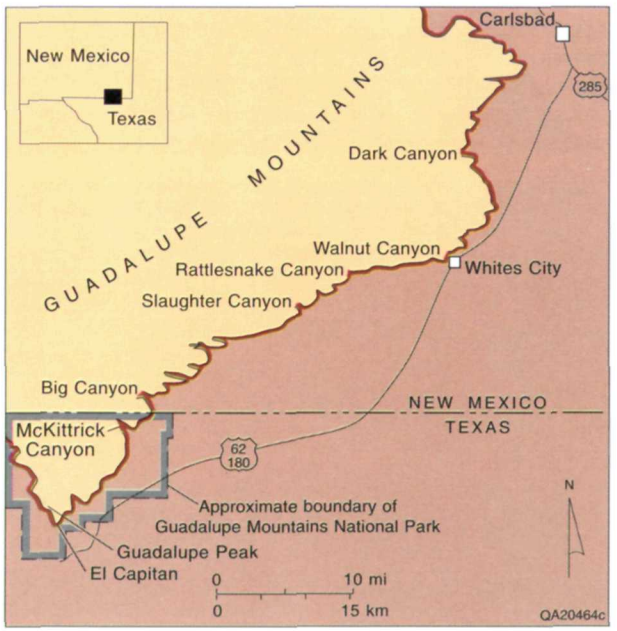

FIGURE 1. Map of the Capitan reef front, Guadalupe Mountains, and location of McKittrick Canyon, other major canyons along the escarpment, Guadalupe Peak, and El Capitan. Modified from King (1948).

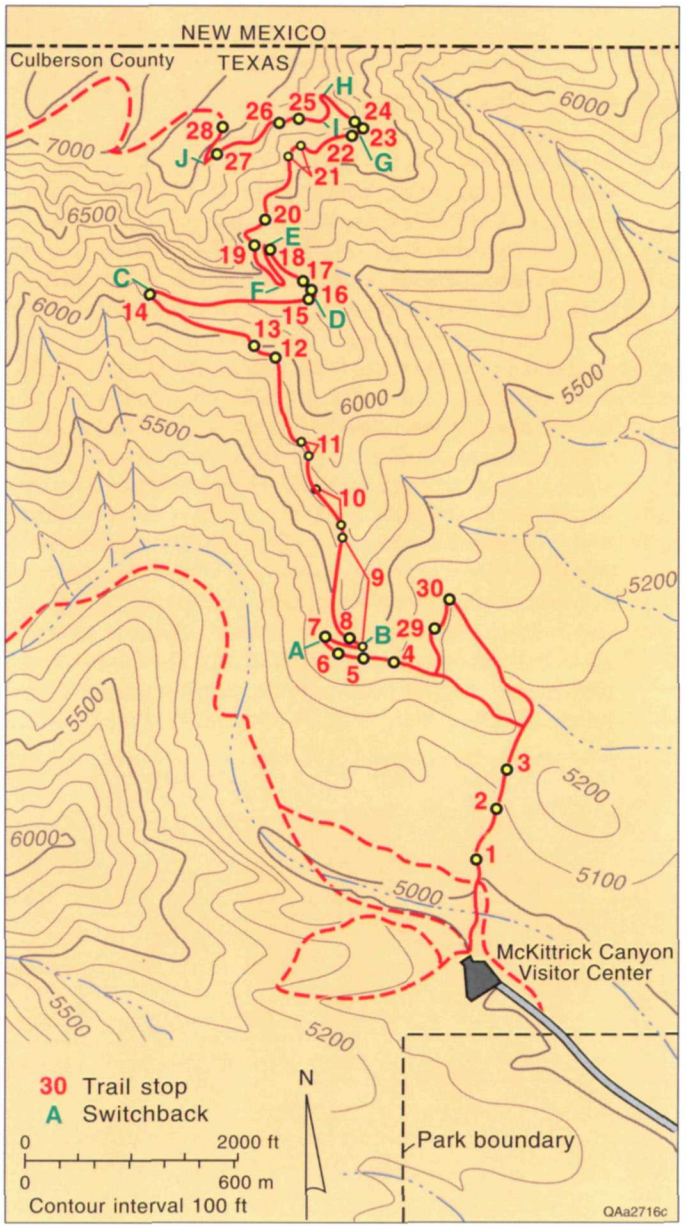

FIGURE 2. Topographic map of the mouth of McKittrick Canyon showing the location of the Permian Reef Geology Trail and trail stops.

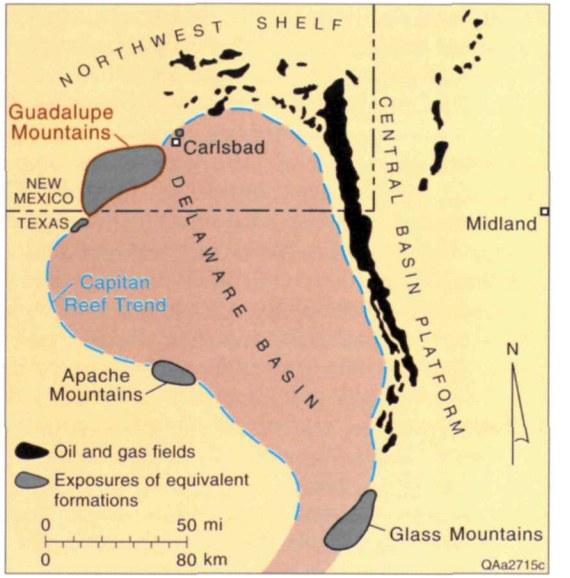

FIGURE 3. Map of the Permian Basin showing the location of the upper Guadalupian reef trend, oil and gas fields producing from equivalent strata in the subsurface, and mountains with exposures of upper Guadalupian formations. Modified from Ward and others (1986).

Geologic Setting

The Capitan reef and its associated upper Guadalupian carbonate platform define the margin of the Delaware Basin of West Texas and New Mexico (fig. 3). Equivalent units occur in the subsurface on the northern (Northwest Shelf) and eastern (western margin of the Central Basin Platform) sides of the basin, where sandstone shelf facies of the

Capitan interval are reservoirs for oil and gas accumulations (fig. 3) (Ward and others, 1986). More than 1.6 Bbbl of oil has been produced from upper Guadalupian (Tansill, Yates, Seven Rivers, and Queen Formations) oil and gas reservoirs in West Texas and New Mexico (Holtz, 1991).

Most of the reef that rims the Delaware Basin is buried; however, Basin and Range-related tilted fault blocks in the Guadalupe, Apache, and Glass Mountains provide Capitan reef outcrops along parts of the western and southern sides of the basin. The Guadalupe Mountains exposures are the most accessible. The west flank of the southern Guadalupe Mountains is a fault scarp that exposes the reef and its basin equivalents in cross section view more than 300 m (>1,000 ft) in the vertical dimension and several miles in the dip dimension. The east side represents an erosionally modified depositional profile of the shelf-to-basin system that was exhumed during late Cenozoic uplift of the Mountains. Canyons, such as McKittrick Canyon, that cut into the platform give access to cross-sectional views. South of McKittrick Canyon, topset beds are largely eroded; north of McKittrick Canyon, most canyons do not incise deeply enough to expose bottomset beds. However, McKittrick Canyon exposes nearly the complete platform section.

The Capitan reef is the youngest of a series of shelf-margin complexes developed around the Delaware Basin. The Capitan reef separates shallow-water deposits to the northwest from deep-water deposits to the southeast. The relatively narrow (16- to 24-km [10- to 15-mi] wide) carbonate facies tract is downdip of a much broader, restricted, evaporite and siliciclastic facies tract. The landward part of the carbonate tract is a broad (4.7- to 12.9-km-wide [6- to 8-mi]) belt of dolomudstones, dolowackestones, and skeletal and coated-grain grainstones deposited in very shallow water, restricted lagoons. The seaward part of the carbonate tract exposed along the trail consists of facies deposited in the following depositional environments: shelf crest and outer shelf, reef, slope, and toe of slope (fig. 7). Deep-water deposits southeast of the carbonate tract are siliciclastic coarse-grained siltstone to fine-grained sandstone with intercalated, basinward-thinning limestone members of the Bell Canyon Formation, Delaware Mountain Group (fig. 4). Water depth in the basin near the shelf margin is estimated to have been approximately 550 m (~1,800 ft) during the latest part of Capitan deposition (Newell and others, 1953).

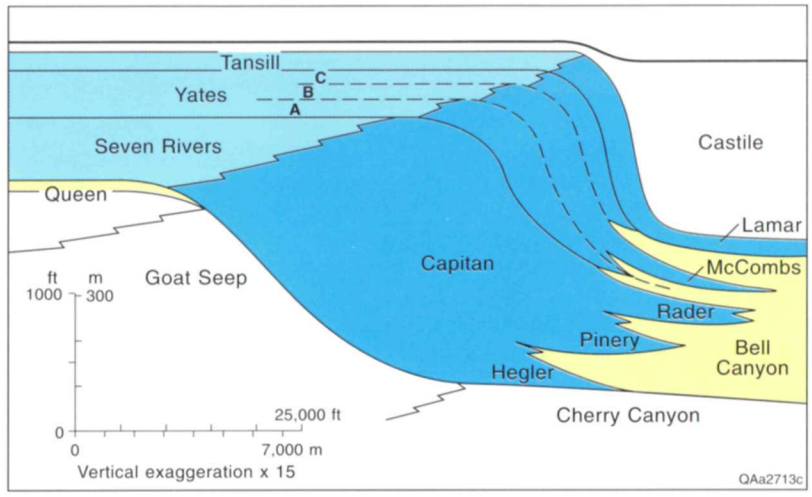

FIGURE 4. Cross section showing shelf-to-basin correlations of the Capitan Formation and equivalents. Blue areas are dominantly carbonates and evaporites, and yellow areas are mostly sandstone. Modified from Garber and others (1989).

In the Guadalupe Mountain area, the Capitan shelf-margin carbonates prograded 4.8 to 8 km (3 to 5 mi) to the southeast to form a thick sheetlike deposit parallel to the basin margin (Garber and others, 1989). After demise of the reef, the basin was filled with evaporites (and the shelf complex was buried) by latest Permian time. Evaporites were dissolved and the reef was exhumed during Pleistocene uplift (Bachman, 1976).

Many formation names have been applied to the rock units along a depositional profile across the Capitan shelf

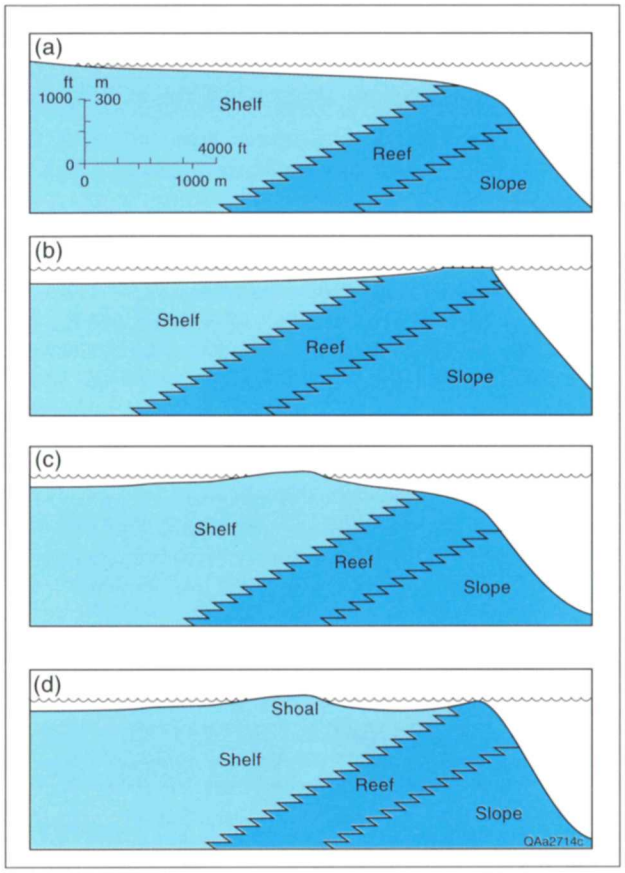

FIGURE 5. Hypothetical paleobathymetric profiles across the Capitan shelf margin. (a) Uninterrupted slope from shelf to basin (King, 1948). (b) Profile showing shoaling at shelf-margin barrier reef (Newell and others, 1953). (c) Profile showing shoaling at pisolite shelf crest landward of the reef (marginal-mound profile of Dunham, 1972). (d) Profile showing shoaling at Tansill-equivalent shelf-margin barrier reef and pisolite shelf crest (Kirkland-George, 1992).

margin. King (1948) used "Capitan Formation" to refer to all massive carbonates separating Artesia Group shelf deposits from sandstones of the Bell Canyon Formation (fig. 4). Hayes (1964) divided the Capitan Formation into the Massive and Breccia members; Newell (1953) used the terms "reef" and "reef talus" for the same divisions. In this trail guide the terms "reef" and "slope" are used to informally subdivide the Capitan carbonates and minor siliciclastics. Shelfward equivalents of the Capitan Formation include the sandstones, carbonates, and evaporites of the Tansill (youngest), Yates, and Seven Rivers Formations (fig. 4). The shelf deposits are mixtures of carbonates, siliciclastics, and evaporites; the Yates Formation contains proportionately more siliciclastics, whereas the Tansill and Seven Rivers Formations are dominantly carbonate. Basinward equivalents are the siliciclastics of the Bell Canyon Formation, and along the edge of the basin, the Lamar (youngest), McCombs, Rader, Pinery, and Hegler carbonate members (fig. 4). The shelf carbonate units interfinger with the siliciclastic-dominated Bell Canyon of the basin center and provide key markers for linking shelf and basin strata.

Several paleobathymetric profiles for the Capitan shelf margin have been proposed over the years. The uninterrupted slope model (fig. 5a) shows gradual deepening of water from the shelf into the basin. All other models suggest shallowing at the shelf margin to form a barrier reef (fig. 5b), or shallowing at a position landward of the reef where pisolite shoals define the shelf crest (fig. 5c), or both (fig. 5d). Examination of exposures along the north wall of McKittrick Canyon (fig. 6), in conjunction with work of Hurley (1977, 1989), demonstrates that the profile varied during deposition of the Capitan Formation. Hurley's (1977, 1989) examination of the lower portion of the Seven Rivers Formation documented 24 to 30.5 m (80 to 100 ft) of paleorelief between peritidal shelf-crest facies and the Capitan reef (fig. 5c) and called the intervening basinward-sloping shelf region the "outer-shelf fall-in beds" (Hurley, 1989, credits the term "fall-in" to L. C. Pray). This basinward slope, estimated at up to 8° (Hurley, 1989) of the outer shelf in the lower Seven Rivers Formation, can be clearly seen in figure 6. The

FIGURE 6. Photomosaic of the north wall of McKittrick Canyon showing the Tansill (T), Yates (Y), and Seven Rivers (SR) Formations (green lines); interpreted depositional profiles (black lines); transition between the outer shelf and reef (yellow line); and Permian Reef Geology Trail (red). Photo by F. J. Lucia.

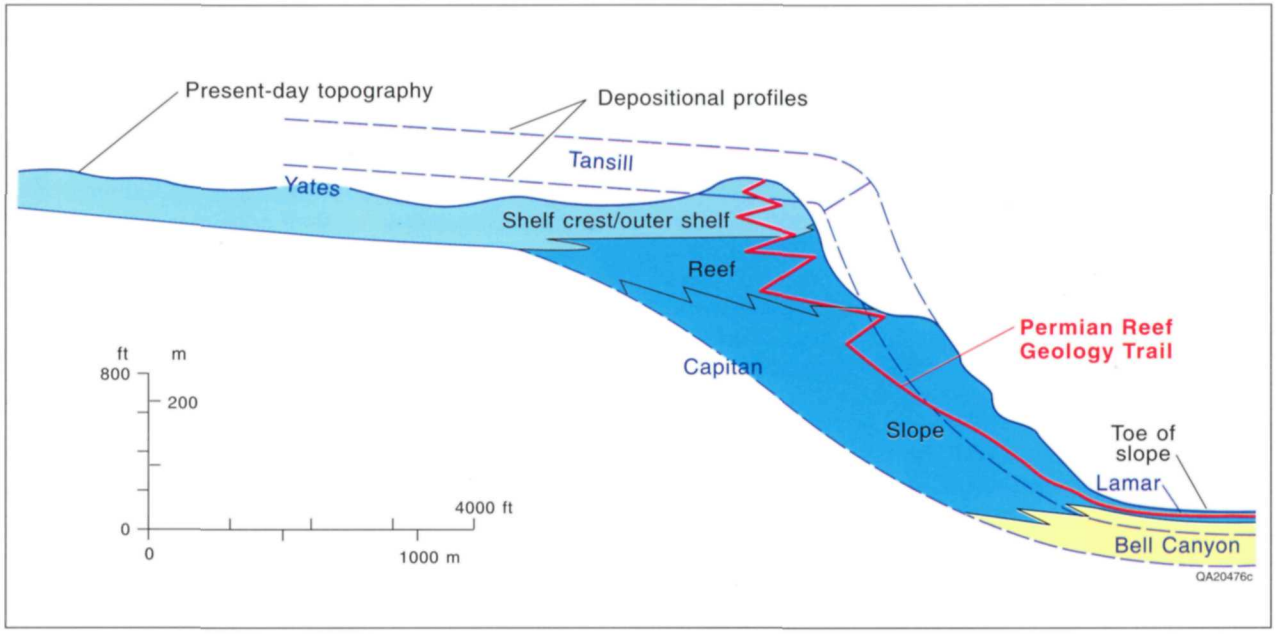

FIGURE 7. Diagrammatic sketch of the north wall of McKittrick Canyon showing the stratigraphy, depositional environments, present-day erosional profile, and general location of the Permian Reef Geology Trail.

Seven Rivers Formation is ~183 m (~600 ft) thick in this area, and the equivalent Capitan reef margin displays 2.4 km (1.5 mi) of progradation. None of the Seven Rivers equivalent Capitan Formation is exposed along the trail.

Yates Formation platform profiles are markedly more flat-topped, as is demonstrated by tracing the distinctive recessive sandstone-rich intervals in the Yates Formation across the shelf. On the north wall of McKittrick Canyon (fig. 6) and in the subsurface (Borer and Harris, 1991) five packages, marked by sandstone beds at the base of each, are considered equivalent to Yates depositional sequences. The upper three packages equate to the Yates A, B, and C divisions of Newell and others (1953) (fig. 4). However, only the youngest two sequences of the Yates Formation (Yates B and C) are exposed on the trail. The Tansill Formation is preserved as a small erosional remnant at the crest of the north wall of the Canyon (figs. 6 and 7). The trail intersects 21 m (70 ft) of the Tansill Formation, which is the Tansill's total thickness in the canyon. Erosion has removed all Tansill-equivalent Capitan reef and most of the slope, leaving only the deeper slope record of the Lamar Limestone Member of the Bell Canyon Formation exposed on the lower third of the trail (fig. 7). Bedding configuration and facies along the upper part of the Permian Reef Geology Trail suggest a Yates profile with a shelf crest coincident with the tepee-pisolite facies tract and an outer-shelf seafloor sloping seaward toward a deeper water reef, like that shown in figure 5c.

The Trail

The remainder of this guidebook is a detailed description and discussion of the facies exposed along the trail (fig. 2). However, the trail crosses only a very small part of the entire Capitan reef complex exposed in McKittrick Canyon (figs. 6 and 7). In addition, postdepositional erosion and cover limit somewhat the continuity of the outcrop along the trail. Erosion has removed all of the Tansill- and uppermost Yates-equivalent reef and most of the Tansill shelf strata. Vegetation and present-day talus cover parts of the upper-slope section, particularly in the critical reef-transition areas, making correlation of these steeply dipping beds difficult. Note also that the slope of the trail is less than both the depositional slope and present-day topographic slope; therefore, facies encountered along the trail are not all from time-equivalent units. For example, along the slope and reef parts of the trail, one encounters progressively older slope facies while walking farther along (up) the trail. The trail traverses facies of the toe-of-slope in Stops 1–8, 29, and 30; slope in Stops 9–14; reef in Stops 15–22; and outer shelf/shelf crest in Stops 23–28 (figs. 2 and 7).

Detailed examination of all stops in this guide will require 2 days. For a 1-day trip, use the guide to select (approximately half) those stops of particular interest to you or your group. The length of the trail is ~5.6 km (~3.5 mi); the vertical climb is 610 m (2,000 ft). As a general guide for a 1-day trip, plan to cover the lower part of the trail (up through Stop 18) by noon and the upper part (to the top) by 2 p.m. Allow 1.5 to 2 hours for return to the McKittrick Canyon Visitor Center at the bottom. Note that gate-closure times are posted at the McKittrick Canyon road entrance. Elevation markers have been installed every 30 m (100 ft) vertically along the trail to provide reference for location of stops (fig. 2). Most markers are located on the uphill side of the trail, generally in an easily visible position ~0.3 to 0.6 m (~1 to 2 ft) above the trail.

Do not disturb or remove any rocks, plants, or wildlife, and do not leave the trail. Hammers and other sampling equipment may not be carried on the trail. These activities are prohibited by law. The important features described in this guide are all well displayed on natural and blasted rock faces visible from the trail. In addition, a collection of rock samples used to prepare this guide has been provided to the park museum study collection and is available through prearrangement at the Headquarters Visitor Center Building 19.3 km (12 mi) south of McKittrick Canyon.

Toe of Slope: Alton Brown and Robert G. Loucks

Rocks exposed along the lower part of the trail are toe-of-slope facies of the Lamar Limestone Member of the Bell Canyon Formation. The toe-of-slope environment occurs where the low depositional dip characteristic of the basin increases to the higher dip characteristic of the slope. The increase in dip is associated with decreasing carbonate mud content and increasing bed thickness. These and other facies changes in the toe of slope can be examined along a time line, because Stops 4–7 expose the same approximate stratigraphic level (fig. 8). Toe-of-slope depositional processes changed during Lamar deposition, so a single time slice, such as observed along this part of the trail, does not exhibit the full variety of lithologies and facies relationships found here. Additional cross sections and overviews fill this gap by illustrating these relationships and providing a stratigraphic framework for interpreting larger scale processes.

The Permian Reef Geology Trail starts on the north side of McKittrick Draw, at the canyon side of the McKittrick Canyon Visitor Center. The trail begins at a fork to the right at the Park Service sign ~46 m (~150 ft) beyond the draw.

STOP 1. Quaternary-Age Alluvial Conglomerate

The cliff at the start of the trail exposes Quaternary-age, calcite-cemented alluvial-fan conglomerate consisting of well-rounded limestone clasts with calcilitharenite matrix. The 5,000-ft elevation marker is located on this exposure. Depositional-flow units are generally less than 1 m (<3.3 ft) thick; cobbles in the coarser units average 20 cm (7.9 inches) long with single boulders up to 50 cm (19.5 inches) across. Large pebbles are locally imbricated.

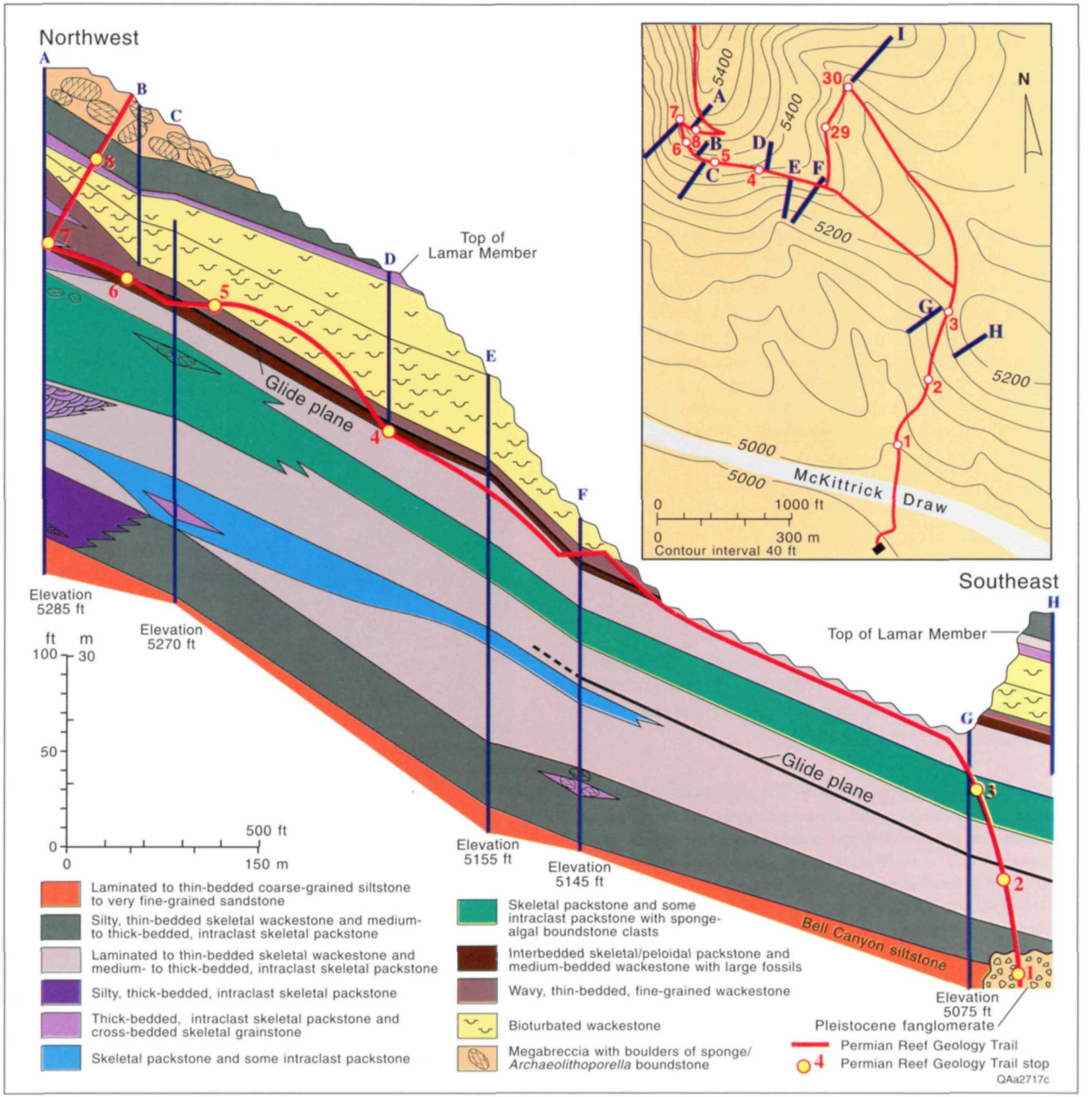

FIGURE 8. Dip-oriented, structural cross section of the toe-of-slope Lamar Limestone exposed on the north wall at the mouth of McKittrick Canyon. Units of Lamar Limestone Member of the Bell Canyon Formation shown on the section generally become more thin bedded and less grainy down paleoslope. Inset shows location of the stratigraphic sections measured for this trail guide. The red line marks the approximate position of the trail on the cross section, and circles mark the position of stops.

A modern analog of these deposits is the gravel of McKittrick Draw. Bachman (1976) dated eroded Guadalupian conglomerates as middle to late Pleistocene, prior to the present downcutting cycle. The conglomerates form a superficial cover over the Bell Canyon siltstones and lowest part of the Lamar for the next few hundred feet along the trail.

STOP 2. Distal Toe-of-Slope Wackestone

Stop 2 is 229 m (750 ft) uptrail from Stop 1 in the lower part of the Lamar. Stop 2 is identifiable by the resistant 3-m-thick (10 ft), cherty limestone bed exposed to the right of the trail (fig. 9a). The dominant lithology at this stop is dark-gray, laminated to thick-bedded skeletal-peloidal wackestone. Most grains in the wackestone are coarse-silt to fine-sand sized (fig. 9b), so the limestone appears to be a mudstone in outcrop. Microfossils are those characteristic of the slope setting, such as foraminifers, spicules, ostracodes, calcispheres, and fragments of larger fossils such as thin-shelled brachiopods. Silicified brachiopods, bryozoans, horn corals, and other body fossils are common in some beds. Fossil constituents and depositional texture are similar to the toe-of-slope wackestones throughout the toe-of-slope section.

Beds immediately below the silicified limestone are dominantly thin- to medium-bedded limestones. Many thin-bedded limestones have a 1.3-cm-thick (0.5 inch), basal, laminated, skeletal packstone unit overlain by graded, skeletal-peloidal wackestone with faint parallel laminations and rare, low-relief ripples that are visible only on polished slabs (fig. 9c). These features suggest deposition by turbidity current.

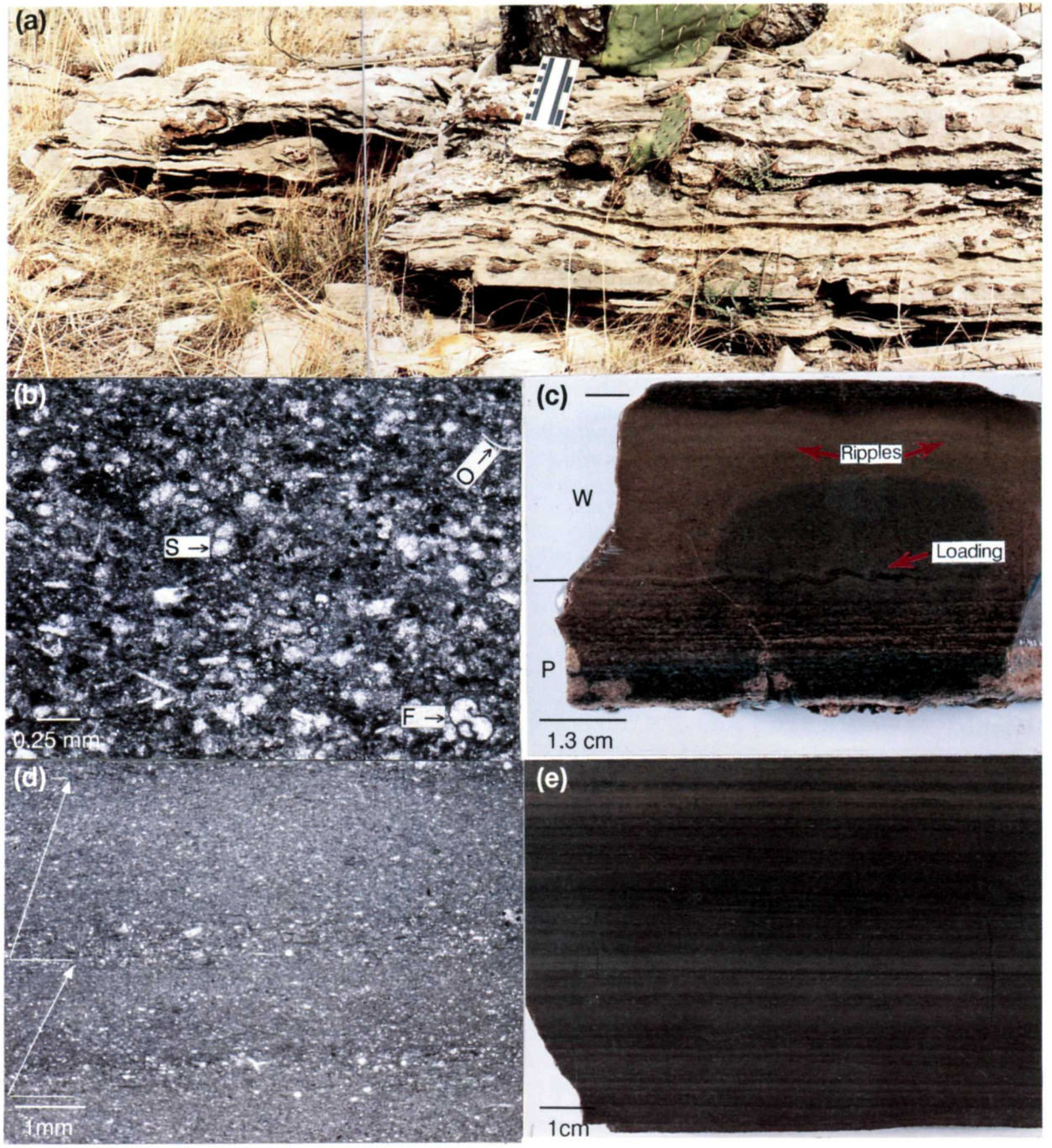

FIGURE 9. Stop 2, trail and thin-section photographs: (a) outcrop photo of cherty, slump-contorted wackestone near the base of Stop 2, (b) thin-section photomicrograph of skeletal peloidal packstone grading upward into a skeletal peloidal wackestone; grains include ostracodes (O), foraminifers (F), sponge spicules (S), and peloids (dark-colored clots), (c) polished slab (scale bar = 1.3 cm [0.5 inch]) of a thin-bedded limestone showing thin, partially silicified, basal packstone (P) and an overlying graded wackestone (W); the packstone has parallel laminations and the wackestone has load-induced structures and faint ripples near the top and a concentric color pattern caused by weathering, (d) photomicrograph of laminated, normally graded, skeletal (small white specks) wackestone; horizontal lines show base of graded units and arrows show upward-grading, skeletal composition similar to that of figure 9b, (e) polished slab of laminated wackestone.

The cherty limestone bed (fig. 9a) has a distinctive convoluted structure caused by proximity to a syndepositional slide. High chert content may be related to the abundance of sponge spicules in this bed. Light-colored, red-weathering silica is common in toe-of-slope wackestones and packstones.

The limestone above the silicified bed is laminated wackestone interbedded with thin-bedded wackestone and skeletal packstone. Each lamina consists of 0.3 to 0.5 mm of wackestone to packstone that grades upward into 2 to 4 mm of wackestone (fig. 9d and 9e). The laminae are interpreted to be low-density turbidity-current deposits. A sparsely burrowed laminated bed about 0.3 m (1 ft) thick occurs about 3 m (10 ft) upsection from the silicified bed. Just below this bed, the laminated wackestone is recumbently folded by syndepositional slope failure. The nose of the fold plunges southeastward, almost directly down paleoslope.

A 1-m-thick (3-ft) erosionally resistant wackestone overlies the laminated wackestone about 4.6 m (15 ft) upsection from the silicified bed. Although grain types are similar to those in the other wackestones, this anomalously thick bed has a faintly convoluted fabric. This unit is tentatively interpreted as a matrix-rich debris flow in which the dominant intraclasts were stiff muds.

For the next 46 m (150 ft), the trail intersects thin-bedded skeletal wackestones interbedded with thin packstone beds. Feeding traces and silicified fossils are exposed on excavated blocks along the trail.

STOP 3. Distal Toe-of-Slope Debris-Flow Deposits

The trail cuts two prominent, erosionally resistant beds separated by about 1.5 m (5 ft) of section just below the crest of the first low ridge (see fig. 8 inset for location). Stop 3 contains one of the few stratigraphic intervals rich in thick- and medium-bedded intraclast and skeletal packstones this far from the reef. Although large clasts are mudstones, wackestones, and packstones derived from the slope (fig. 10a), small clasts of sponge-algal boundstone occur in the intraclast packstones, indicating that this flow was derived from high on the slope (fig. 10b). These packstones are interpreted to have been deposited by debris flows and high-density turbidity currents (fig. 11). Chert bodies in these beds are diagenetic features, not depositional clasts.

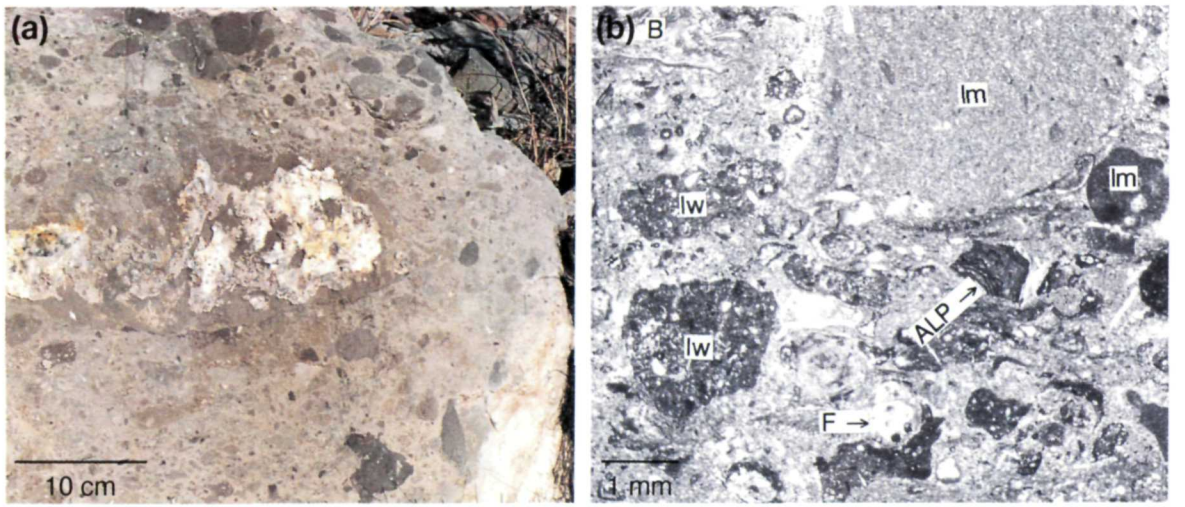

FIGURE 10. Stop 3, trail and thin-section photographs: (a) outcrop photograph (scale = 10 cm [4 inches]) of the intraclast skeletal packstone at the middle of Stop 3; large clasts are mudstone, wackestone, and packstone pebbles to cobbles derived from the lower slope; *Archaeolithoporella* boundstone is represented as sand- and granule-sized clasts, (b) thin-section photomicrograph (plane-polarized light) of an intraclast skeletal packstone. Skeletal grains include brachiopods (B) and foraminifers (F); intraclasts include *Archaeolithoporella* boundstone (ALP), skeletal/peloidal wackestone (lw), and mudstone (lm).

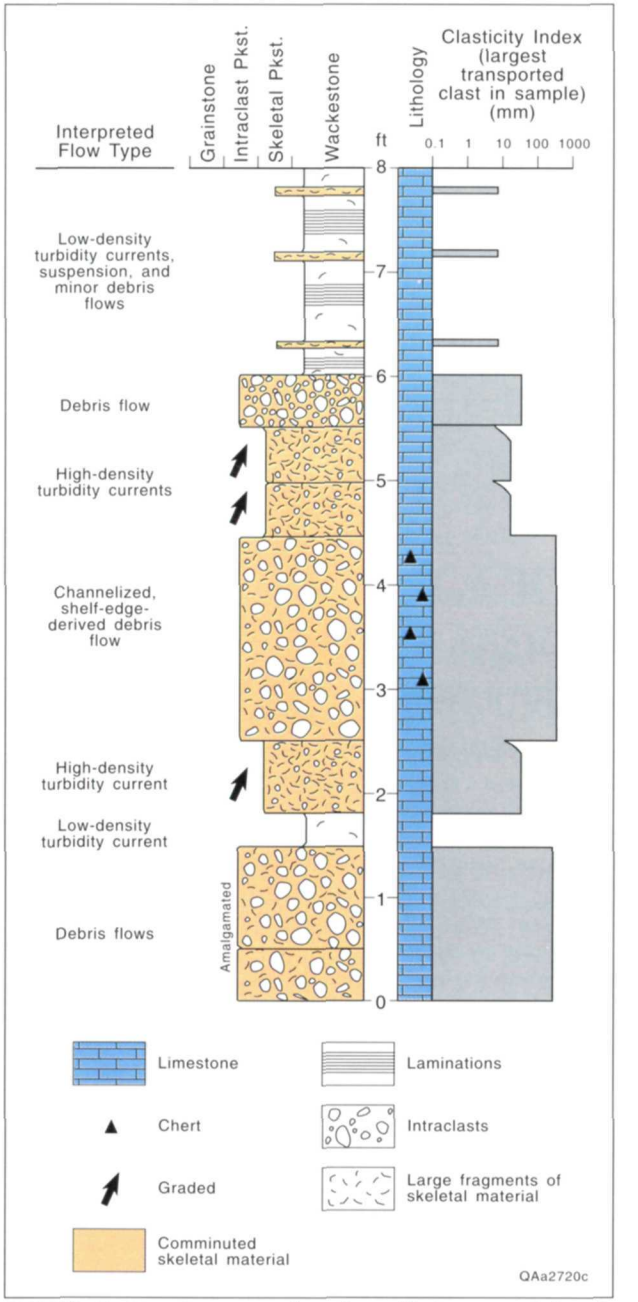

FIGURE 11. Stop 3, measured section with interpreted depositional processes. Position of laminated wackestone and thin skeletal packstone beds in the upper part of the section is schematic due to poor exposure.

The junction of the Geology Loop Trail (straight) and the Permian Reef Geology Trail (sharp left) is marked by a sign. The Geology Loop Trail exposes depositional-strike-oriented facies changes in the toe-of-slope setting. These stages are described in a separate section beginning on page 44.

The Permian Reef Geology Trail continues up a dip slope in the upper part of the Lamar Limestone Member following the crest of the low ridge separating McKittrick Canyon from drainage to the northeast (fig. 8 inset). The flaggy bedded laminated wackestones exposed along the ridge crest in the vicinity of the 5,200-ft elevation marker are similar to those discussed at Stop 2. Above the upper junction with the Geology Loop Trail, the Permian Reef Geology Trail follows the base of a low cliff. Echinoid spines, gastropods, and scaphopods are common on some bedding planes of the thick-bedded wackestones exposed on the trail just before the Grottos (Stop 4).

STOP 4. Vertical and Lateral Changes in Toe-of-Slope Sedimentation

Farther along the trail are shady, protected areas called the Grottos. Stop 4 is located at the down-trail end of the Grottos. Limestones exposed at Stop 4 are predominantly very fine grained wackestones and mudstones with skeletal constituents similar to those described at Stop 2. Four stratigraphic units are exposed here (fig. 12a); these units can be traced along the cliff downdip and updip from Stop 4 (fig. 12c) and to the cliff on the south side of McKittrick Canyon. The lowest unit is a thin-bedded, fine-grained wackestone with thin skeletal packstone layers similar to rocks at Stop 2. Overlying this lower unit is a recessively weathered unit of microporous, coarse skeletal-peloidal packstone (fig. 12b) interbedded with medium-bedded wackestone with large fossils. Because of its recessively weathered profile and unique lithology, this unit forms a key correlation bed with Stop 7 and measured sections even farther updip and downdip. This unit is separated by a paleoglide plane from the third unit, a thin-bedded, sparsely bioturbated, fine-grained wackestone. The upper two-thirds of the cliff is a wackestone with a characteristic bioturbated fabric (fig. 12d). Most burrows are unbranched, oblique to horizontal, tortuous, smooth-walled, cylindrical traces. Observed characteristics are similar to the form ichnogenus *Planolites*.

The lower three units are interpreted to be low-density turbidity current deposits with different fractions of coarser material. Depositional mechanism of the upper unit is unknown. Variations in burrow intensity record changing biological activity in the toe-of-slope setting. Absence of bioturbation indicates anoxic conditions in the Delaware Basin, whereas extensive bioturbation indicates dysaerobic to aerobic conditions (Babcock, 1977). This burrowed wackestone has been correlated about 8 km (5 mi) into the basin and onto the slope (Stop 10), so it may mark a major incursion of oxygenated water into the otherwise anoxic Delaware Basin (Babcock, 1977).

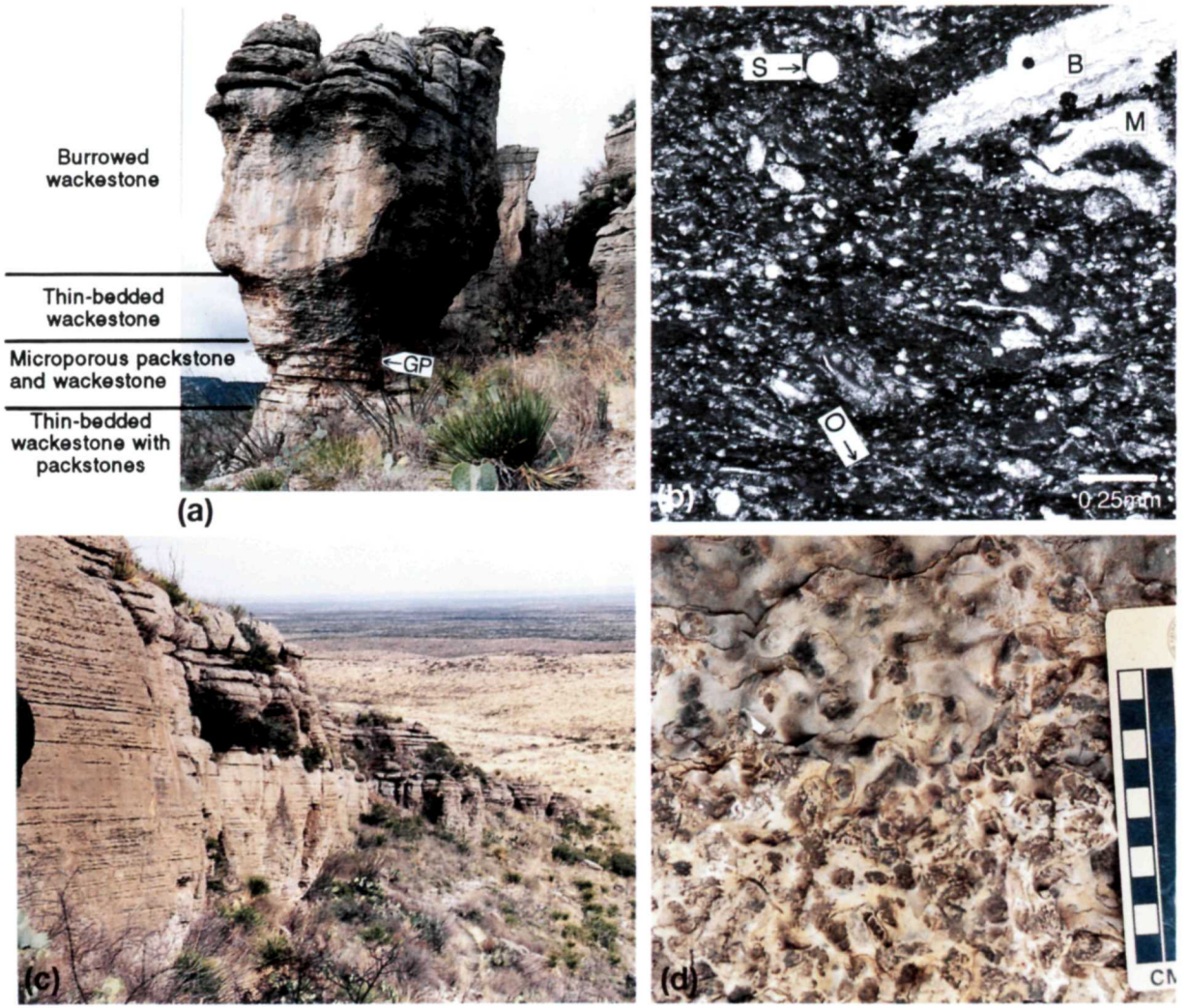

FIGURE 12. Stop 4, trail and thin-section photographs: (a) outcrop with unit marked GP identifying paleoglide zone, characterized by bedding convolution, separating two of the units, (b) thin-section photomicrograph of microporous peloidal packstone with grains of brachiopods (B), sponge spicules (S), ostracodes (O), and mollusks (M) and dark matrix including many deformed peloids, (c) view along the Lamar cliff of burrowed wackestone from Stop 4 showing continuity of bedding and preserved depositional dip, (d) outcrop of weathered bedding plane of the *Planolites*-burrowed wackestone.

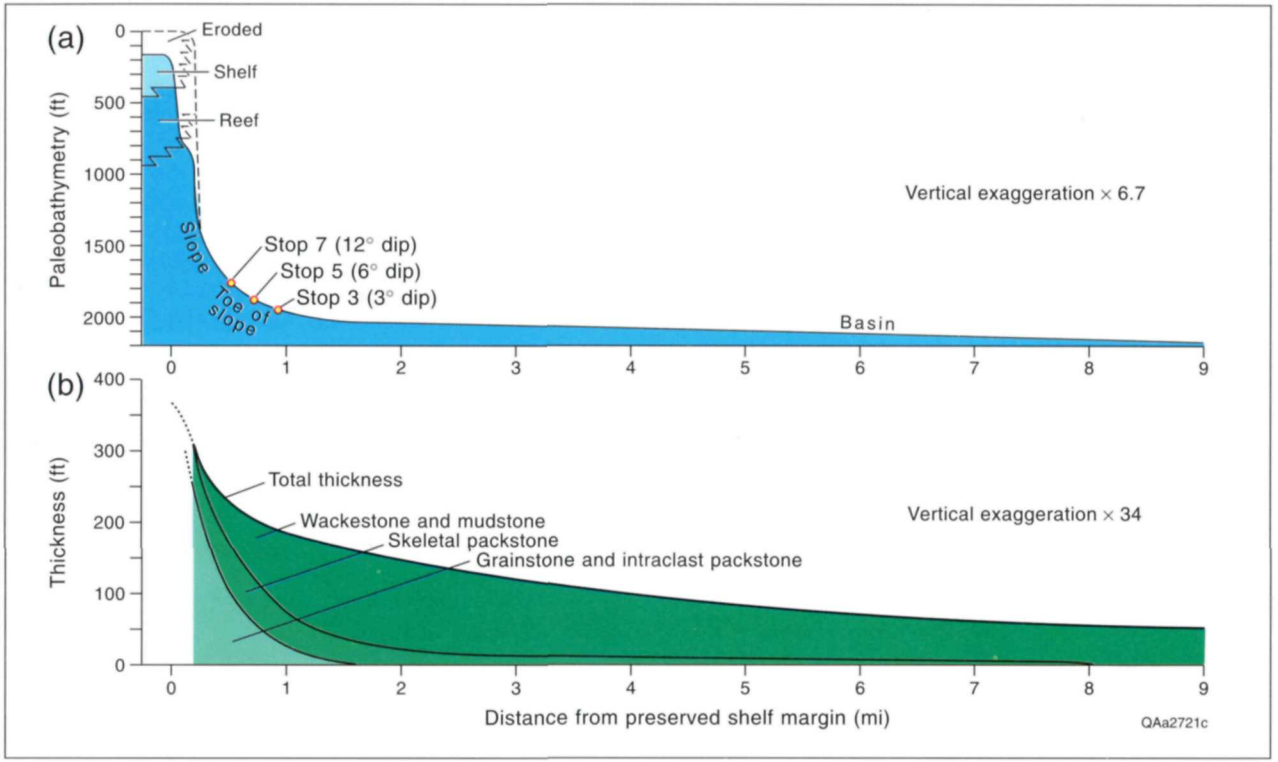

FIGURE 13. Regional variations along a reef-to-basin cross section of (a) depositional dip and (b) lithology and thickness of the Lamar Limestone Member. The reconstructed paleobathymetry of the top of the Lamar Limestone Member is based on modern structural relief and assumes no compaction. The top of the Lamar is correlated with the base of the Ocotillo Member of the Tansill Formation about 61 m (200 ft) above the base of the Tansill. Lithology and thickness data are from measured sections in Tyrrell (1962), Babcock (1977), and this study.

The upslope change from laminated wackestone, as observed at Stop 2, to thin-bedded wackestone, here at Stop 4, is one of many changes in the Lamar Limestone Member that reflects proximity to the shelf margin. The paleoslope steepens dramatically from the basin to the toe of slope (fig. 13a). The Lamar interval thickens, and the percentage of grainy facies increases (fig. 13b). The scale of changes is best appreciated by looking toward the basinal Lamar outcrops here. Although there is a northeasterly structural dip of about 2° in the originally flat-lying basin units, their dip in the paleoslope direction (southeast) is less than 13 m per 1.6 km (<70 ft/mi), so present-day dip measured perpendicular to the platform margin closely approximates that of depositional slope. The distant cuestas to the southeast are almost directly down paleoslope from McKittrick Canyon. They are capped by a thin (9- to 12-m-thick [30- to 40-ft]) section of Lamar wackestones and mudstones. Just outside the park, near the mouth of McKittrick Canyon, the low hills expose more than 46 m (>150 ft) of limestone, but depositional dip is gentle, and the Lamar Limestone is still more than 95 percent wackestone. From this point, paleoslope steepens, and the fraction of grainy rocks increases significantly. Depositional dip increases from ~3° at Stop 3 to an average of 6° at Stop 4 (fig. 13a).

Updip from the Grottos, paleoslope steepens, and the fraction of grainy limestone greatly increases. Stops 4, 6, and 7 expose the same stratigraphic interval in different paleobathymetric positions (fig. 14). The slightly burrowed, thin-bedded wackestone above the recessively weathered peloidal packstone at Stop 4 contains no skeletal packstone beds. At Stop 6 the same unit has numerous thin skeletal packstone beds, and at Stop 7 the same unit is thicker and contains thick intraclast packstone beds (fig. 14).

STOP 5. Stratigraphic Relations on the South Side of the Canyon

Outcrops at the second Grotto are more weathered and poorly exposed, but updip thickening and lithology changes in the toe-of-slope setting can be examined in the Lamar exposed in the cliff on the south wall of the canyon (fig. 15). At first glance, the beds in the upper half of the cliff appear to downlap onto beds in the lower half of the cliff. Closer inspection of bedding relationships indicates an overall thinning in a downdip direction, but no single downlap surface. Convergence of bedding is caused by thinning and termination of individual beds. There are two prominent bedding-termination surfaces that are planar, basinward-dipping surfaces of onlap, which truncate underlying, shallow-dipping beds (fig. 15). These surfaces are interpreted to be glide planes wherein intact sections of overlying strata slid basinward as subtle slumps, but they may represent large-scale scour-and-fill structures. The upper, continuous recessively weathered unit corresponds to the recessively weathered unit here and at Stop 4. Stop 5 approximately corresponds to a paleobathymetric position near the southeast end of the cliff, whereas Stop 7 corresponds to a position to the right of the large pine tree at switchback A.

Stratigraphic relationships between basin and slope beds can also be viewed on the south wall of McKittrick Canyon (fig. 16). The Bell Canyon siliciclastic members are the vegetated, tan-to-yellow slopes. The McCombs, Lamar, and Rader Limestone Members of the Bell Canyon Formation weather into resistant white or gray beds. These carbonate members thicken and merge updip with the lower part (slope) of the Capitan Formation as the siliciclastic members thin.

STOP 6. Turbidites and Debris-Flow Deposits

Stop 6 is about 46 m (150 ft) beyond the end of the cliff, past a clump of low trees. The low exposures on the north side of the trail are thin- to medium-bedded, homogeneous, fine-grained wackestone containing thin-bedded 5- to 15-cm-thick (2- to 6-inch) packstone beds with skeletal fragments up to 1.3 cm (0.5 inch) across (fig. 17). The same stratigraphic interval at Stops 4 and 5 lacks packstones

and has less depositional slope (fig. 13a). Some packstones are ungraded; others are normally or inversely graded. Fossils within the packstones are brachiopods, bryozoans, and foraminifers, all of which are characteristic of slope settings. Some wackestone beds show boudin structures (fig. 17). Contacts between the grainy and muddy units are slightly convoluted. Convolution and boudin structures are thought to be caused by creep associated with incipient slope failure of muddy sediment on these steeper paleoslopes. The wackestones are interpreted to be low-density turbidity-current deposits, whereas the graded packstones are interpreted to be suspension layers within high-density turbidity current deposits (S3 layers of Lowe, 1983). The ungraded packstones are either debris-flow or high-density turbidity current deposits.

STOP 7. Transition from Toe of Slope to Slope

The updip transition from units dominated by thin-bedded wackestones (toe of slope) with thin skeletal packstones to units dominated by thick, mud-clast-rich packstones (slope) is exposed at Stop 7 at switchback A (fig. 18a). The cut at the switchback exposes a thick-bedded, erosionally resistant packstone and an underlying, recessively weathered, thin-bedded, peloidal packstone with thin peloidal-skeletal grainstone beds (fig. 19). This is the same peloidal packstone unit that occurs at Stop 4, but at Stop 7 the unit contains thin grainstone beds (fig. 18b) and megafossil packstone beds instead of wackestone beds with megafossils as at Stop 4. The thicker packstone bed is amalgamated from three flows; the lowest is rich in wackestone clasts, the middle unit is rich in brachiopods (fig. 18c), and the upper unit is a mixture of constituents of both the lower and middle units. None of the units contain clasts with boundstone fabric or reef organisms, indicating that these intraclast packstones were derived from the slope. The base of the amalgamated packstone cuts into the underlying recessive packstone at the switchback. Surrounding units and depositional interpretations are shown in figure 19.

The stratigraphic relationships at this transition are as important as the suite of sedimentary structures. The intraclast packstones maintain approximately the same thickness updip from switchback A, yet they abruptly thin and terminate in a relatively short distance down paleoslope from the switchback

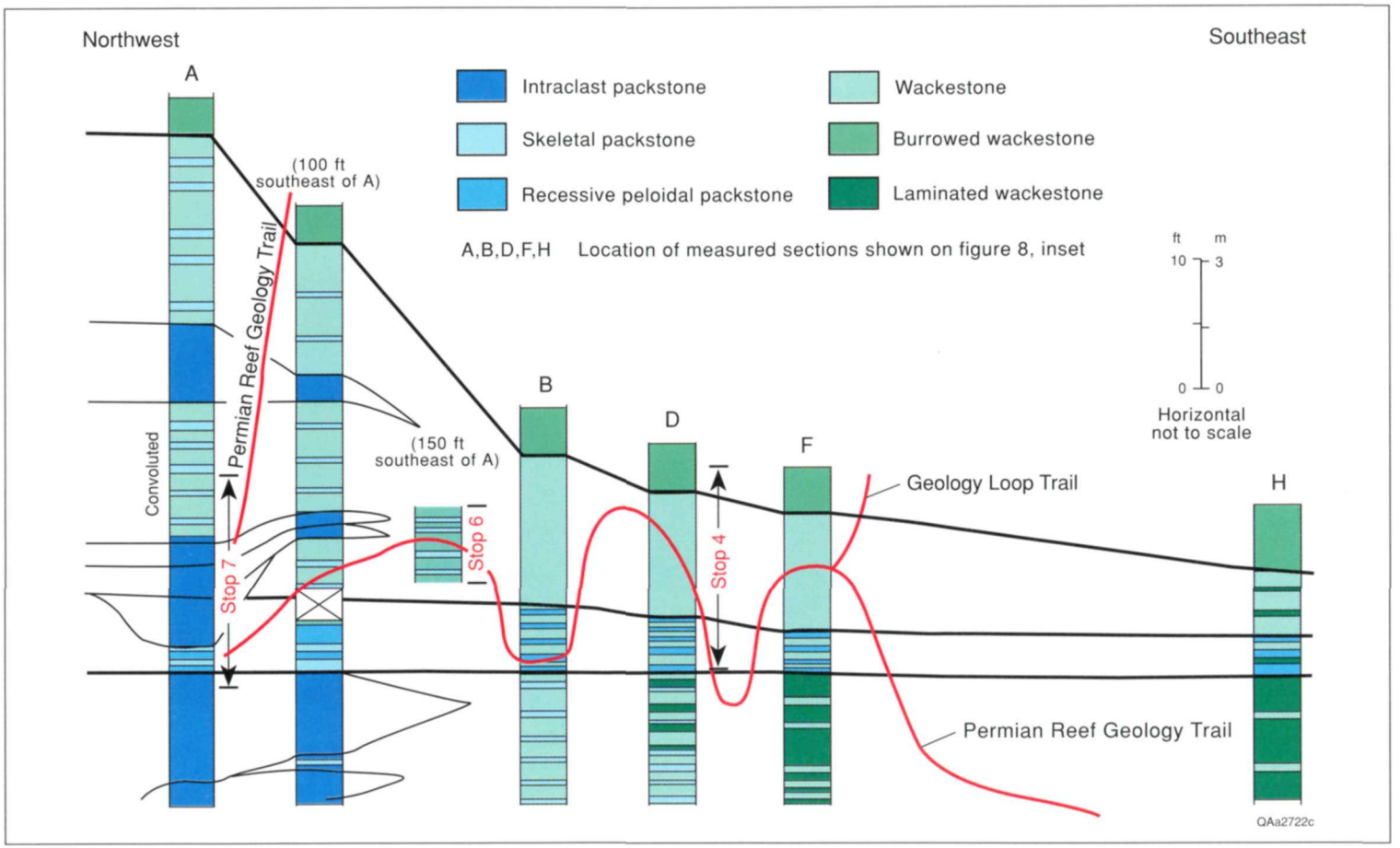

FIGURE 14. Cross section of toe-of-slope facies between Stops 4 and 7 along the north wall of McKittrick Canyon. Wackestone units vary systematically from laminated in downdip sections to thin bedded in updip sections. Skeletal packstones thicken and become more abundant up paleoslope, and intraclast packstones are present in the sections proximal to the shelf margin.

(figs. 14 and 18a). This transition is also visible on the upper part of the cliff on the south side of the canyon.

Up the trail from switchback A are poorly exposed thin- to medium-bedded wackestones with thin, skeletal packstone beds and other intraclast packstones. The burrowed wackestone exposed in the path about 46 m (150 ft) up the trail from switchback A is correlative with the burrowed wackestone unit at Stop 4.

STOP 8. Top of Lamar Limestone Member

Stop 8 is at a resistant-weathering, thick, intraclastic packstone bed with large wackestone clasts and muddy skeletal matrix stratigraphically above the burrowed wackestone, about 30 m (100 ft) uptrail from switchback A (fig. 2). The packstone is interpreted to be another slope-derived, debris-flow deposit. Overlying thin-bedded mudstones contain flat bivalve fossils and a small amount of quartz silt along dolomitic partings. These units are interpreted to be low-density turbidity current deposits. The packstone bed is interpreted to be the top of the Lamar Limestone Member of the Bell Canyon Formation. The overlying, slightly silty (quartz) mudstones and thin-bedded wackestones are in the post-Lamar member of the Bell Canyon Formation (fig. 8). This silty interval also correlates to the silty interval in the slope near Stop 12.

Summary

The dominant lithology exposed along the lower part of the trail is very fine grained, laminated to thin-bedded, skeletal wackestone with thin layers of skeletal packstone. Most of these units were deposited by low-density turbidity currents. The deposits are best interpreted as a type of periplatform ooze in which clay- and silt-sized carbonate was derived from the shallow-water shelf, and the coarse silt and larger skeletal grains and intraclasts were derived from the slope.

Three types of grainy limestones are exposed along the trail in the toe of slope: (1) thin 1.3-cm to 25-cm thick (0.5 inch to 10 inches) packstone and graded grainstone beds containing slope-derived skeletal material, (2) thick (25-cm to 10-m thick [10 inches to 4 ft]) pebble to cobble conglomerate beds with a packstone fabric and slope-derived wackestone clasts and skeletal grains, and (3) channelized, thick to very thick bedded, pebble to cobble conglomerates with a packstone matrix and clasts derived from both the shelf margin and slope.

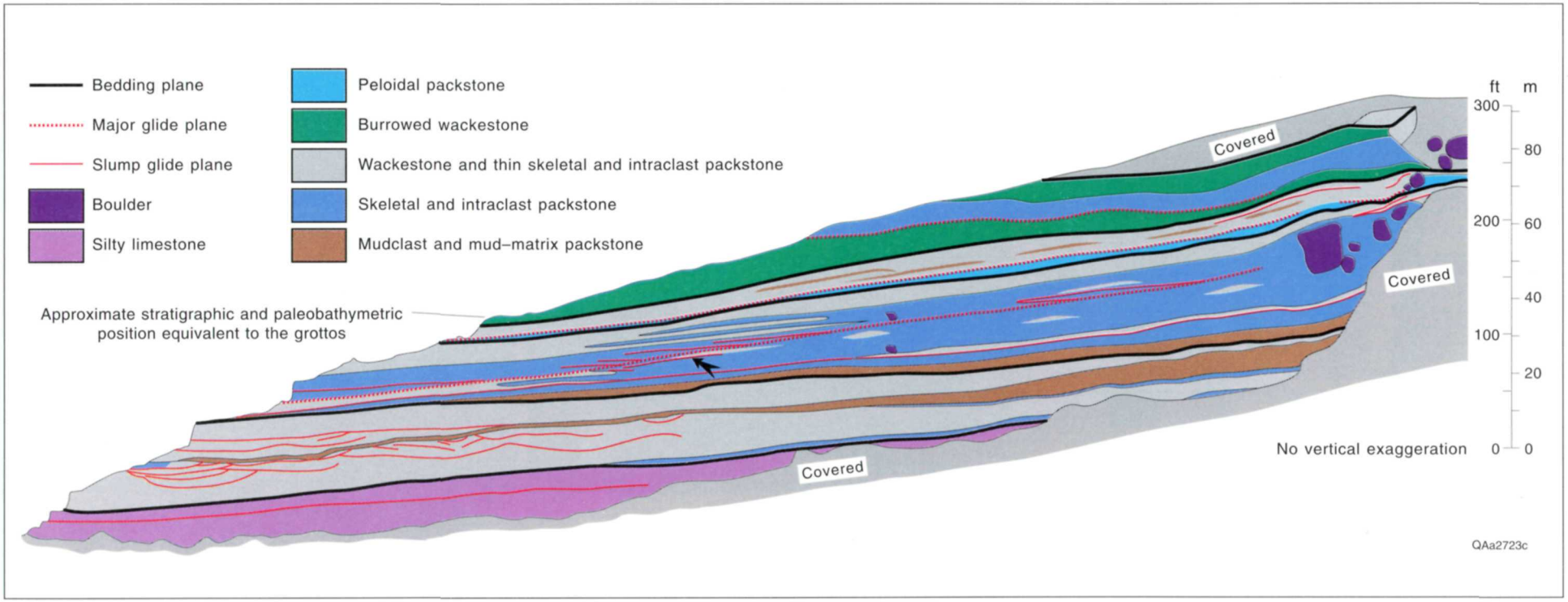

FIGURE 15. Interpretation of lithology and bedding relationships on the cliff of Lamar Limestone on the south side of McKittrick Canyon (Stop 5). Large boulders and packstones occur in the updip part of the cliff. Packstones terminate downdip by thinning of the debris-flow depositional units and by glide-plane truncation (large arrow). Thin wackestone beds were deformed and eroded by the debris flows, and slumps in the lower part of the cliff are at the same stratigraphic position as the deformed wackestones at Stop 2. Lithology in the central part of the cliff is interpreted from weathering patterns and correlation to the ends of the cliff. Beds are thin and variable in the central part of the cliff, so the lithology shown there is schematic. Area of outcrop shown in figure 16.

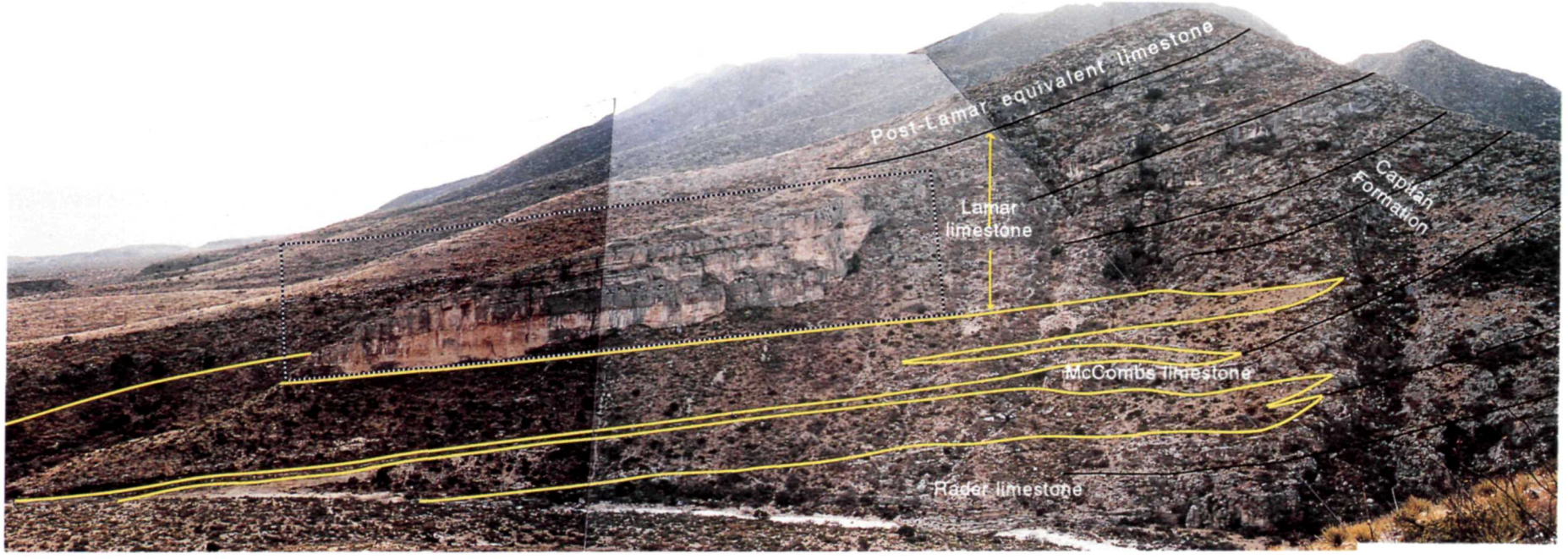

FIGURE 16. Photograph of the south wall of McKittrick Canyon across from Stop 5 showing the basinal carbonate members merging with the Capitan Limestone. The transition from updip carbonate to downdip siltstone is shown with the yellow lines; the black lines mark bedding within the limestone. The area of figure 15 is outlined by the dashed line. Stratigraphic relationships after Newell and others (1953).

At the same paleoslope position, some stratigraphic intervals are characterized by abundant packstones, whereas other intervals are dominated by wackestones (fig. 8). This pattern indicates that toe-of-slope deposition alternated between deposition of carbonate-mud-rich, low-density turbidity current deposition and grain-rich, debris-flow and high-density turbidity current deposition. Most tongues of thick, coarse-grained, slope-derived intraclast packstones do not extend as far basinward as do tongues containing the channelized packstones derived from the shelf margin (fig. 8). The slope-derived gravity flows apparently had less momentum than the gravity flows generated at the shelf margin.

In contrast to the abrupt downdip termination of the intraclast packstones, the skeletal packstones thin as they interfinger downdip with the thin-bedded and laminated wackestones (fig. 14). This interfingering indicates that the debris flows and high-density turbidity currents that deposited the skeletal packstones changed downslope into low-density turbidity currents that deposited the thin-bedded and laminated wackestones farther downslope.

FIGURE 17. Photograph of ungraded skeletal packstone along the trail at Stop 6. The large siliceous bodies in the center of the bed are diagenetic, not transported clasts. This bed is interpreted to be a slope-derived debris flow. The overlying wackestone has been deformed by boudins by downslope creep (red arrow).

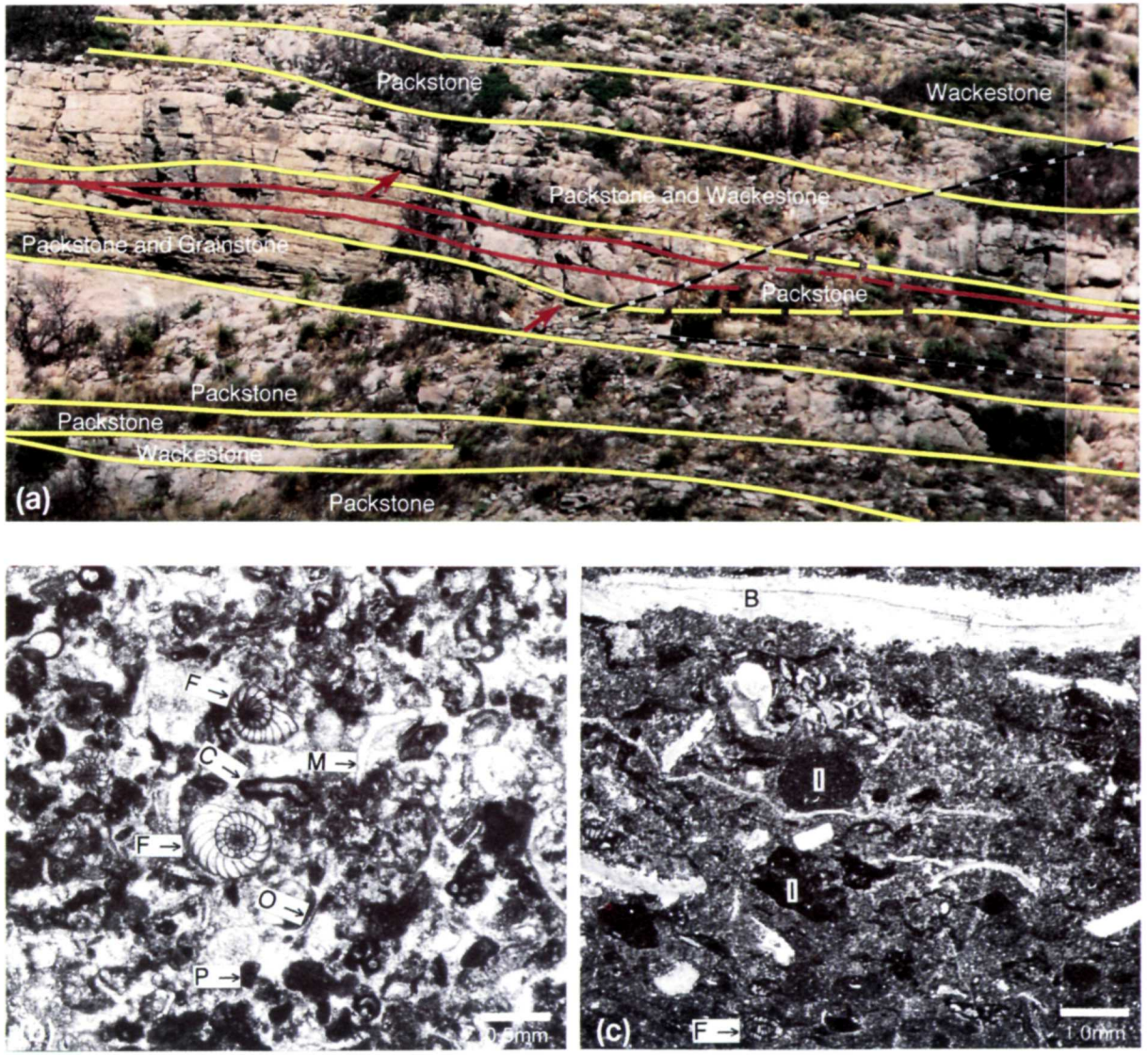

FIGURE 18. Stop 7, trail and thin-section photographs: (a) stratigraphic section around Stop 7 showing the downdip thinning of intraclast packstone units (yellow) that cross the trail (dashed), amalgamation surfaces (red), and truncation of units underlying packstone (red arrows); (b) peloidal-skeletal grainstone from recessively weathered packstone and grainstone interval with mollusk fragments (M), smaller fusulinids (F), algal/foraminifer coated grains (C), peloids (P), and ostracodes (O); (c) skeletal-intraclast packstone from the middle member of the amalgamated debris flow at Stop 7 with brachiopods (B) and mud intraclasts (I).

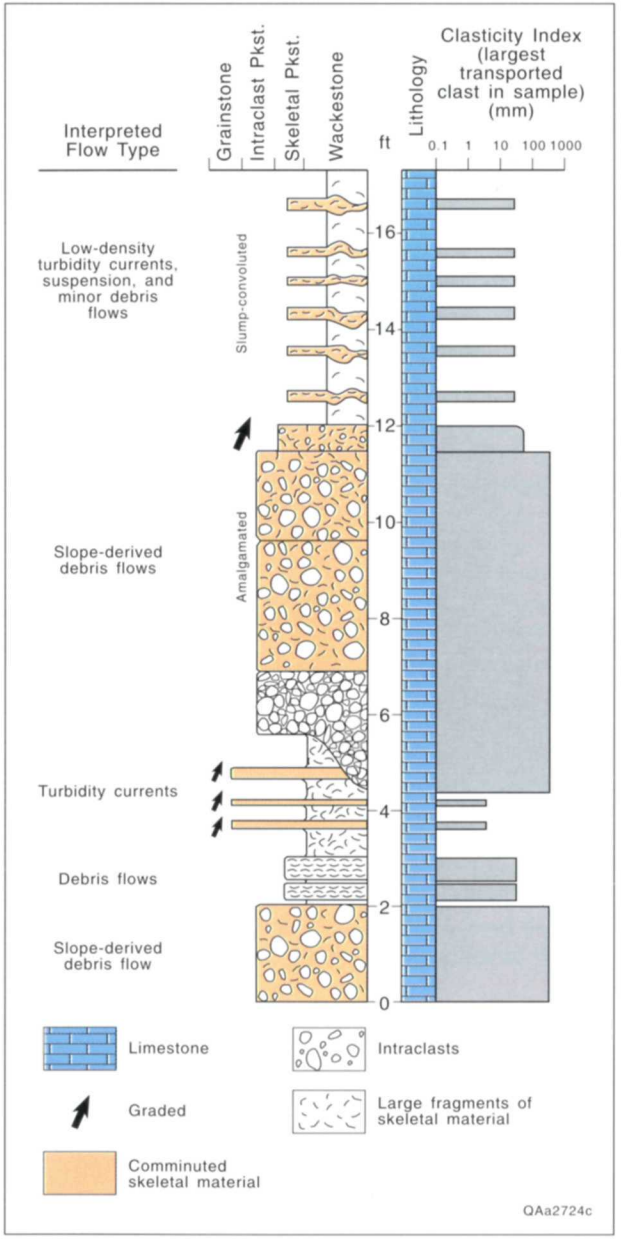

FIGURE 19. Measured section at Stop 7 with depositional interpretations. The switchback intersects the section 1 m (3 ft) above the base of the section, at the base of a recessively weathered peloidal packstone interval. Abbreviations and symbols are the same as those in figure 4, except for the peloidal packstone interval, which is plotted with the wackestones.

Slope: Denise Mruk and Don G. Bebout

The slope is a transitional depositional/physiographic region between the shallow-water carbonate shelf and the deep-water toe of slope and basin. Slope deposits reflect this transition and record components of two basic end-member sedimentary processes: gravity-induced flows from outer-shelf, reef, and slope environments and suspension sedimentation of the basin. Transport mechanisms characteristic of the slope include rock-fall, slump, grain-flow, high-density turbidity current, and debris-flow. Deposits formed by each of these processes will be examined in slope outcrops exposed along the Permian Reef Geology Trail.

The slope facies tract of the Capitan Formation is discussed at seven locations (stops) along the trail from just below switchback B to switchback D (fig. 20). The present structural dip, which approximates the depositional dip of the Permian slope beds, is steeper than the slope of the trail; therefore, younger rocks are exposed along the lower part of the trail, and older rocks along the upper part. Tansill-equivalent slope facies are exposed at Stops 9–12. The Tansill-equivalent reef facies have been eroded in McKittrick Canyon; therefore, the only preserved reef facies are in debris-flow blocks in the Tansill-equivalent slope beds. Yates-equivalent outcrops are exposed at Stops 13 and 14. The Yates-equivalent slope beds correspond to the massive reef facies and lower two-thirds of the shelf beds exposed along the higher parts of the trail beyond switchback D (fig. 20).

STOP 9. Mud-Dominated Gravity-Flow Deposits

Tansill-equivalent, mud-dominated gravity-flow deposits are well exposed along the lower third of the slope part of the trail and are designated as Stop 9. Numerous examples of the very thick bedded, lithoclast megabreccias are exposed from ~30 m (~100 ft) beyond switchback A up the trail to the 5,700-ft marker (fig. 20). The contact of the Lamar Limestone Member, described in the previous section of this guide, with the overlying slope megabreccias is identified by the change from thin-bedded, dark-colored, fine-grained limestone of the toe-of-slope and basinal facies to very thick bedded, light-colored, slightly silty, dolomitic wackestone of the megabreccia facies. Angular clasts 1 to 30 cm (0.4 to 12 inches) in diameter are incorporated within the dolomitic wackestone. Large, rounded boulders of sponge-*Archaeolithoporella* boundstone are at the contact on either side of the trail.

The megabreccia exposed at switchback B is part of a 24-m-thick (80-ft) amalgamated unit of alternating clast-supported and matrix-supported limestone beds (fig. 21a). Bedding within the amalgamated unit dips at 15° to 20°. Some beds demonstrate inverse grading from pebble-size clasts to boulder-size blocks. The clasts include reef-derived sponge-*Archaeolithoporella* boundstone (Toomey and Babcock, 1983), slope-derived skeletal wackestone and packstone, and dark-gray wackestone derived from the underlying toe-of-slope beds (fig. 21b). In the reef-derived blocks, the problematical alga *Archaeolithoporella* (fig. 21c) commonly encrusts small, elongate sponges; also present are brachiopod spines, the pinnate bryozoan *Acanthocladia*, and quartz silt. Brachiopods and crinoids in the matrix between the blocks may have been indigenous to the slope environment. Calcite-filled evaporite molds are visible in the sandy dolomitic wackestone below switchback B. The amalgamated unit exposed at Stop 9 is interpreted to represent repeated deposition by cohesive debris flows. Bedding planes within this unit probably indicate boundaries between individual debris flows. These debris-flow deposits overlie post-Lamar-age siltstone (fig. 20).

Analysis of geopetal fabrics is one of the most useful tools for distinguishing between allochthonous reef blocks and autochthonous massive reef beds. Variously oriented geopetal structures occur within the reef blocks of the lithoclast megabreccias and indicate that the blocks were transported after initial deposition and early cementation.

The boundstone fabric in the reef blocks was formed in shallower water on the slope or shelf margin. Oversteepening of the reef as it extended over unstable upper-slope sediments resulted in mass slumping of reef material and transportation down the slope. The most distinctive features of the Tansill-equivalent reef facies are the lack of internal sediment, lower sponge diversity, and large amount of botryoidal-fan cement. These features contrast with the older Yates-equivalent reef facies to be discussed in the next section of this guide. The botryoidal fibrous cement, readily recognized as the dark-gray to black, fanlike bodies of calcite cement that fill large cavities within the organic framework, is an early marine cement (fig. 21b). The thick layers of cement, intercalation of cement and encrusting algae, and suspension of skeletal components (floating) in cement suggest a rapid rate of cementation in the Tansill-equivalent reef (Toomey and Babcock, 1983).

Beyond switchback B, the trail follows an irregular, undulatory base of the amalgamated debris-flow unit and exposes a sandy dolomitic wackestone at its base. The carbonate adjacent to this sandy bed is also commonly dolomitized, reflecting movement of dolomitizing fluids along permeable siliciclastic zones (Melim, 1991). Slope dolomitization is discussed further at Stop 13.

STOP 10. Slope/Toe-of-Slope Burrowed Wackestone

Slope strata equivalent to the upper part of the Lamar Limestone Member are exposed at Stop 10, which begins at the 1.2-m-thick (4-ft) dolomitic siltstone forming the yellow-brown exposure just before the 5,700-ft marker. This siltstone correlates to the base of the post-Lamar Limestone Member of the Bell Canyon (fig. 20). Underlying the siltstone are beds of burrowed wackestone equivalent to the Lamar. The first occurrence of wackestone at Stop 10 is on the floor of the trail at the 5,700-ft marker.

The relationship of the burrowed wackestone to the upper-slope gravity-flow deposits is best demonstrated in the third burrowed wackestone exposure beyond the 5,700-ft marker (fig. 21d and 21e). The wackestone contains small, rounded intraclasts, crinoids, brachiopods, and the small fusulinid *Reichelina* (fig. 21f). The burrowed wackestone here correlates to the toe-of-slope burrowed wackestone exposed at the Grottos (Stop 4) and between switchbacks A and B (Stop 8). Wackestone at Stop 10 is more extensively burrowed than the equivalent limestone in the basin and presumably records periods of more oxygenated conditions in the toe-of-slope setting.

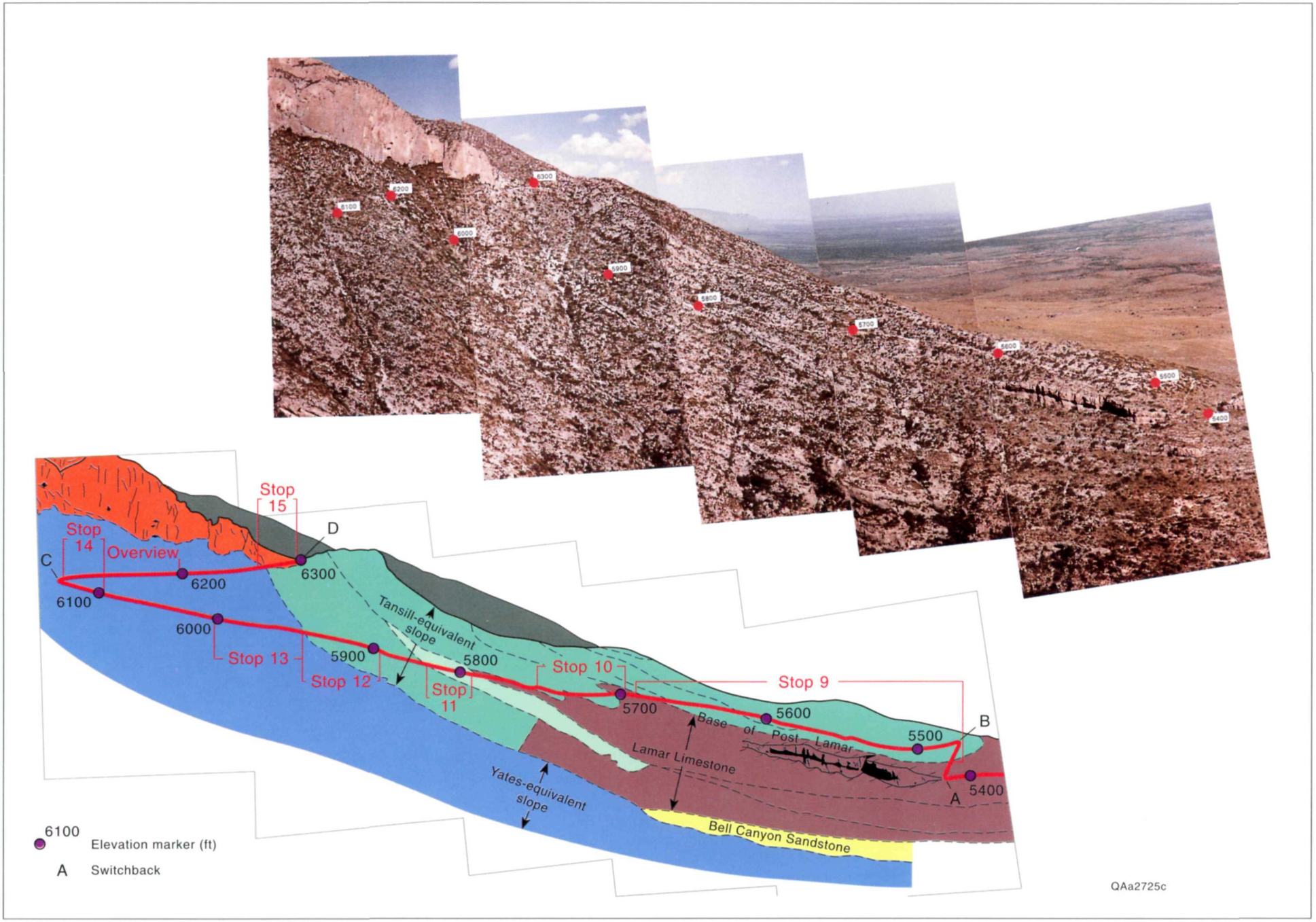

FIGURE 20. Dip-oriented oblique aerial photograph and an interpretive tracing of the slope and toe-of-slope portion of the Permian Reef Geology Trail. Locations of slope Stops 9–14, reef Stop 15, and elevation markers are noted along the trail.

Coarse-grained skeletal grainstone overlies the burrowed wackestone. The laminated grainstone is made up of fragments of crinoids, brachiopods, and dasycladacean algae presumably derived from the shallow-water shelf. The contact between the wackestone and the overlying grainstone is irregular and apparently erosional (fig. 21e). The grainstone was most likely deposited by high-density turbidity currents.

Downtrail from this exposure, the burrowed wackestone and overlying grainstone are truncated by a sequence of grain-rich, gravity-flow deposits. These beds are well exposed 15 m (50 ft) up the trail where the outcrop forms a slight overhang. These beds dip at 25° and consist of interbedded, dolomitized, skeletal lithoclast wackestone, packstone, and grainstone. Brachiopods, bryozoans, sponges, and crinoids are the dominant skeletal grains. Elongate, light-tan, mudstone lithoclasts are aligned parallel to the slope dip, but grading is not apparent. The skeletal lithoclast wackestones are interpreted as debris-flow deposits and the packstones and grainstones as high-density turbidity current deposits.

STOP 11. Grain-Dominated Gravity-Flow Deposits

Tansill-equivalent, grain-dominated, gravity-flow deposits are characteristic of the middle and upper portion of the Capitan slope. Stop 11 includes the gravity-flow deposits exposed along the trail from just below the 5,800-ft marker to ~9 m (~30 ft) up the trail beyond the marker. Nine stratigraphic units are distinguished within the gravity-flow deposits at Stop 11 (figs. 22 and 23a, 23b).

The slope beds exposed at Stop 11 dip at 25° to 30°. The beds are lithoclastic, skeletal-peloidal wackestone

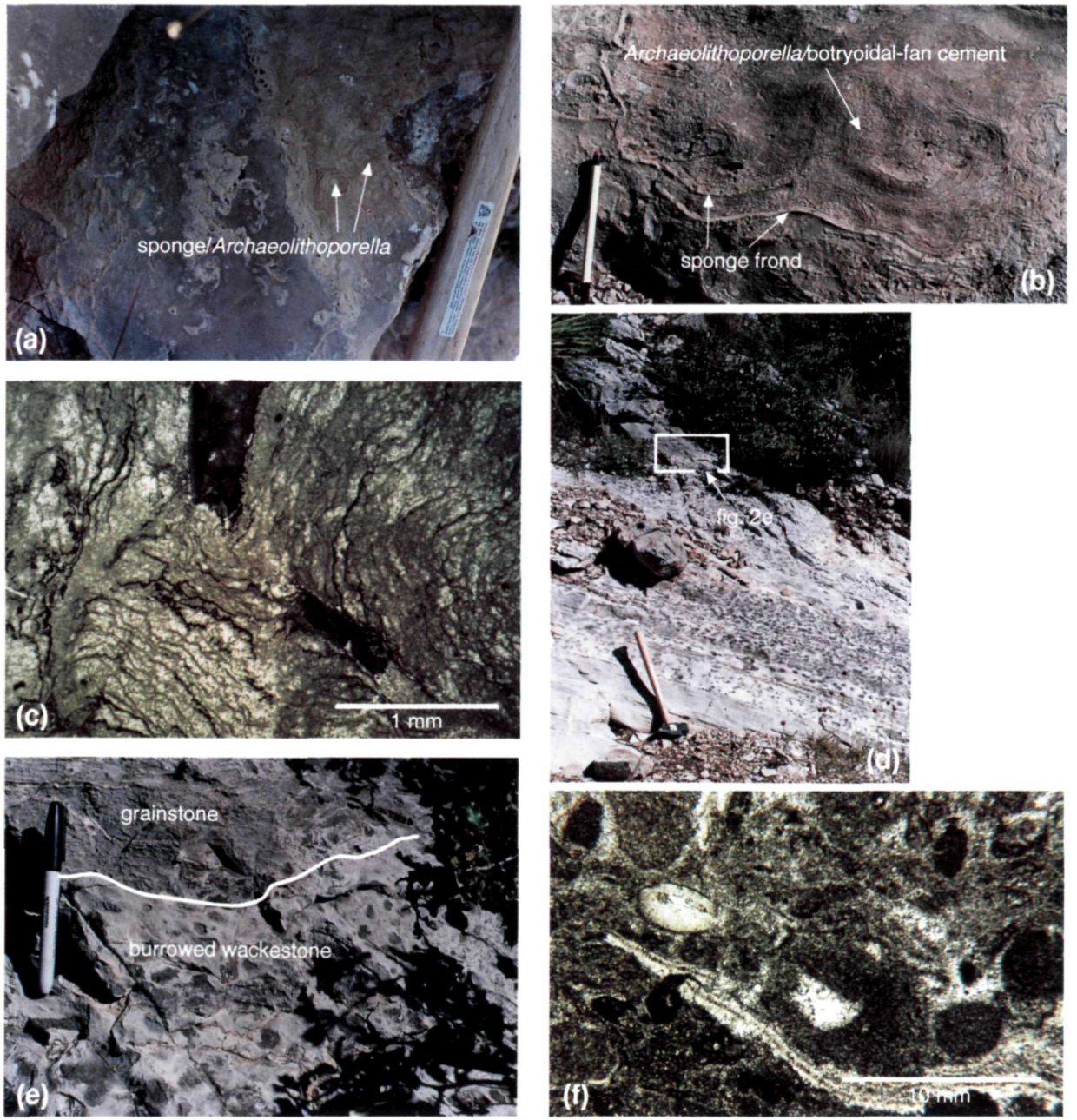

FIGURE 21. Stop 9, trail and thin-section photographs: (a) sponges encrusted with *Archaeolithoporella* standing out in relief against the undolomitized skeletal-peloidal wackestone-packstone matrix; hammer handle on right side of photo for scale, (b) reef block with large sponge fronds and *Archaeolithoporella* and botryoidal-fan cement, (c) thin section of *Archaeolithoporella* showing the characteristic irregular, concentric laminations. Stop 10, trail and thin-section photographs: (d) toe-of-slope burrowed wackestone, with 20° dip, preserved between debris flows of the slope, (e) interpreted erosional contact between the wackestone and grainstone, (f) thin section of the burrowed wackestone showing abundant peloids.

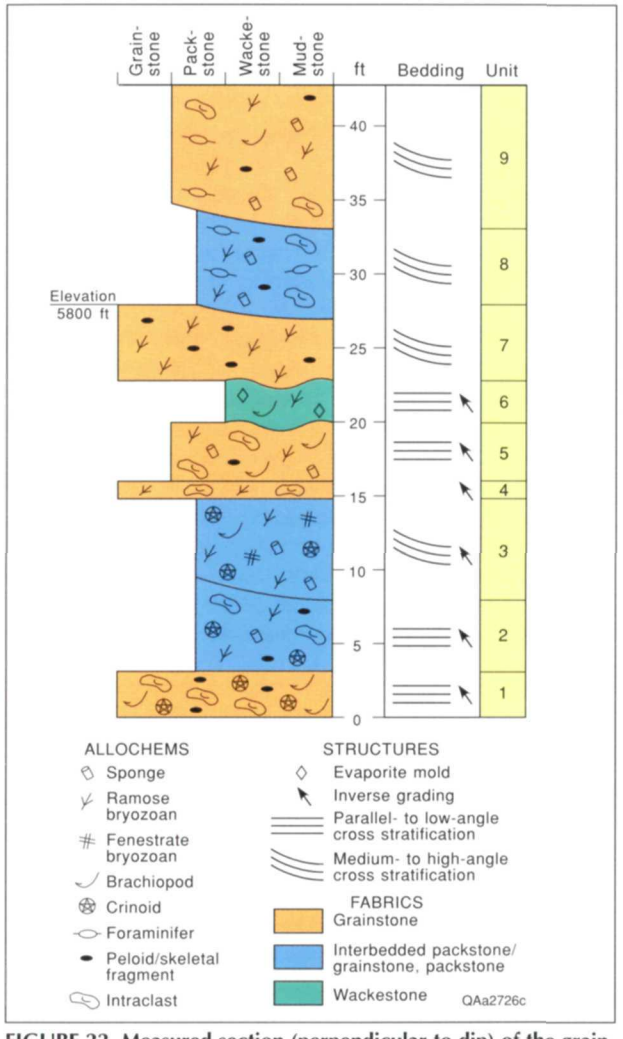

FIGURE 22. Measured section (perpendicular to dip) of the grain-dominated gravity-flow deposits at Stop 11.

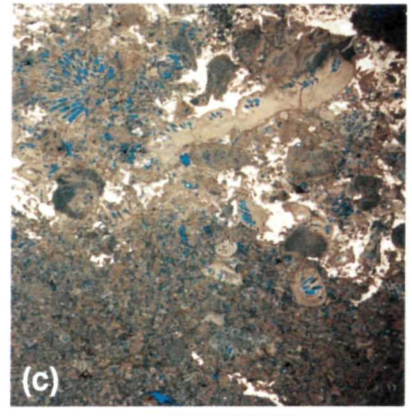

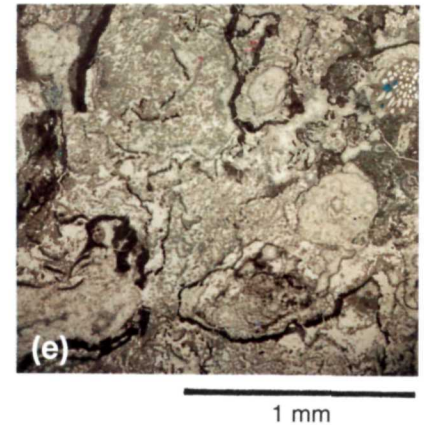

FIGURE 23. Stop 11, trail photographs of the grain-dominated gravity-flow deposits: (a) units 1–3, (b) units 4–9, (c) thin-section photograph of fine-grained skeletal-peloidal grainstone at base to coarse-grained bryozoan-skeletal grainstone at top. Stop 12, trail photographs and thin-section photographs: (d) sponge-bryozoan-*Archaeolithoporella* boundstone over dark-gray, fine-grained skeletal-peloidal wackestone, (e) thin section of sponge-bryozoan-*Archaeolithoporella* boundstone, (f) bryozoan wackestone with lens of packstone.

to grainstone. Contacts between the major units are irregular to scoured. The upper beds are cross stratified, and most beds show inverse grading and internal scour. Fossils include fragments of bryozoans, brachiopods, foraminifers, *Tubiphytes*, and sponges (fig. 23c). Plates and columnals of robust crinoids are characteristic of the skeletal grains in the older units 1–3. Intraclasts are common throughout and consist of light-colored shelf packstone and dark-colored slope wackestone and packstone.

The gravity-flow units at Stop 11 (fig. 23) are interpreted to represent deposits of predominantly high-density turbidity currents. Internal scour and inverse grading provide evidence of traction sedimentation and traction carpet sedimentation, respectively. Large-scale crossbedding in units 8 and 9 (fig. 23b) may represent small dune forms that were deposited from the bed load of very thick, high-density turbidity currents. Exposures at Stop 11 may record deposition from the proximal end of cohesive debris flows that were deposited on the less steeply dipping lower slope.

The stratigraphic position of the gravity-flow deposits at Stop 11 relative to other units can be determined by correlating these beds to basin and reef facies on the photomosaic (fig. 20). Gravity-flow deposits exposed at Stop 11 can be traced down slope to where they thin into the lower part of the Lamar. The slope beds have been traced updip to the steeply dipping beds that overlie the massive Yates-equivalent reef exposed at switchback D. These correlations indicate that the gravity-flow deposits at Stop 11 were derived from Tansill-equivalent reef beds and were deposited at the same time as the lower part of the Lamar.

The grain-dominated, gravity-flow deposits suggest that reef growth was active and abundant carbonate sediment was being transported into the basin while the Lamar interval was accumulating. The steeply dipping beds of the upper part of the slope exposed at switchback D (fig. 20) suggest that sediment was shed from a largely aggradational reef. Gravity-flow deposits on the slope may reflect periods when the slope became oversteepened and unstable from high rates of carbonate production on the reef. These observations on the slope beds are consistent with the conclusions of Babcock and Yurewicz (1989) and Garber and others (1989) that the crest of the shelf-margin buildup gradually shoaled during the depositional history of the Yates- and Tansill-equivalent reefs.

STOP 12. Slope Mud-Rich Carbonate

Stop 12 displays reef blocks and mud-rich, fine-grained deposits of the upper part of the slope that are poorly bedded relative to the very thick bedded, gravity-flow deposits examined at Stops 9–11. A block of reefal boundstone is well exposed just before the 5,900-ft marker (fig. 23d and 23e). Note that the 5,900-ft marker is located ~1.5 m (~5 ft) above the trail. The outcrop consists of boulders of massive, sponge-bryozoan-*Archaeolithoporella* boundstone and fine-grained, skeletal-peloidal wackestone to packstone (fig. 23d). Reef blocks exposed here have a higher density and diversity of frame-building sponges than the reef blocks examined in the younger debris-flow deposits at Stop 9. The amount of *Archaeolithoporella* and botryoidal fibrous cement is also

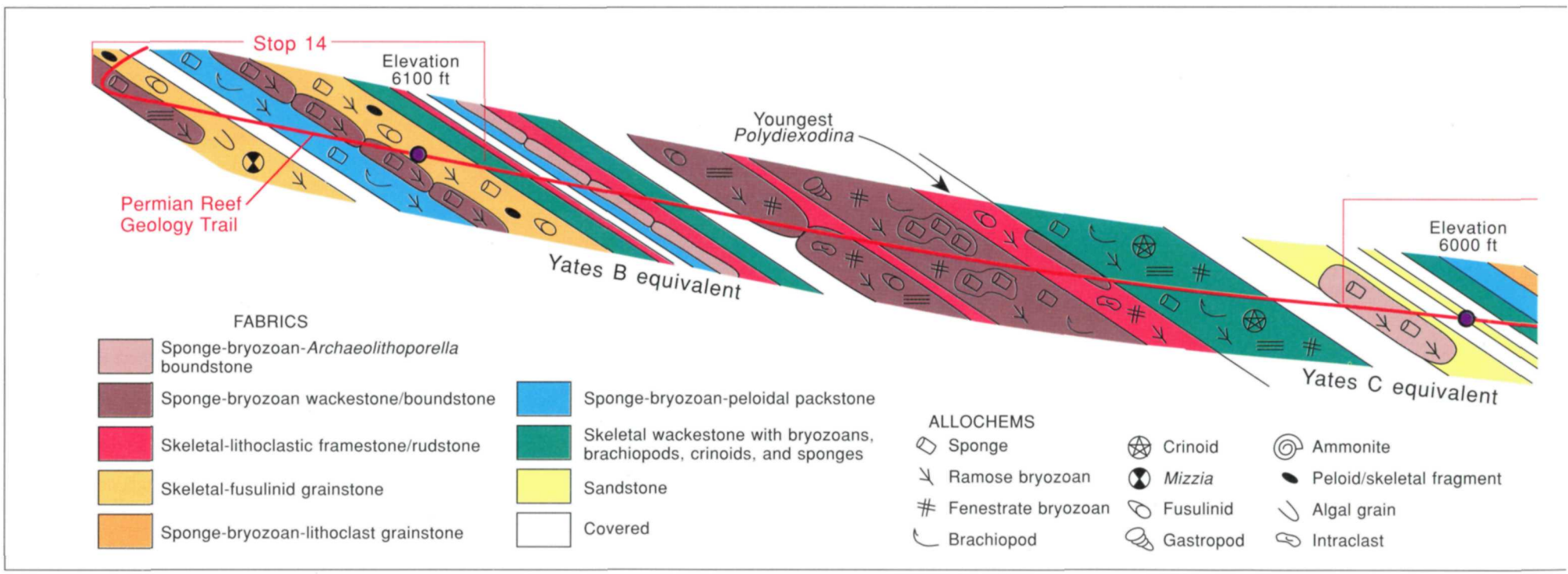

proportionately reduced. Reef blocks at Stop 12 and on the upper part of the slope crop out as matrix-encased piles of boulders and as isolated blocks encased in mud-rich, upper-slope beds. This distribution suggests that the reef blocks accumulated as rock fall and may have locally formed talus cones.

The best exposures of the mud-rich upper part of the slope beds are located ~9 m (~30 ft) up the trail from the 5,900-ft marker and past a prominent gully at the point where the trail bends slightly to the left. The mud-rich carbonate is thin- to very thick-bedded, with dips between 15° and 20°. The bedding in outcrops exposed above the trail appears to be deformed or slumped. Massive, fine-grained peloidal wackestone and packstone dominate the section, but small lenses of grainstone and lithoclast wackestone and packstone are present (fig. 23f).

The mud-rich carbonate contains a diverse, deep-neritic fauna of ramose and fenestrate bryozoans, sponges, brachiopods, and crinoids. Cephalopods are also abundant. Some of the well-preserved fossils appear to be indigenous, especially the articulated brachiopods and large fenestrate bryozoans. The poorly developed bedding suggests that the sponges and bryozoans were transported as individual grains to form debris cones, rather than as components of debris flows or turbidity currents. An alternative explanation for the origin of the massive, fossiliferous limestone on this portion of the slope is deposition from submarine slumping. The steep slopes, fine-grained sediment, and lack of binding or cementation favor this interpretation. Evidence of synsedimentary internal deformation is inconclusive.

Mud-rich, fossiliferous limestone exposed in the gully area at the up-trail end of Stop 12 coarsens downward into thin-bedded, coarse-grained, sponge-bryozoan lithoclastic grainstone. Lithoclastic grainstone is best examined farther up the trail, where the trail turns back to the right and exposes an outcrop less oblique to bedding. The grainstone is dolomitized and much lighter in color than the dark-brown massive limestone. The base of the grainstone is sharp, irregular, and probably erosional. The skeletal and lithoclast grainstone beds are interpreted as high-density turbidity current deposits. Similar thin, dolomitized gravity-flow deposits punctuate the massive mud-rich limestones throughout the slope section.

STOP 13. Slope Mixed Siliciclastics and Carbonates

Stop 13 includes two siliciclastic sandstone beds and intervening carbonates that were deposited on the upper part of the slope (fig. 24). This stop begins where the trail steepens at the first extensively weathered, yellow siliciclastic interval (younger). The contact of the siliciclastics with the overlying carbonate examined at Stop 12 crops out on the floor of the trail (fig. 25a). The intervening carbonate beds are present farther up the trail and are well exposed at the light-tan grainstone outcrop just beyond the trees that cover the trail. The second siliciclastic interval (older) crops out at the 6,000-ft marker.

The first sandstone bed is a recessively weathered, ~6-m-thick (~20-ft) bed that is concordant with other slope beds. All units within the siliciclastic interval have dips between 25° and 32°, and there is no apparent angular discordance between any of the units. The siliciclastic beds are discontinuous and cannot be traced

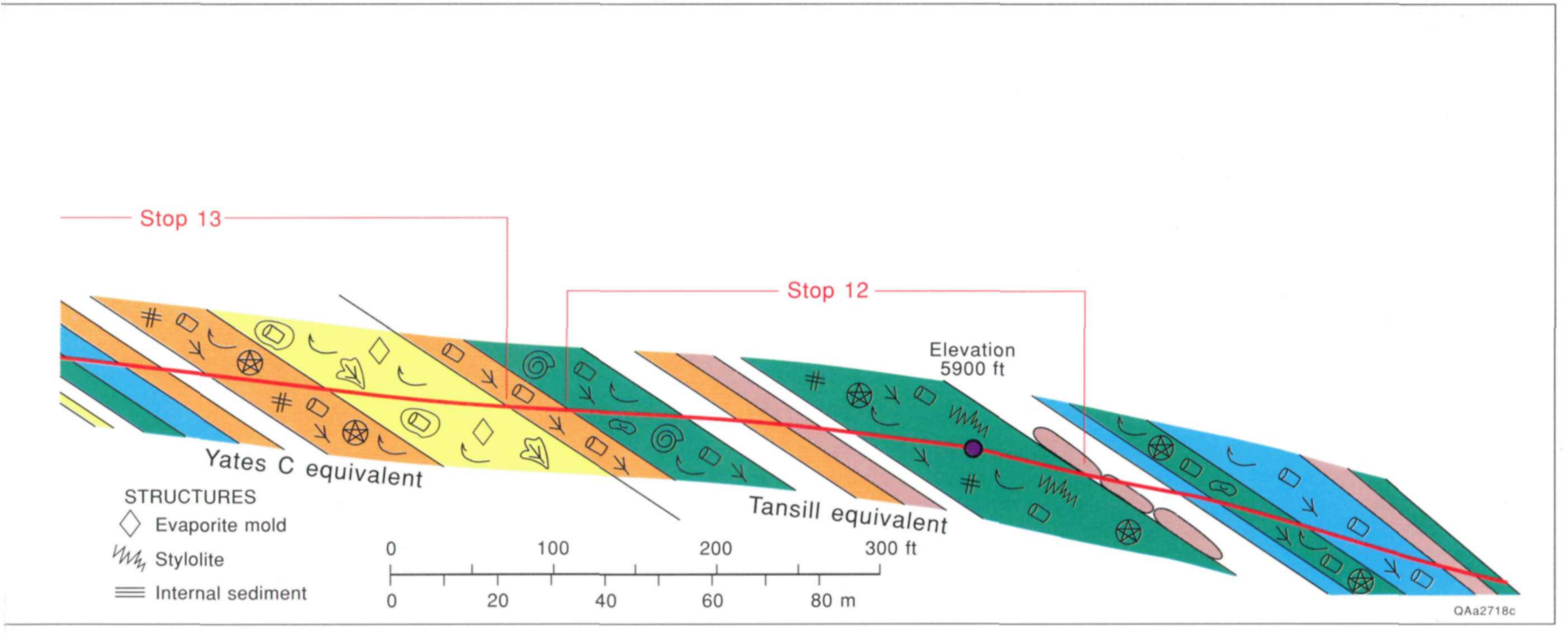

Figure 24. Diagrammatic sketch of the slope beds of Stops 12–14 showing carbonate textures and fabrics encountered along this part of the trail and location of stops relative to elevation markers and geographic features. The section was measured along the trail perpendicular to slope dip; areas marked as cover are not to scale.

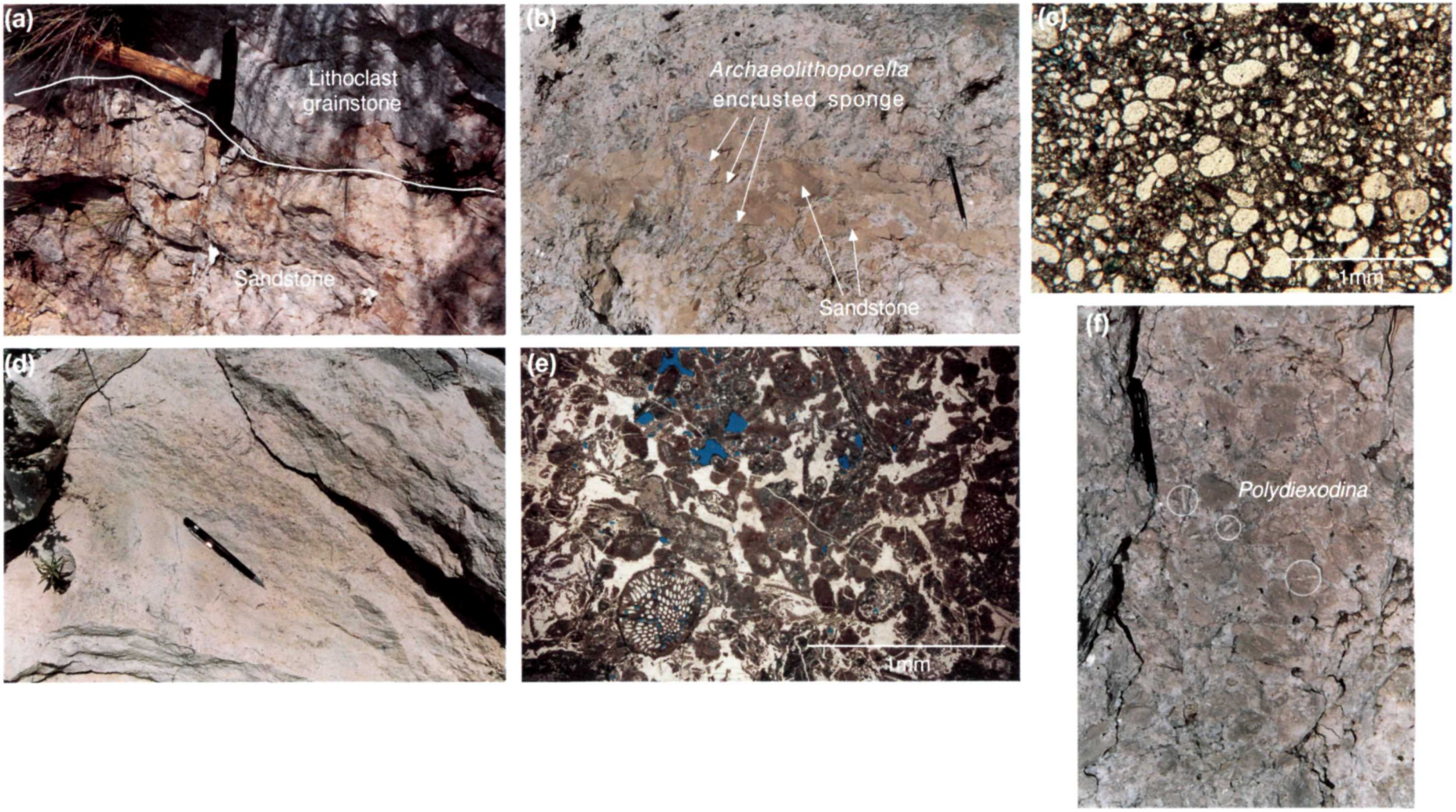

FIGURE 25. Stop 13, trail and thin-section photographs: (a) irregular contact between sandstone and overlying lithoclastic grainstone, (b) sandstone filling in apparent growth-framework voids in *Archaeolithoporella*-encrusted sponge colony, (c) thin-section photomicrograph of very fine- to fine-grained, well-rounded sandstone with a dolomite matrix and kaolinite-filled molds of dissolved feldspar grains, (d) dolomitized thin-bedded, fine- to coarse-grained skeletal packstone and grainstone, (e) thin-section photomicrograph of dolomitized skeletal grainstone with skeletal grains cemented by isopachous fibrous cement, a thin rind of dolomite, and late poikilolitic calcite, (f) skeletal-lithoclast rudstone with clasts of fine-grained skeletal wackestone and the youngest occurrence on the slope of the fusulinid *Polydiexodina*, cemented by late-stage calcite.

in outcrop into the basin or onto the shelf. Sedimentary structures within the sandstone are not apparent in outcrop. The second siliciclastic unit was deposited around boulders of sponge-*Archaeolithoporella* boundstone and has limited exposure along the trail.

The siliciclastic beds are composed of very fine grained to fine-grained, well-rounded quartz grains in a dolomite matrix (fig. 25b). Rounded molds containing authigenic kaolinite are interpreted to be dissolved feldspars (fig. 25c). Calcite pseudomorphs after gypsum crystals are also randomly distributed throughout the sandstone. The sandstone contains a reef fauna of *Tubiphytes, Archaeolithoporella,* sponges, and bryozoans, some apparently in growth position. Where the skeletal grains are preserved, they are dolomitized and have a white, chalky appearance. Molds of dissolved fossils are filled with calcite.

The dolostones between the siliciclastic beds are thin-bedded, fine- and coarse-grained, skeletal packstone and grainstone that were probably deposited on the steep upper part of the slope by high-density turbidity currents and grainflows, respectively (fig. 25d and 25e). The skeletal grains include sponges, ramose bryozoans, crinoid plates and columnals, brachiopods, foraminifers, phylloid and dasycladacean algal fragments, and peloids. The skeletal grains have been micritized and cemented by a thin isopachous fibrous cement, a thin rind of dolomite rhombs, and late poikilotopic calcite. The late calcite is interpreted to have replaced earlier evaporites (Scholle and Melim, 1988). The light-tan dolostone grades laterally into undolomitized, dark-tan packstone and wackestone.

The sandstone and carbonate outcrops at Stop 13 illustrate selective dolomitization of permeable, siliciclastic and grain-rich carbonate beds on the slope. The primary stage of dolomitization in the slope is interpreted to have formed during early burial by seepage reflux of penecontemporaneous, back-reef lagoonal brines (Melim, 1991). Isotopic composition of the dolomites indicates that the brines were mesosaline; that is, concentrations are greater than seawater but less than gypsum saturation (Melim, 1991). The mesosaline brines initially descended via joints and fractures driven by the density contrast between brine and seawater. The mesosaline brines migrated from the joints along the most permeable pathways into slope deposits, commonly the grainstone and siliciclastic beds. Selective dolomitization of debris-flow deposits adjacent to siliciclastic beds in the lower portion of the slope (Stop 9) demonstrates the basinward extent of permeability-controlled, density-driven dolomitization. Gypsum molds preserved in the sandstone (Stop 13), high density-turbidity current deposits (Stop 11, unit 6), and debris-flow deposits (Stop 9, switchback B) suggest that the early mesosaline brines may have been followed by a later stage of more concentrated, hypersaline brines. Other examples of interpreted joint- and permeability-controlled dolomitization are visible in the beds that intersect the upper portion of the trail above Stop 13, grainstones exposed at switchback D, and shelf beds exposed at Stop 23.

The slope sandstone and carbonate sequence at Stop 13 overlies carbonate beds that contain the youngest occurrence of *Polydiexodina* on the trail (fig. 25f). *Polydiexodina* ranges upward to near the top of the Yates B interval on the shelf and to the McCombs Limestone Member of the Bell Canyon Formation in the basin (Newell and others, 1953). The sandstones at Stop 13 are stratigraphically higher than the *Polydiexodina,* so they are interpreted to correlate to the Yates C member on the shelf and the sandstone that rests between the McCombs and Lamar Limestone Members of the Bell Canyon Formation in the basin. According to biostratigraphy and slope-to-basin correlations, the siliciclastic beds at Stop 13 mark the top of the Yates Formation on the slope. The shelf siliciclastic beds that correlate to slope siliciclastics are exposed at Stop 26.

Outcrops between the sandstones at Stop 13 and the 6,100-ft marker at Stop 14 are thin- to medium-bedded skeletal wackestones and packstones surrounding sponge-*Archaeolithoporella* boundstone reef blocks in beds that dip at 27°. These slope beds with reef blocks are generally similar to those discussed at Stop 12.

STOP 14. Fusulinid-Rich, Shelf-Margin Talus

Stop 14 is located between the 6,100-ft marker and switchback C and includes the very distinctive, steeply dipping (27° to 66°) *Polydiexodina* beds that were deposited in the area of shelf-margin talus exposed at the 6,100-ft marker (figs. 20 and 26a and 26b).

The exposure of the youngest occurrence of *Polydiexodina* consists of poorly sorted, skeletal-lithoclastic rudstone. Skeletal grains include the pinnate bryozoan *Acanthocladia* and fenestrate bryozoans, in addition to *Polydiexodina.* Lithoclasts are fine-grained skeletal wackestone and are subangular. These clasts were apparently derived from underlying slope wackestones and packstones. Examination of lithoclastic beds beneath the reef blocks shows apparent in situ brecciation of the slope sediments. The lithoclasts and rudstone texture may have developed during dislocation and movement of reef-derived boulders as submarine slides on the slope.

The trail cuts through ~9 to 12 m (~30 to 40 ft) (measured perpendicular to bedding) of skeletal-fusulinid packstone and grainstone (fig. 26b and 26c) at Stop 14. Dips of the fusulinid beds are highly variable and range from 27° to 66°. This wide range of dips is a result of deposition between and over allochthonous blocks of reef facies. Fusulinids in the beds with steepest dip have variable orientations and occur in lenses. Where fusulinid beds have dips closer to the observed depositional slope dips of 27° to 32°, the beds are inversely graded, with long axes of the fusulinids parallel to dip. These beds are inversely graded from peloidal-skeletal packstone to very coarse-grained, fusulinid-algal grainstone. The skeletal component includes segments of the dasycladacean alga *Mizzia,* fusulinids, crinoid plates and columnals, platy algae, and bryozoans. The inversely graded beds are best exposed directly beneath the 6,100-ft marker.

The proximity of Stop 14 to the reef (fig. 20) places it in the zone of shelf-margin talus. This is an area that on modern reefs is typically characterized by an apron of reef blocks encased in skeletons of perireefal sediments, reef-building organisms, carbonate sand grains, and lime mud (Land and Moore, 1977; James and Ginsburg, 1979). Reef blocks observed at Stop 14 were probably deposited by rock fall off the Yates-equivalent reef. The steep dips and inverse grading of the surrounding fusulinid grainstones suggest that the fusulinids were deposited as grain flows. The concentrated occurrence and channelized appearance of the fusulinids and associated skeletal grains at this location may indicate that they have been funneled through a pass or channel in the reef.

Fusulinids are benthic foraminifers that lived on shallow-water shelves and shelf margins in water depths of 14 to 18 m (45 to 60 ft) (Ross, 1983). The abundance, robust size, and excellent preservation of fusulinids on the slope suggest that they thrived on the shelf and were transported downslope. The accumulation here

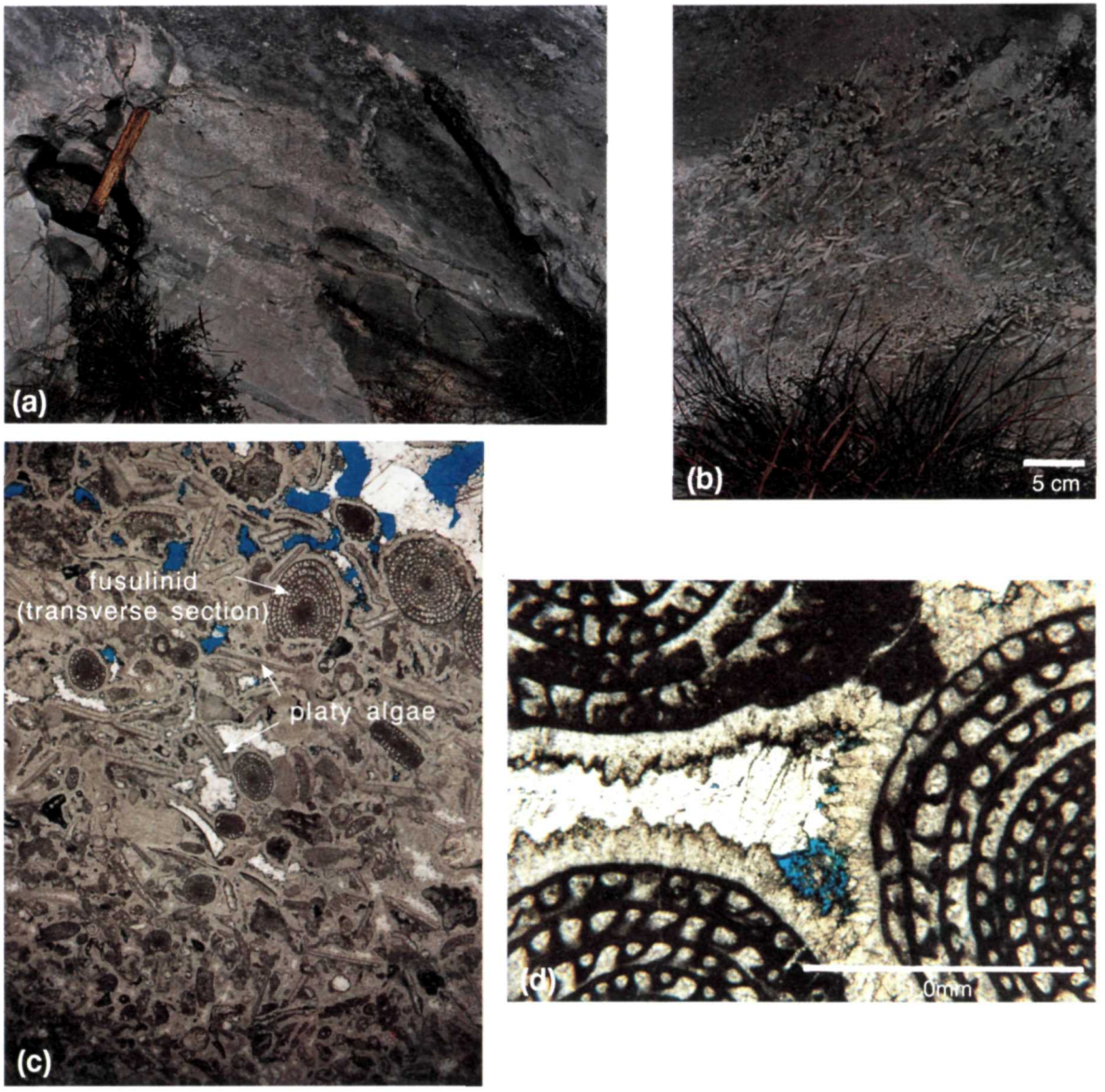

FIGURE 26. Stop 14, trail and thin-section photographs: (a) inversely graded skeletal-fusulinid packstone to grainstone with the long axes of the fusulinids aligned parallel to dip of 27° to 32°, (b) plan view of steeply dipping fusulinid grainstone, fusulinids are ~2 cm long (~0.8 inch), (c) thin-section photomicrograph of inversely graded peloidal-skeletal grainstone to fusulinid-algal grainstone, the dolomitized skeletal grains (fusulinids, platy algae) are coated with isopachous fibrous cement, a thin rind of dolomite, and coarse calcite, (d) thin-section photomicrograph of fusulinid grainstone showing the isopachous fibrous cement around fusulinid grains and equant calcite cement filling most of the remaining interparticle space.

of numerous fusulinids of the same size, shape, and specific gravity was probably controlled by local hydrodynamic conditions.

Summary

The perspective of the slope beds from the 6,200-ft marker near the top-of-slope portion of the trail offers an excellent opportunity to summarize the lithologies, slope depositional processes, and stratigraphic relationships of Stops 9–14.

The first four slope stops (Stops 9–12) are Tansill-equivalent (1) lithoclast megabreccia interpreted to be lower slope cohesive debris-flow deposits, (2) burrowed wackestone toe-of-slope deposits equivalent to the Lamar Limestone Member, (3) lithoclastic-skeletal wackestone-grainstone interpreted to be high-density turbidity-current deposits, and (4) slumped reef blocks and fine-grained peloidal wackestone-packstone of the upper part of the slope. These carbonate facies represent periods of active growth at the shelf margin and transportation of carbonate into the basin. Several intervals of high-volume sediment transport are identified in the Tansill-equivalent, slope beds (fig. 20). Grain-dominated, high-density turbidity current deposits are characteristic of the upper and middle portions of the slope, where the slope dips are 20° to 35°, and mud- and boulder-dominated cohesive debris-flow deposits are typical of the 10° to 20° dip of the lower part of the lower slope.

The last two stops are in Yates-equivalent slope beds. Dolomitic, fine-grained siliciclastics, sponge boundstone, and dolomitized grainstones are exposed at Stop 13 and are equivalent to the youngest Yates "C" member of Newell and others (1953) (fig. 4) or the Yates-Tansill sequence of figure 35 and are interpreted to represent a major sea-level lowstand. Lowstand beds can be correlated biostratigraphically with equivalent shelf and basin strata. Steeply dipping, skeletal-fusulinid packstone-grainstone and shelf-margin talus are exposed at Stop 14. The thick accumulation of fusulinids and variable dips may indicate the presence of a pass or channel in the Yates-equivalent reef.

Reef: Brenda L. Kirkland, Susan A. Longacre, and Emily L. Stoudt

The next portion of the Permian Reef Geology Trail cuts through ~152 m (~500 ft) of reef facies—the massive Capitan Formation (Richardson, 1904; King, 1942, 1948). At an elevation of ~1,905 m (~6,250 ft) (figs. 2, 7, and 20), the in-place reef facies interfingers with forereef debris. The reef facies extends up to ~2,060 m (~6,750 ft) where reef boundstones are interbedded with outer-shelf grainstones. The presence of the fusulinid *Polydiexodina* along part of the trail and stratigraphic correlations up-canyon indicate that the Capitan Formation along the trail is equivalent to the middle and upper Yates Formation (Yates B and C of Newell and others, 1953) (fig. 4). This part of the reef is older and stratigraphically below the Tansill-equivalent reef facies frequently visited in Walnut and Dark Canyons located 43 km (27 mi) and 55 km (34 mi), respectively, to the northeast.

Before considering features present in the reef facies of the Capitan Formation, it is helpful to review some fundamental aspects of reefs. A modern reef community consists of a diverse array of organisms, many with calcareous skeletons, living from sea level down to a depth of ~91 m (~300 ft) (James, 1983). Essential components of a modern reef can be categorized into four groups. First is the community of frame-building and binding organisms that form the structure of the reef. Second is marine cement, which, along with binding organisms, lithifies the reef. Third is the group of bio-eroders that, by their activities, break down the reef and create the fourth component, internal sediment. Along with marine cement, internal sediment can fill any available space within the reef structure (Ginsburg and Lowenstam, 1958; Moore, 1989; Tucker and Wright, 1990). Evidence of most of these components is displayed in the stops along this part of the trail.

In contrast with the transported blocks of Tansill-equivalent reef that occur on the slope, reefal boundstones along this part of the trail are preserved in place. Compared with the Tansill-equivalent reef exposed at the mouth of Walnut Canyon and in the slope blocks at McKittrick Canyon, the Yates-equivalent reef along the Permian Reef Geology Trail exhibits a greater diversity of sponges, less *Archaeolithoporella*, and fewer and smaller fans of botryoidal cement. Also in contrast to the slope section is the apparent lack of both disseminated quartz silt and interbedded siltstones through the segment of the reef exposed by the trail.

Debate about depth of water above the living Permian reef continues. As noted in the introduction, the depositional profile for Capitan sediments varied vertically and laterally through time. Yurewicz (1977), Babcock (1977), and Toomey and Babcock (1983) suggested that the Capitan reef accumulated in progressively shallower water from the time of deposition of the Seven Rivers Formation to that of the Tansill Formation. Babcock (1977) interpreted the presence of *Collenella*, abundance of algal and other shallow-water elements, and biotic diversification in the youngest, shelfward facies of the reef in Walnut and Dark Canyons as indicative of shallower water depths. *Collenella* is present in the uppermost outcrops of the Yates-equivalent Capitan in McKittrick Canyon (Stop 22), suggesting a similar shallowing of the Yates-equivalent reef. The abundance of framework and binding components suggests that the reef could resist waves, but water depth above the reef cannot be estimated from the reef unit alone.

As discussed in the next section of the trail guide, the geometry of the outer-shelf beds suggests "fall-in" toward the equivalent reef (figs. 5a, c and 43). The fall-in bed geometry suggests that the reef was deposited downdip from the highest part of the shelf profile, in water depths from 30 to 43 m (100 to 140 ft) during Seven Rivers deposition (Yurewicz, 1977; Hurley, 1978) and in depths as shallow as 9 to 15 m (30 to 50 ft) during deposition of the Yates-B-equivalent reef (Kerans and Harris, this volume, p. 32). Different conclusions were reached in a sedimentologic study of the upper Capitan and Tansill Formations by Kirkland-George (1992), who proposed that the Tansill-equivalent reef grew to sea level and protected a shallow-water lagoon on the outer shelf (fig. 5d).

Key features within the reef portion of the trail include organisms, cements, and internal sediments. The Guadalupian-aged fauna of the massive Capitan is diverse, but it is dominated by a variety of calcareous sponges and bryozoans, rather than corals as in modern reefs. Volumetrically the most important binding element of the reef is the rhodophyte *Archaeolithoporella*, which occurs along with prodigious amounts of marine botryoidal-fan cement (fig. 27a). Other marine cements include isopachous rims of calcite that are visible without a hand lens (Stop 21). Macroscopic examples of layered internal sediment filling both framework voids and possible neptunian dikes are abundant along the trail (Stop 19).

Diagenetic events recorded in the Capitan reef will be discussed in greater detail at Stop 21, but note that typical cements that are present along the trail are dominantly (1) marine botryoidal fans, (2) marine isopachous fibrous crusts, and (3) several generations of calcspar.

STOP 15. Interbedded Basal Reef and Slope Deposits

Stop 15 includes a series of locations beginning at ~1,905 m (~6,250 ft), at the first rock exposure beyond the grassy, scree-covered slope below the steep walls of the massive reef. This stop extends for 142 m (465 ft) along the trail to just around switchback D (figs. 2 and 20) in the saddle east of the massive reef outcrop. A large cephalopod and a mass of *Tubiphytes* (a tiny, porcellaneous, problematic organism that weathers whitish on outcrop) are displayed in the first major exposure along this part of the trail. Twenty-seven meters (90 ft) farther up the trail is a reddish-weathering recess (fig. 27a) that shows the typical reef boundstone of sponges and bryozoans encrusted with *Archaeolithoporella*, botryoidal-fan cements, and *Tubiphytes*. Laminated internal sediment also occurs in reef cavities. A variety of ramose and fenestellid bryozoans, including *Acanthocladia*, are exposed

in the floor and north side of the trail just below switchback D (figs. 20 and 27b). Several cephalopods (fig. 27c) are present in the trail ~3 m (~9 ft) beyond the 6,300-ft marker just above switchback D.

Interbedded with the reefal boundstone immediately below switchback D are steeply dipping, Yates-C-equivalent skeletal grainstones and packstones deposited in the transitional reef/slope environment. The bedded packstones and grainstones exposed at switchback D on the east side of the saddle are Tansill-equivalent slope deposits.

STOP 16. Well-Exposed Sponge-*Archaeolithoporella* Boundstone

Stop 16, which straddles the trail ~64 m (~210 ft) beyond switchback D (fig. 27d), is another excellent exposure of typical Yates-equivalent Capitan reef framework. The three common elements of the Capitan reef—organisms, marine cement, and laminated internal sediment—are all well displayed in this exposure. The more common sponges occurring throughout the reef are illustrated in figure 28. Based on a census of the sponges along the trail, the most common sponge is an elongate form with geometrically regular pores that represents *Lemonia cylindrica* (formerly *Guadalupia cylindrica*); both small and large forms of this sponge are found in almost all localities. Other sponges mixed with this form are *Guadalupia, Amblysiphonella, Cystauletes, Girtycoelia,* and *Cystothalamia.* Almost all reef outcrops also contain several growth forms of delicate to robust ramose

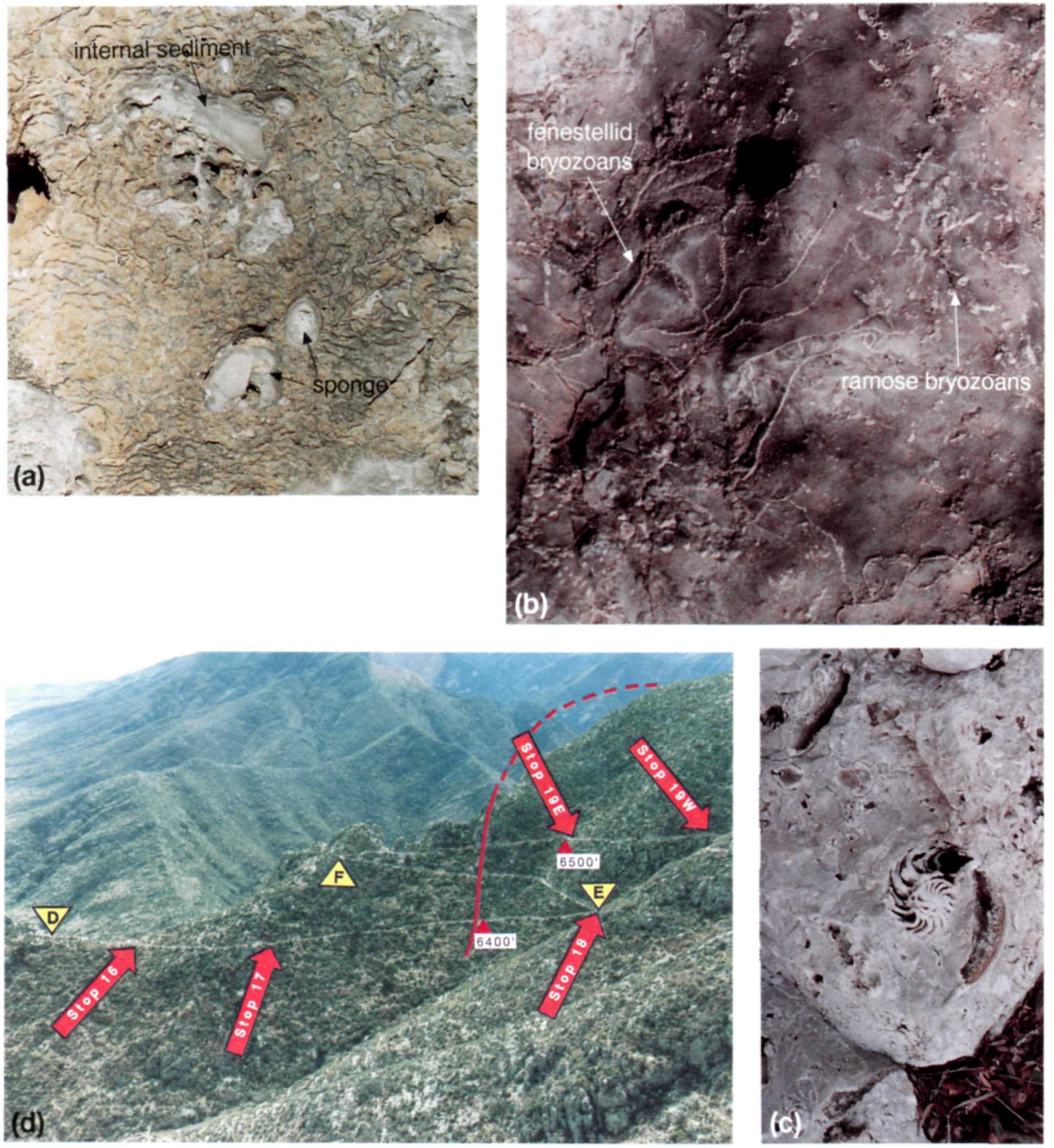

FIGURE 27. Stop 15, basal reef: (a) typical reef boundstone with interlaminated *Archaeolithoporella* (dark-gray thin lines) and rust-colored botryoidal-fan cement encrusting sponges; some voids filled with internal sediment (1/4 actual size), (b) bryozoans in floor of trail (1/2 actual size), (c) cephalopod in wall of trail (1/4 actual size), (d) view looking south of reef trail showing locations of switchbacks D through F, Stops 16–19, and an approximate time line through the reef derived from plotting the youngest occurrence of the fusulinid *Polydiexodina*. In the reef exposures along the trail, this fusulinid has been found only west (right) of this red line.

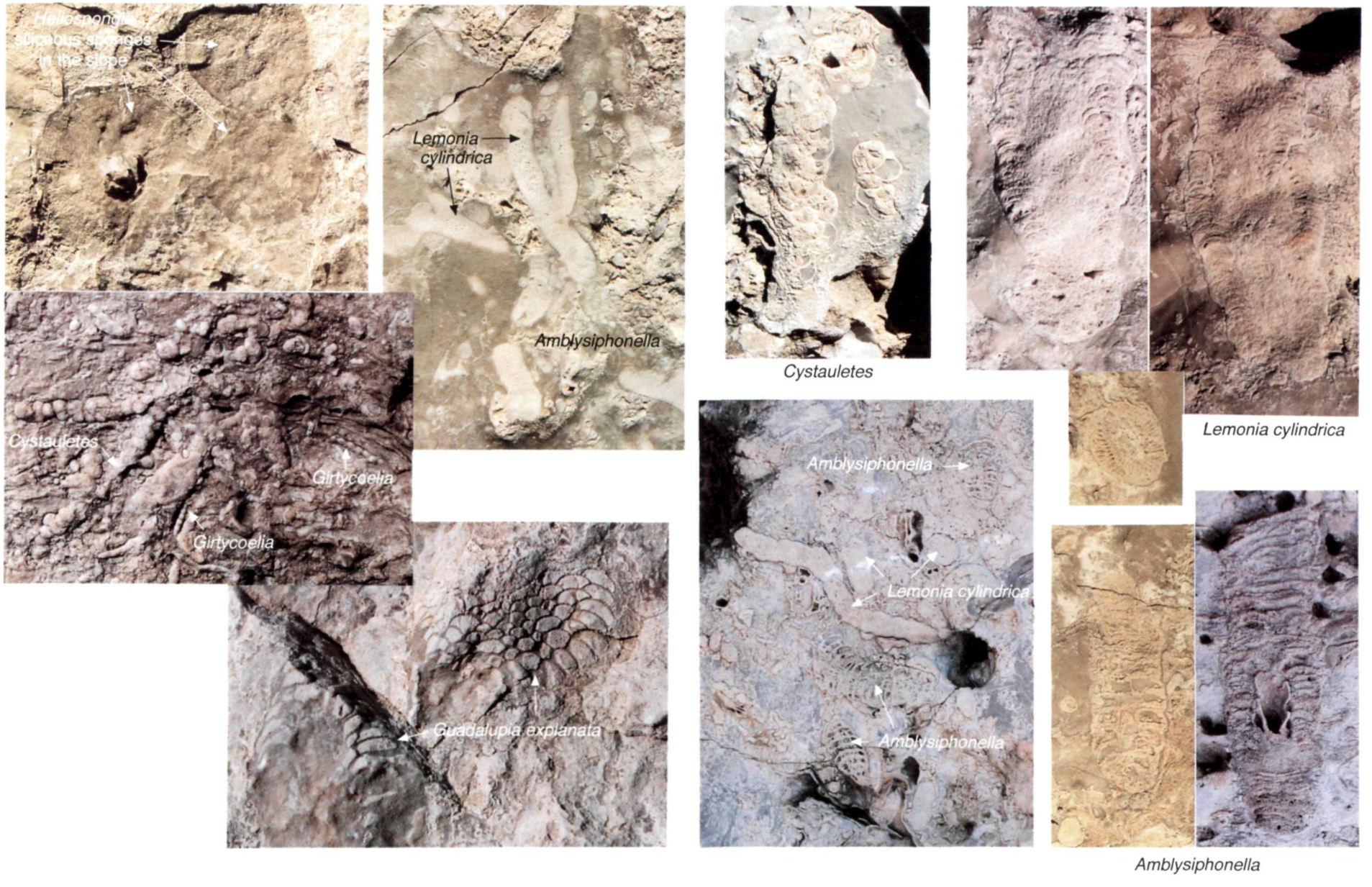

FIGURE 28. Stop 16, sponges of the Capitan reef. Photographs are almost 1/2 actual size.

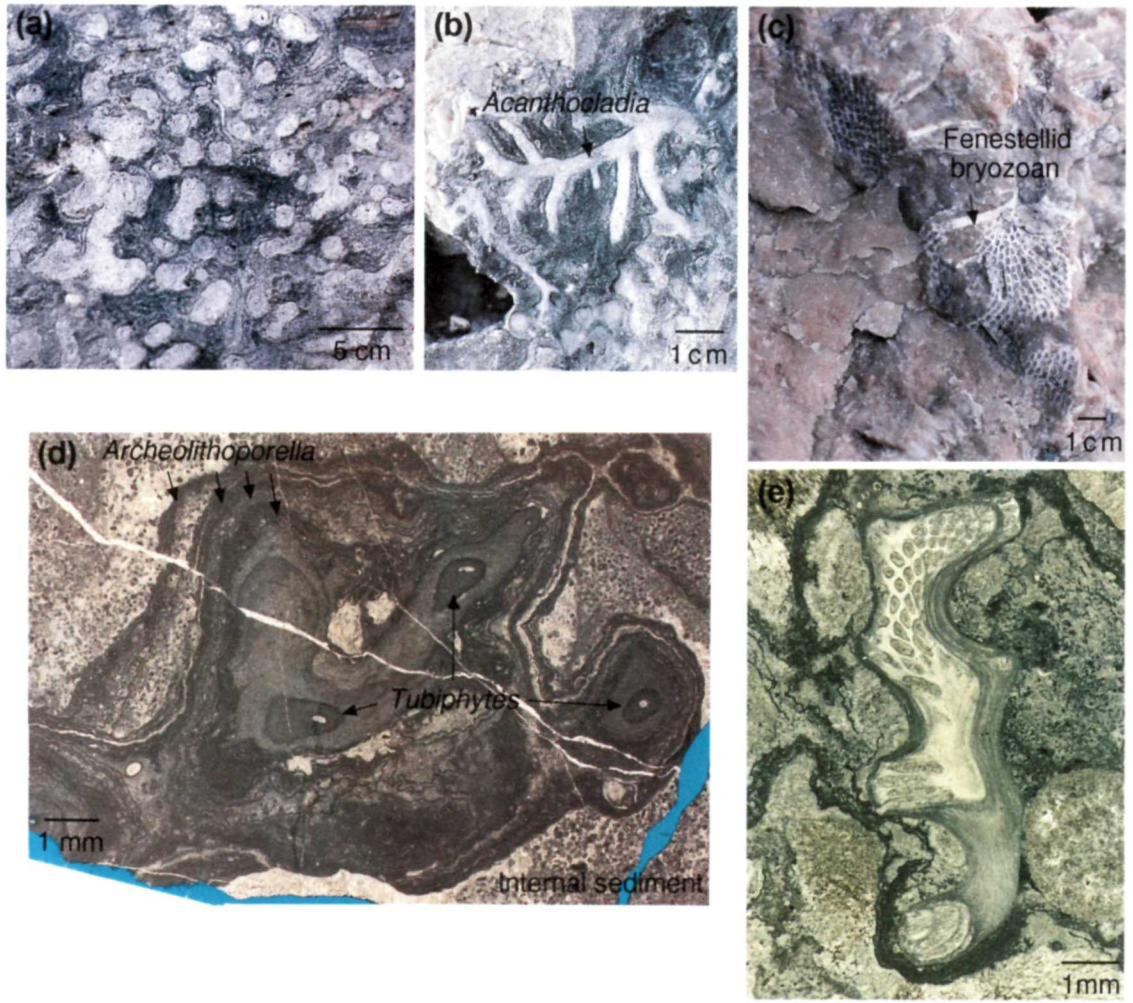

FIGURE 29. Stop 17, *Tubiphytes* and *Acanthocladia* in reef: (a) *Tubiphytes* colony (1/6 actual size), (b) branching *Acanthocladia* (1/2 actual size), (c) fenestellid bryozoan exposed in trail (1/4 actual size), (d) photomicrograph of *Tubiphytes* colony encrusted by *Archaeolithoporella*, (e) photomicrograph of cross section of *Acanthocladia*.

and fenestellid bryozoans. With the exception of the transition into the shelf sediments (Stop 22), neither spatial nor temporal zonation was detected in the fauna. The lack of zonation can be accounted for by the filter-feeding habits of most of the organisms that compose this Permian reef; in contrast to modern corals, they were not constrained by the occurrence of light-sensitive zooxanthellae.

STOP 17. *Tubiphytes/ Acanthocladia* Boundstone

Stop 17, ~46 m (~150 ft) beyond Stop 16 (figs. 27d and 34), contains a large mass of *Tubiphytes/Acanthocladia* boundstone. The 6,400-ft marker is ~100 m (~300 ft) beyond this exposure; that marker is 46 m (150 ft) from switchback E. At Stop 17, typical *Acanthocladia* fronds are well displayed in a whitish specimen located 0.6 m (2 ft) above and to the left of the trail (fig. 29b and 29e). Although encrusting *Tubiphytes* is common throughout the reef, it is particularly well developed here (fig. 29a) along with fenestellid bryozoans (fig. 29c). Some organisms appear to be preserved in growth position, although others are debris of probably broken specimens. Voids between the branches of the organisms are filled with isopachous, fibrous, radiaxial cement and laminated internal sediment (fig. 29d). Although the best exposure along the trail measures only 2 by 3 m (6.6 by 10 ft), the mass extends for at least 25 m (75 ft) along and above the trail.

STOP 18. Fusulinids within the Reef

Stop 18 is located at switchback E (figs. 27d and 34) where the large, age-diagnostic fusulinid, *Polydiexodina* (fig. 30a), occurs among upright sponges (fig. 30b). *Polydiexodina* is 25 to 38 mm (1 to 1.5 inches) long, easily seen, and characteristic of the Seven Rivers to Yates B (middle Yates) interval in the shelf facies (Newell and others, 1953). Observed occurrences of *Polydiexodina* are on the north side of the line drawn on figure 27d, making this portion of the reef equivalent to the Yates B. Its absence between the line and the base of the Tansill-equivalent

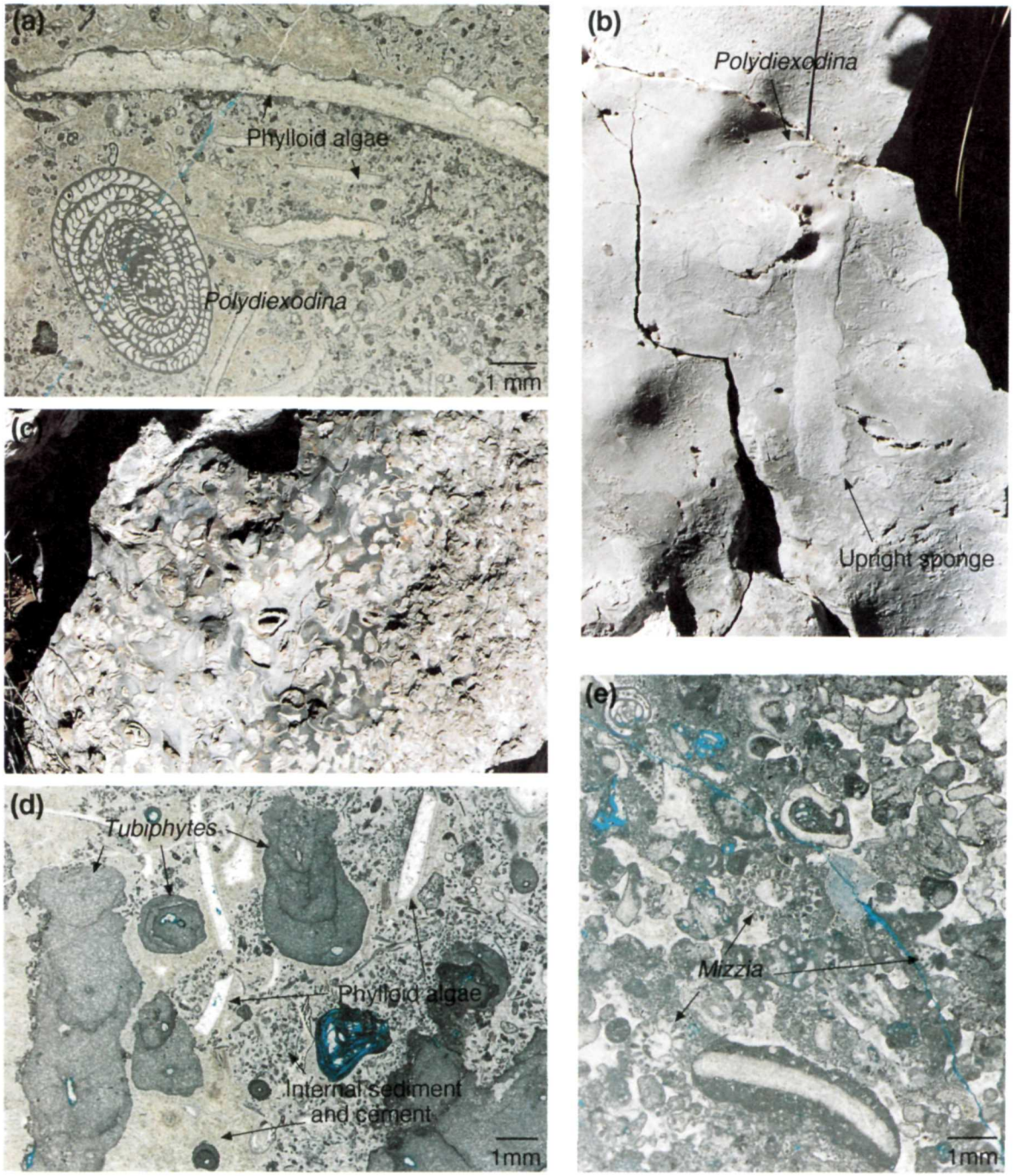

slope deposits (switchback D, fig. 20) suggests that the reef interval along this part of the trail is equivalent to the younger Yates C. Note that the slope of the line, which may approximate a time line, is near vertical, suggesting a rather steep-fronted reef profile.

The trail crosses the Yates B/C boundary twice more before reaching Stop 19, ~126 m (~415 ft) up the trail beyond switchback F (fig. 27d). Along the trail are several pockets filled with yellowish-orange-stained, silt-sized dolomite. As discussed in the slope section of the trail guide, similarly colored layers in the slope are composed of shelf-derived quartz siltstone and very fine grained sandstone. Although similar sandstone layers may occur within the Yates-equivalent reef, they are not obvious along the trail.

STOP 19. Pockets or Neptunian Dikes within the Reef

Stop 19 includes a series of locations along 78 m (255 ft) of trail (figs. 27d), beginning ~21 m (~69 ft) beyond the 6,500-ft marker. At least three sites along this part of the trail contain organisms that either are markedly different from the typical reef organisms or are badly broken and clearly not in place. These assemblages may represent (1) fill within neptunian dikes that cracked open during reef growth and later were infilled by allochthonous grains, (2) pockets within the reef that were infilled with allochthonous debris, or (3) anomalous microcommunities within the reef.

The first and most striking of these sites predominantly contains large brachiopods (fig. 30c) but also contains gastropods and *Polydiexodina*. This location displays a distinct size zonation from coarser material in the center

FIGURE 30. Stop 18, fusulinids in reef, and Stop 19, pockets or neptunian dikes: (a) photomicrograph of fusulinid *Polydiexodina* and phylloid algal fronds, (b) outcrop photo of upright sponge and *Polydiexodina* (1/4 actual size), (c) outcrop expression of a neptunian dike containing large brachiopod shells (1/5 actual size), (d) photomicrograph of *Tubiphytes* and phylloid algal fragments encased in internal sediment and marine cement from dike site 2, (e) photomicrograph of *Mizzia* and other backreef skeletal grains observed at third dike or pocket in reef.

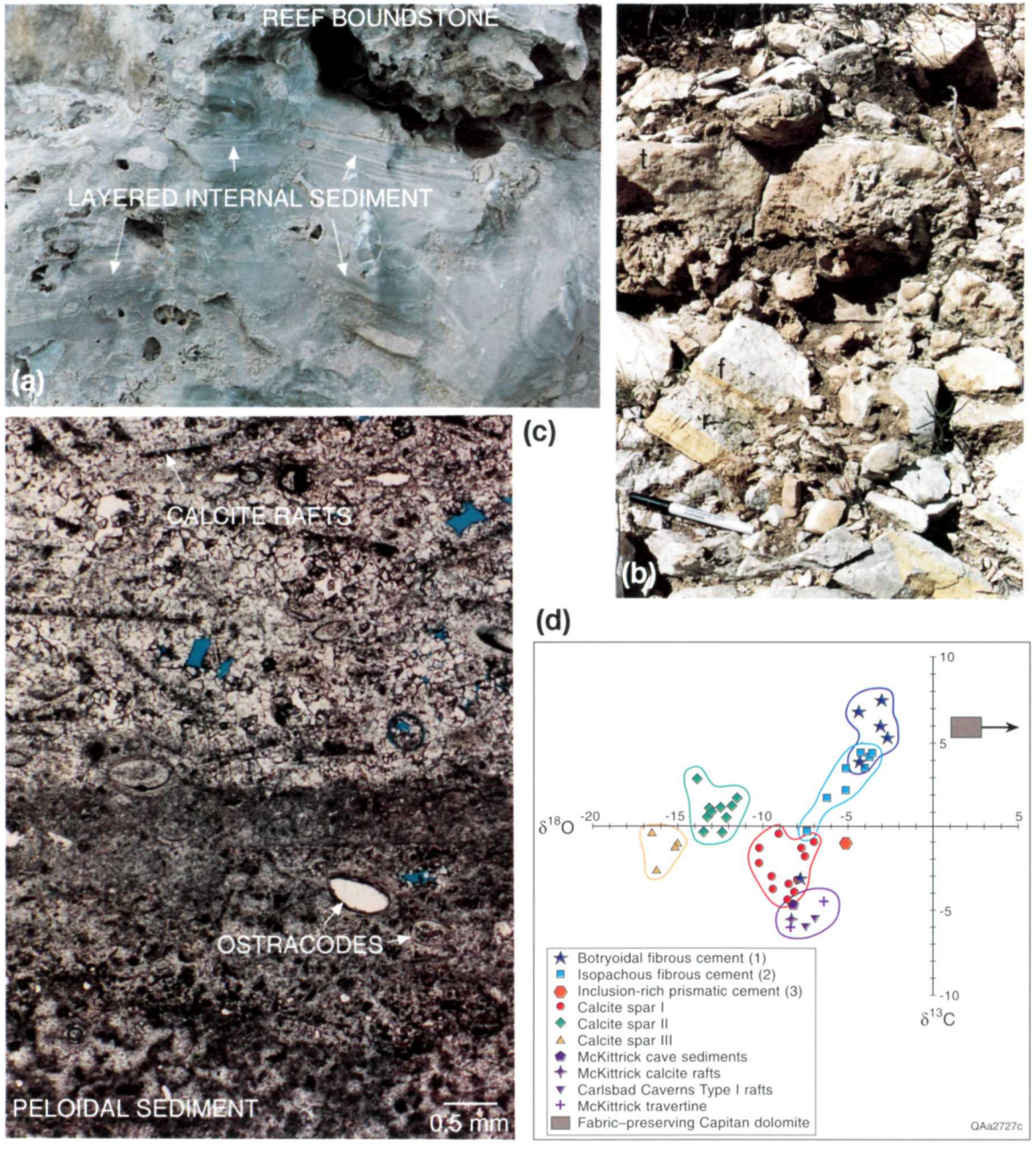

of the deposit to finer material along the margin. Two cephalopods occur along the trail between the first and second sites of Stop 19. The second site, ~23 m (~75 ft) farther up the trail, is dominated by fragmented *Tubiphytes* (fig. 30d), scattered plates of phylloid algae, sponges, and *Polydiexodina*. The grains are cemented with isopachous marine cement. Very small peloids (probably internal sediment) are surrounded by isopachous rims of marine cement. The third site, 53 m (174 ft) beyond site 2, contains a distinctive assemblage of *Polydiexodina*, other foraminifers, *Mizzia* (a green alga common in shelf deposits), phylloid algal plates, echinoderm and brachiopod fragments, and intraclasts/oncolites (fig. 30e). Most of these grains are cemented by thin rims of isopachous marine cement.

Overall, these pockets or dikes appear to coincide with the location of Tertiary fracture sets that are clearly visible when the trail is viewed from Stop 20. Note that the fractures virtually parallel the line marking the youngest occurrence of *Polydiexodina* in figure 27d. These Tertiary fractures may represent reactivation associated with Permian neptunian dikes or they may coincide with "growth surfaces" on the reef face.

STOP 20. Typical Reef Outcrops and Cave Fill

Stop 20 incorporates ~46 m (~150 ft) of trail (figs. 27d and 34). The outcrops along this stop display particularly well developed layers of internal sediment (fig. 31a) within reef boundstone. However, the most interesting feature of this portion of the trail is a small outcrop of

FIGURE 31. Stop 20, Permian internal sediment and cave fill in reef: (a) outcrop of layered internal sediment overlain by marine-cemented reef boundstone containing sponges and *Archaeolithoporella* (1/5 actual size), (b) outcrop exposure of small collapsed cave with layered, iron-stained sediment fill (f), calcite rafts (r), and honeycomb-weathered travertine (t), (c) photomicrograph of cave sediment fill containing peloids, ostracodes, and calcite rafts, plane light, (d) isotopic data from principal reef cements, dolomite, and speleothems (from Given and Lohmann, 1986; Hill, 1987; Mruk, 1989; Melim, 1991). Dolomite values plotted as average ± standard deviation; arrow indicates shelfward trend toward heavier oxygen isotopes, suggesting increasing salinity of dolomitizing fluids (Melim, 1991).

cave fill (fig. 31b) preserved about 5 m (15 ft) down trail from the ridge point. This relict cave is filled by probable waterlaid floor sediments (fig. 31b) consisting of brownish-yellow carbonate containing peloids and ostracodes, interbedded with calcite rafts (fig. 31c) (Chafetz and Butler, 1980; Folk and others, 1985). Directly above these deposits is an exposure of banded travertine consisting of elongate columnar blades of light-tan calcite (fig. 31b). Petrographically similar travertine fills many Tertiary-age fractures throughout the Guadalupe Mountains.

D. Mruk (personal communication, 1992) measured carbon and oxygen isotopes from the brownish-yellow sediments, calcite rafts, and travertine (fig. 31d). Her data fall in the same range as that of similar Quaternary calcite rafts from Carlsbad Caverns described by Hill (1987). When this small cave formed is uncertain; it may have developed concurrently with numerous other caves in the Guadalupe Mountains. However, the oxygen isotope values fall in the same range as spar I (see next stop), whose time of precipitation was most probably Permian.

STOP 21. Reef Diagenesis

Stop 21 begins 46 m (150 ft) beyond the 6,600-ft marker (fig. 34) in a distinctive, fresh cliff-face and extends for 91 m (300 ft) along the trail. The complex diagenetic sequence in the Capitan reef, as described in detail by Mruk (1985, 1989), Crysdale (1986), and Melim (1991), is well developed. Many of the cements (fig. 32a) are visible on outcrop; others require examination of thin sections in plane light, or in some cases cathode luminescence, for recognition.

The earliest-formed diagenetic components are dark-gray and light-brown botryoidal fans (cement 1) filling framework voids within the reef (fig. 32a–32f); the botryoids are large 1.5 to 5 cm (0.6 to 2 inches) and interlaminated commonly with the alga *Archaeolithoporella*. Petrographic and isotopic evidence (figs. 31d and 32b) suggests an aragonitic precursor and a marine origin (Newell, 1955; Loucks and Folk, 1976; Mazzullo and Cys, 1978; Given and Lohmann, 1985, 1986; Mruk, 1985, 1989). A second type of marine cement, which is smaller but also visible on outcrop, is an isopachous cement that encrusts surfaces of botryoids and lines framework voids (cement 2; fig. 32a). These isopachous rims are thin (0.5–4 mm) with up to four layers visible on outcrop (fig. 32c and 32e). In thin section, isopachous rims were followed by inclusion-rich prismatic cement (Mruk, 1989) (cement 3; figs. 32d and 33a). In many cases, cements 2 and 3 have radiaxial extinction patterns. Morphology and isotopic signatures (fig. 31d) of these cements indicate formation from marine fluids.

Mruk (1989), Melim and Scholle (1989), and Melim (1991) recognized significant dolomitization, dissolution, fracturing, and brecciation events after marine cementation and before precipitation of the first calcspar cements. Scattered dolomite crystals also postdate calcspar I (fig. 33b and 33c). Although the Capitan reef is not as extensively dolomitized in the Guadalupe Mountains as it is in the subsurface (Garber and others, 1989), dolomite is present in varying amounts in the reef and slope deposits. In addition to pervasive dolomitization along fractured and brecciated zones described at Stop 22, petrographic examination reveals scattered small (0.2 mm) dolomite rhombs and leached rhombic pores (fig. 33c).

Three generations of spar are present in the reef; each is distinguished by cathodoluminescence and isotopic composition (Mruk, 1989) (figs. 31d and 33a). The first and third generations are distinguished only by luminescence in thin section. Spar I (using the terminology of Given and Lohmann, 1986, and Mruk, 1989) consists of small crystals (0.25 to 0.5 mm) formed in optical continuity with the inclusion-rich prismatic cement (fig. 32d). Spar II, particularly abundant along this portion of the trail (fig. 32c and 32e), formed as much larger crystals (0.5 to 10's of cm [0.6 to 4 inches]) and composes 10 percent of the cement in the massive facies (Mruk, 1989). Spar II probably formed during Mesozoic burial of the Capitan carbonates, as indicated by isotopic signatures and two-phase fluid-inclusion studies (Crysdale, 1986; Mruk, 1989). An episode of dissolution and corrosion (fig. 33d) preceded precipitation of spar III (Mruk, 1989) on and within corroded spar II crystals. Spar III is distinguished by dull luminescence (fig. 33a). Vugs filled with calcite spar are prominent along the trail; however, cores from the subsurface reef display similar vugs that are filled with anhydrite and/or gypsum (Garber and others, 1989). Melim and Scholle (1989) suggested that evaporites originally filled vugs in the Guadalupe Mountains but later were replaced by calcite spars II and III.

STOP 22. Upper Reef—*Collenella*, Fusulinids, and Dolomite

Stop 22 occurs ~18 m (~60 ft) below switchback G (fig. 34). The fusulinid *Polydiexodina* is present, indicating that this highest reef exposure along the trail is no younger than Yates B. The fauna is dominated by *Collenella* (a problematic alga that occurs in upper reef facies in other canyons) (fig. 33e), *Acanthocladia*, and partly articulated crinoids; the diverse fauna also includes corals, gastropods, bivalves, cephalopods, several types of sponges, and *Archaeolithoporella*. The presence of *Collenella* here but not elsewhere within the reef section suggests that water depths may have shallowed during deposition of the Yates B. Kerans and Harris (this report) describe evidence of exposure of the outer-shelf facies at the top of Yates B (Stop 24). Although water level probably did not drop below the top of the reef at this time, the presence of *Collenella* and the diverse fauna may reflect the shallowing or fall of relative sea level that resulted in exposure further up on the shelf. Shelf grainstones and reef boundstones are interbedded just below switchback G.

A brecciated zone occurs near the reef/outer-shelf transition on both sides of the nearby spur where the trail crosses it twice, just below and above switchback G. During shallow burial, the rigid, marine-cemented reef fractured, probably due to compaction of the underlying, unconsolidated slope facies. Dolomitization altered the rock along fracture walls, creating dolomite halos (fig. 33f). Dolomite is also present in permeable beds in the slope, with the amount of dolomitization decreasing downslope.

Average carbon and oxygen stable isotope values for fabric-preserving dolomite are increasingly heavy shelfward of the reef (fig. 31d), suggesting that the salinity of the dolomitizing fluid was increasing across the shelf (Melim, 1991). On the basis of (1) isotopic values, (2) distribution of dolomite (decreasing basinward), and (3) petrographic evidence for timing of dolomitization, Melim (1991) attributed dolomitization to refluxing of Permian saline fluids from the shelf down into the reef and slope along fractures and permeable zones, similar to the model of Adams and Rhodes (1960).

Summary

The massive Capitan reef along the trail exposes a diverse marine fauna dominated by a variety of calcareous sponges and several forms of bryozoans and algae. Little biological zonation is apparent within the reef along the trail. As indicated by the distribution of the fusulinid *Polydiexodina*, the trail crosses reef facies equivalent to both Yates B and C of the shelf, thus providing an important correlation marker that can be traced through the slope, reef, and shelf beds. The configuration of that correlation marker suggests that the Yates-equivalent Capitan reef had a very steep profile, similar to that of modern reefs. The Tansill-equivalent reef, well-exposed at Walnut Canyon, has been eroded at McKittrick Canyon; the only Tansill-equivalent reef present at McKittrick occurs as fallen blocks in the slope facies. Yates- and Tansill-equivalent reef deposits differ in that the older reef contains more internal sediment, less *Archaeolithoporella*/botryoidal-fan cement, and perhaps a greater variety of sponges.

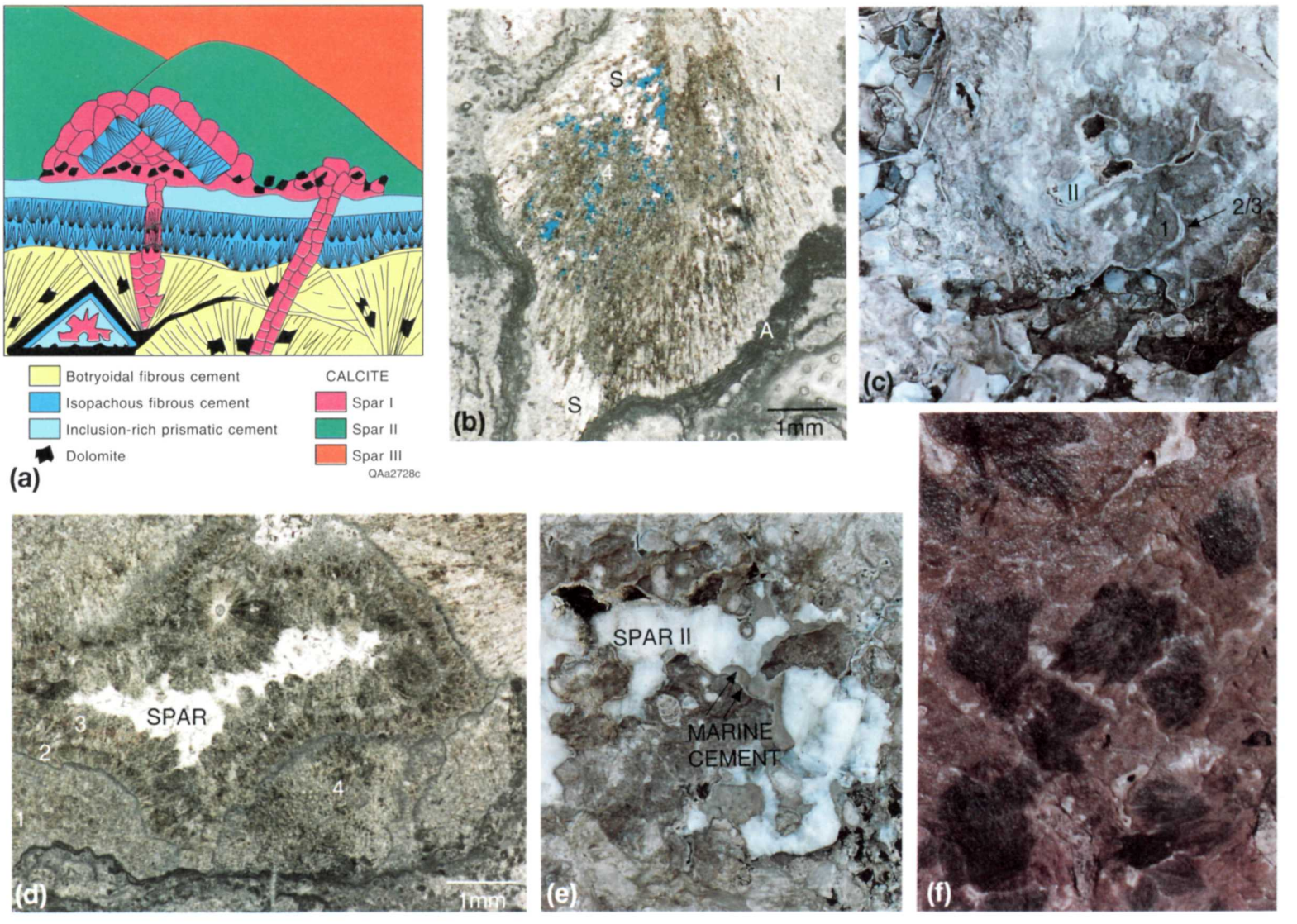

FIGURE 32. Stop 21, reef cement: (a) schematic diagram of cement types in reef (modified from Mruk, 1989), (b) botryoidal-fan cement (note relict aragonite needle morphology) and encrusting layers of *Archaeolithoporella* (A). Aragonite alteration varies from almost unaltered (1) to replaced by sparry calcite (S) to dissolved and/or replaced by dolomite (4), (c) outcrop expression of major cement types (1/5 actual size), (d) photomicrograph of major cement types, (e) outcrop expression of calcspars and marine cements (1/5 actual size); coarse-crystalline milky spars are primarily spar II, (f) outcrop photo of light- and dark-colored botryoidal fans (1/5 actual size).

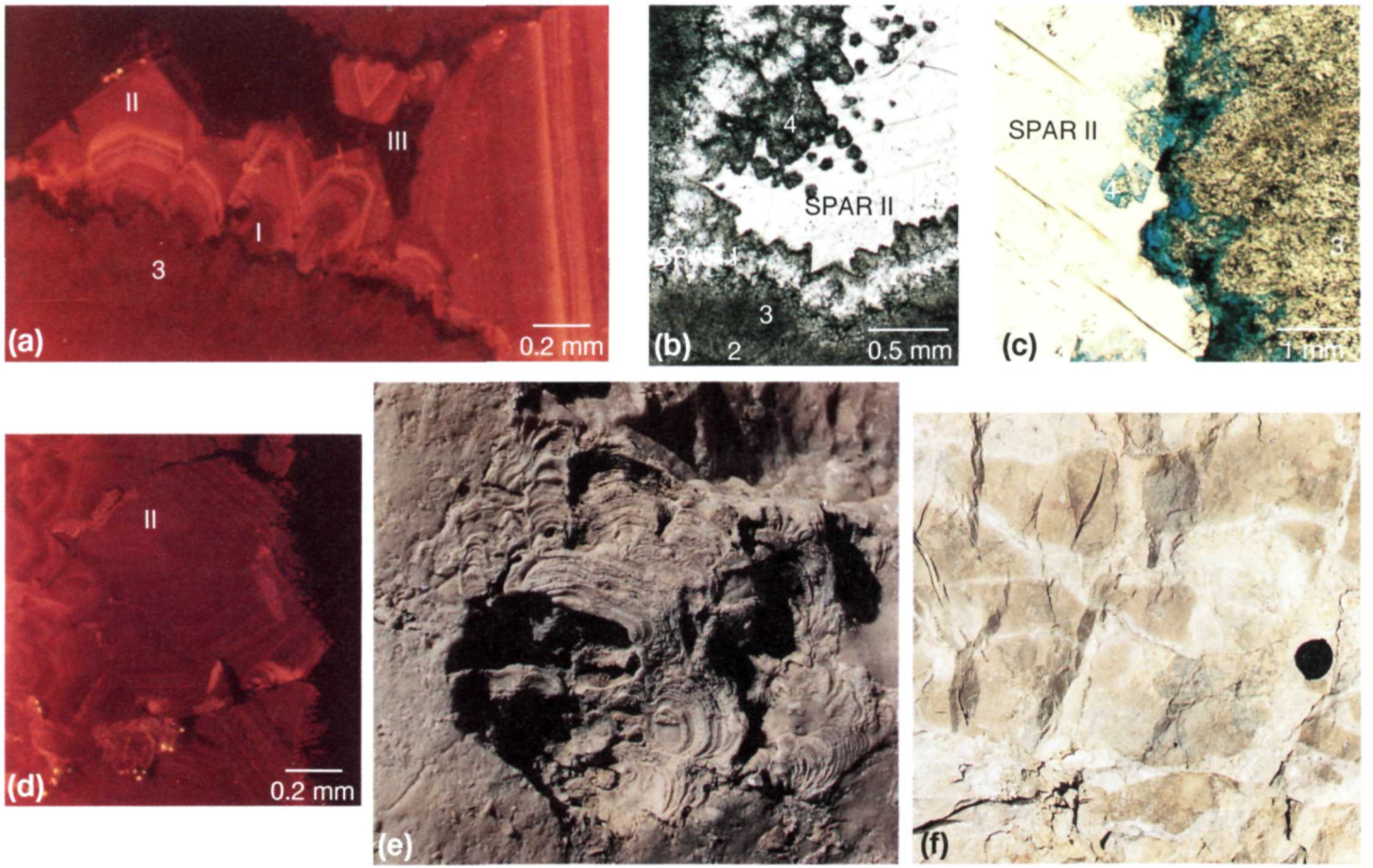

FIGURE 33. Stop 21, reef cement, and Stop 22, *Collenella* zone: (a) photomicrograph of cathodoluminescence patterns in spar I (zoned dull to bright), spar II (zoned mostly bright), and spar III (unzoned dull), (b) dolomite cement 4 capping spar I and marine cements, (c) partial dissolution of dolomite 4, dissolved rhombs infilled with blue epoxy, (d) photomicrograph of luminescent spar II showing corroded crystal margins, (e) *Collenella* head, shown 2/3 actual size, (f) upper reef displaying dolomitization (light cream color) associated with fractures (lens cap for scale).

Outer Shelf and Shelf Crest: Charles Kerans and Paul M. Harris

This segment of the Permian Reef Geology Trail includes progradational outer-shelf facies of the uppermost Yates Formation and both shelf-crest and possibly outer-shelf facies of the basal Tansill Formation (fig. 7). The reef/outer-shelf transition occurs at Stop 23 (switchback G), and this portion of the trail extends to the ridge crest (Stop 28) just above 7,000 ft (fig. 34). The total stratigraphic interval exposed in this section of the trail is 60 m (200 ft), slightly less than the total topographic relief because of 1° to 2° structural dip to the northeast (Hayes and Koogle, 1958). The Yates Formation as exposed along the trail is 33 m (110 ft) thick (fig. 35). Farther up canyon, in an updip position where the uppermost portions of the Yates Formation are removed by post-uplift erosion, Newell and others (1953) measured a maximum thickness of 88 m (290 ft) for the Yates Formation. On the Northwest Shelf, Borer and Harris (1991) demonstrated from subsurface correlations that the Yates exceeds 122 m (400 ft) in thickness. Thinning of Yates shelf strata toward the basin occurs as Yates-equivalent Capitan reef facies climb stratigraphically. Thus, the Permian Reef Geology Trail, which cuts the Yates in a position close to its terminal shelf-margin position, records only the upper quarter to third of the Yates section (figs. 7 and 35). Tansill strata compose the uppermost 26 m (85 ft) of stratigraphic section along the trail. In more complete sections to the north along depositional strike, Tansill Formation thickness reaches 122 m (400 ft) (Hayes, 1964).

Key observations concerning this portion of the trail are (1) the range of depositional facies characteristic of the outer-shelf and shelf-crest facies tracts of the Yates and Tansill Formations (cf. Neese and Schwartz, 1977; Esteban and Pray, 1983; Hurley, 1989; Neese, 1989; Borer and Harris, 1991), (2) the primary depositional dip (fall-in bed geometry) of the Yates shelf profile from the shelf crest downward to the shelf-edge reef, (3) the vertical arrangement or stacking patterns of these facies in small-scale (3 to 9 m [10 to 30 ft]), upward-coarsening cycles, (4) a key exposure surface that may represent a sequence boundary within the Yates outer shelf, and (5) the progressive upward increase in dolomitization of shelf strata following the overall progradation of evaporitic inner-shelf facies tracts over outer-shelf, open-marine deposits.

Six stops are described in this portion of the trail (figs. 34 and 35). The first four stops are in the Yates Formation: (1) the reef/outer shelf transition (Stop 23), (2) an exposure surface within the outer shelf (Stop 24), (3) outer-shelf upward-coarsening cycles (Stop 25), and (4) mixed siliciclastic/carbonate outer-shelf cycles (Stop 26). The remaining two stops are in the Tansill Formation: (5) shelf-crest cycles (Stop 27) and (6) outer-shelf dolopackstones (Stop 28). As in other portions of the trail, one must be aware that the trail cuts vertically through the section as well as laterally across depositional strike and dip. Most of the across-dip facies changes occur between Stops 24 and 26. Stop 25 contains lateral facies changes within outer-shelf cycles as they are traversed by the trail through several hundred feet of depositional dip in a seaward to landward direction.

STOP 23. Reef/Outer-Shelf Transition Zone

At Stop 23 the trail turns from a northeast to a northwest heading as it passes from the reef into the shelf at switchback G (figs. 34 and 35). This position represents the downdip termination of inclined outer-shelf or fall-in beds as they pass into the massive reef facies. The panoramic view from the trail to the northeast displays well the geometric relationship among the nearly flatlying, uppermost shelf-crest strata, the more steeply basinward-dipping, crudely stratified outer-shelf beds, and the massive reef. This fall-in bed geometry is best developed in older Seven Rivers strata (Hurley, 1989) but is also apparent throughout the Yates Formation and to a lesser degree in the Tansill Formation. Hurley (1989) used geopetal fabrics to show an original depositional dip of 8° for Seven Rivers fall-in beds and an additional postdepositional overprint of 2° to 3° due to tectonic or compactional tilting, for a total of 10° to 11°. As the Capitan reef generally shallowed through time (Babcock and Yurewicz, 1989) the dip of the fall-in beds became progressively less. However, stratification on the north wall of McKittrick Canyon (fig. 6) shows apparent repeated shallowing of the reef and progressive flattening of fall-in bed dips that are related to more short-term variations of the shelf margin.

For ~15 m (~50 ft) shelfward along the trail from switchback G, outcrops of limestones with minor dolostones display a mix of depositional fabrics including boundstone, wackestone, packstone, and grainstone. Bedding is poorly developed and neither crossbedding nor bioturbation has been observed. One area of boundstone may represent a low-relief mound. A high percentage of grains displays micritic (cyanobacterial?) coatings. The skeletal component includes mollusks (both bivalves and large bellerophon gastropods) (fig. 36a), green algae (minor *Mizzia*), sponges, crinoids, and rare foraminifers, including the fusulinid *Reichelina* (fig. 36b). One bedding surface displaying largely intact specimens of crinoids and clusters of sponge spicules represents slightly reworked filter-feeding communities that attest to moderate wave energy or preservation by rapid burial or both.

A recessively weathered zone above iron-stained packstones 3 m (10 ft) above the base of the outer-shelf strata marks the position of a laterally discontinuous 0.2-m-thick (0.5 ft) siliciclastic siltstone bed. Siltstone beds typically mark high-frequency (5th order?) cycle boundaries, and sections containing several stacked cycles rich in siltstone can be used to subdivide the Yates Formation into mappable units (Candelaria, 1989; Borer and Harris, 1991). This siltstone is very well sorted,

FIGURE 34. Oblique aerial photograph of upper portion of Permian Reef Geology Trail showing reef Stops 17–22 and shelf Stops 23–28, elevation markers, major switchbacks, and key stratigraphic relations. Stop 24 details relations associated with the lower sequence boundary shown, Stop 26 covers key sandstone marker beds used to define the top of the Yates Formation, and Stop 28 illustrates facies changes reflecting maximum flooding within the uppermost (Tansill 1) sequence.


Tansill Formation
Yates Formation
Capitan Formation
Tansill 1 Sequence
Yates/Tansill Sequence
Yates 4 Sequence
SB
Yates "C"
Yates "B"
SB-J
SB-I
SB-H
SB-G
SB-E
SB-F
7000'
6900'
6800'
6700'
6600'
6500'
6400'
28
27
26
25
24
23
22
21
20
19
18
17
Reef and Slope of Upper Yates Sequences

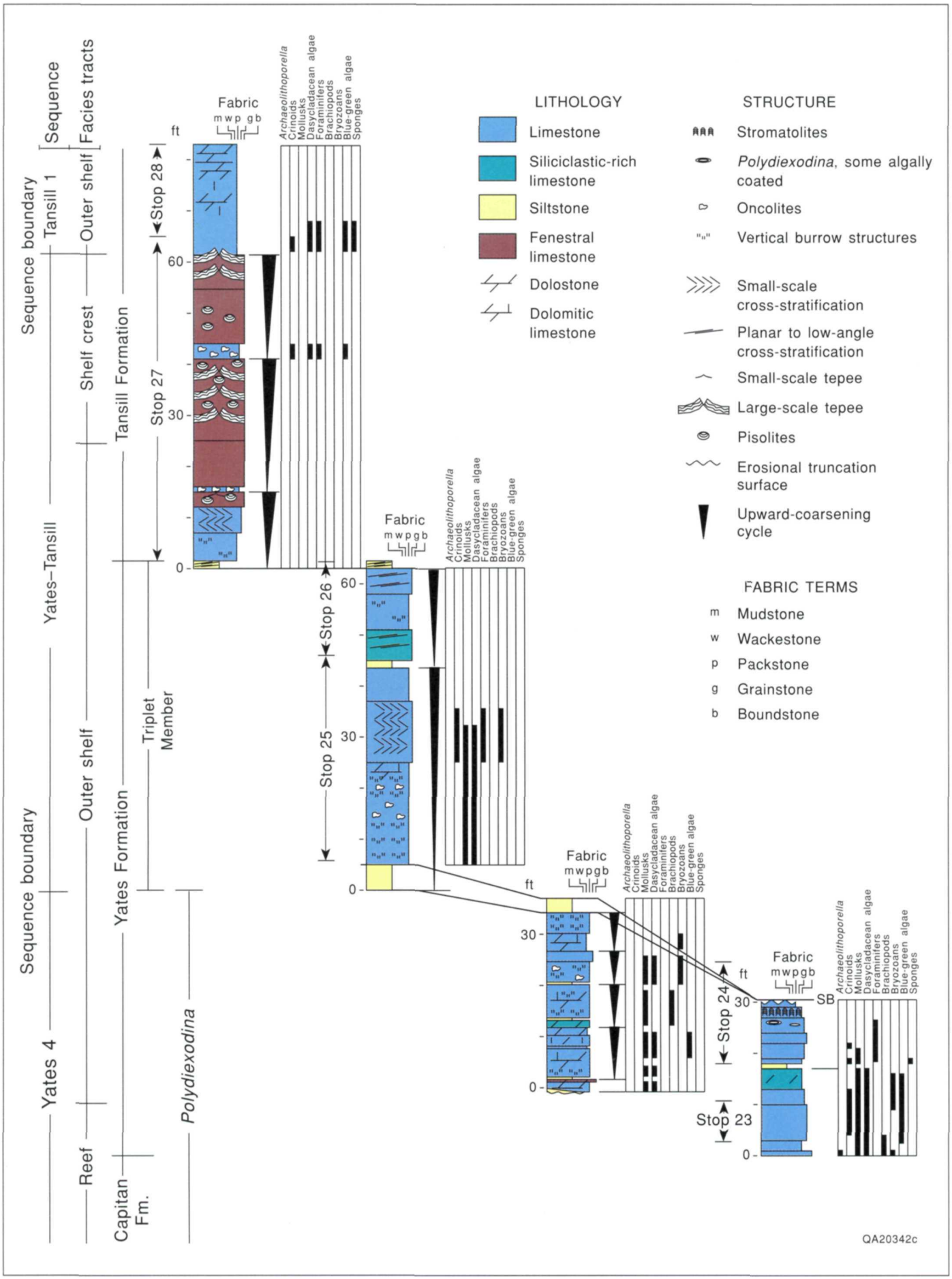

FIGURE 35. Measured sections for the outer shelf and shelf-crest portion of the trail showing stratigraphic nomenclature, sequences and cycles, and the position of Stops 23–28.

fine to medium grained, and dolomitic (fig. 36c), similar to siliciclastic-rich shelf facies from elsewhere in the Permian Basin (Candelaria, 1989; Borer and Harris, 1991). Siltstone porosity is largely restricted to secondary pores after dissolved feldspars. Photomicrographs from 1.5 m and 1 m (5 and 3 ft) below the silt bed (fig. 36d and 36e) illustrate the gradual introduction through time of siliciclastics onto the distal outer shelf before deposition of the siltstone bed proper. This relationship suggests that some siliciclastic detritus was transported across the outer shelf while it was still submerged or was mixed with underlying sediments by burrowing during the ensuing transgression. Several mechanisms have been proposed for siliciclastics bypassing the shelf, including eolian or desert fluvial transport (Mazzullo and others, 1986; Fischer and Sarnthein, 1988), offshore marine currents on a submerged shelf (Candelaria, 1989), bypassing during sea-level lowstands with trapping of sediments during reflooding (Borer and Harris, 1991), or by shelf-lagoon-derived saline density currents (Harms, 1974).

Diagenetic fabrics in the reef/outer shelf transition include an early generation of cloudy isopachous-fibrous calcite (probably relict Mg calcite, fig. 36d and 36e) and later clear, equant spar cements. Farther shelfward from the reef margin, the percent of early fibrous cement decreases markedly. Some iron sulfide and iron oxide

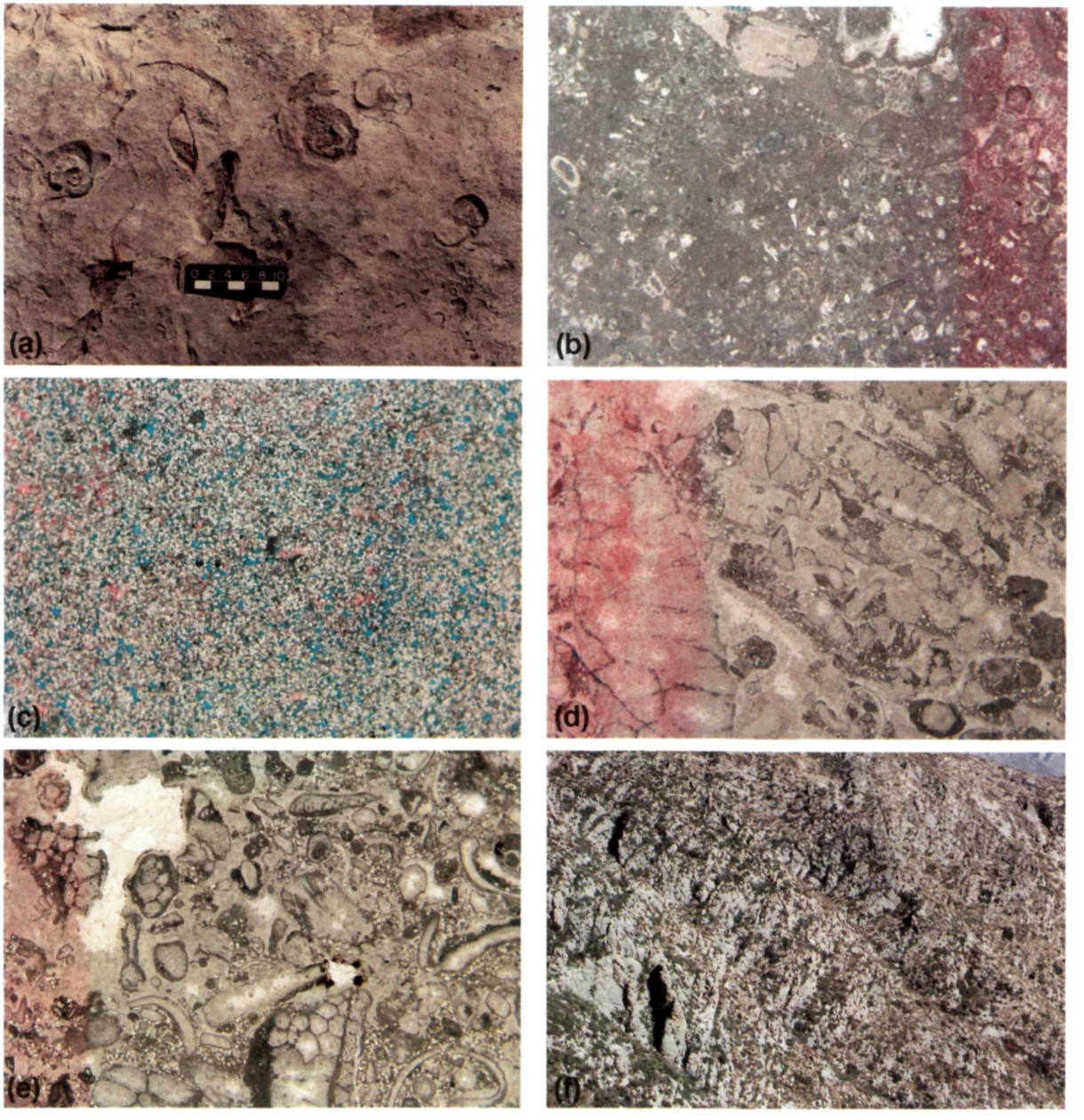

FIGURE 36. Outcrop and thin-section photographs of Stop 23 reef/outer shelf transition: (a) bedding surface showing large gastropods in skeletal packstone (scale bar in cm), (b) photomicrograph of lithoclast-skeletal-peloid packstone with pelmatozoan fragments, gastropods, various foraminifers (including *Reichelina*), and minor *Mizzia*, (c) photomicrograph of very well sorted, fine- to medium-grained, dolomitic siltstone with abundant secondary porosity resulting from feldspar dissolution and late-stage calcite cement, (d) photomicrograph of bryozoan grain-dominated packstone with quartz silt, grains rimmed by early-generation isopachous-fibrous calcite cement, and interparticle porosity filled with later clear blocky spar; (e) photomicrograph of skeletal packstone with abundant quartz silt; skeletal grains include mollusks, bryozoans, gastropods, and minor *Mizzia*. (early generation of cloudy isopachous-fibrous calcite shows possible corrosion prior to porosity occlusion by calcite spar); and (f) view to NE showing intense strike-parallel jointing in reef and slope portions of Yates-equivalent Capitan. Less well developed shelf-perpendicular jointing is seen in figure 34.

appear as later phases, probably derived from leaching of iron-bearing siliciclastics from the siltstone.

Vertically oriented, tabular breccia bodies 10 to 40 cm (4 to 16 inches) wide occur in joints at switchback G. These brecciated joints, described at Stop 22, are selectively dolomitized and weather recessively, defining a distinctive reef parallel joint set (fig. 36f).

STOP 24. Exposure Surface within Yates Outer Shelf

Immediately above, and in part superimposed upon, the reef/outer-shelf transition facies is a distinctive fenestral laminite/breccia unit that displays evidence of subaerial exposure and significant facies offset (fig. 37). The first evidence of this exposure event seen on the trail is at Stop 24, halfway between switchbacks G and H (figs. 34 and 35), ~6 m (~20 ft) before reaching the three large ponderosa pine trees that cover the trail. Fenestrally laminated columnar stromatolites and laminar fenestral cyanobacterial mats rest directly on packstones with a diverse outer-shelf fauna, suggesting that water depth shallowed abruptly (facies offset) (figs. 37, 38a, and 38b). The stromatolites are composed of light-gray micrite and are surrounded by gray to tan skeletal packstone. They display a slightly upward-widening profile in cross-sectional view in low outcrops along the south side of the trail (fig. 38a). Plan views display an interlocking network of cyanobacterial mats with intercolumnar sediment defining circular shapes (fig. 38b).

From this stromatolite outcrop shelfward along the trail to switchback H, a variety of features including breccia and fenestral structures are superimposed on typical outer-shelf *Polydiexodina* wackestones (figs. 37 and 38c). Just above switchback H ~3 m (~10 ft) beyond the 6,800-ft elevation marker the trail crosses the exposure surface again in a more shelfward position where sheet cracks and incipient tepee structures are capped by a recessive but persistent siltstone unit 0.3 m (1 ft) thick that is locally stromatolitic. Laterally along this surface sheet-crack breccia complexes up to 7.6 m (25 ft) thick are developed (fig. 38d) with peloidal internal sediment and paleoaragonite botryoids filling sheet cracks.

The recessively weathered siltstone resting atop the massive sheet-crack/breccia complex of the exposure surface creates a distinctive ledge (fig. 34) that can be traced from McKittrick Canyon northward along strike at least 4 km (2.5 mi) northeast to the next major dip-oriented reef exposure at Big Canyon (fig. 1) and is also traceable updip for several hundred feet (figs. 6, 36c, and 37). The combination of fenestral fabrics, shallow-water columnar stromatolitic growth forms, and thick sheet-crack breccia complexes with peloidal internal sediments suggests that this portion of the outer shelf, down to a point almost level with the reef, underwent prolonged subaerial exposure. The abrupt transition from open-marine to subaerial setting (facies offset), rather than the typical upward-shallowing facies progradation, supports interpretation of a major shallowing event and probable sequence boundary.

The top of the exposure surface along the trail is also equivalent to the top of the Yates "B" member of Newell and others (1953) as defined by physical correlation with their McKittrick Canyon sections and by the presence of the fusulinid *Polydiexodina* up to, but not above, this surface (fig. 35). The unit immediately below this exposure surface is the Yates 4 sequence. *Polydiexodina* also occurs in the slope no higher than the McCombs Limestone Member of the Bell Canyon Formation. If this correlation (Tyrrell, 1969) is valid, then it is possible to construct a time line from Stop 24 of the outer-shelf Yates Formation through Stop 19 within the reef to Stop 14 of the Capitan slope (fig. 39). In the toe of slope, the Bell Canyon sandstone interval between the McCombs and Lamar carbonate tongues may represent periods of shelf bypassing of siliciclastics during repeated shelf emergence (see fig. 4 and Stop 26 discussion). These Bell Canyon sandstones pinch out abruptly upslope into carbonate debris of the Capitan slope (fig. 20; King, 1948; Newell and others, 1953; Reeckmann and Sarg, 1986).

At switchback I the trail turns again to an oblique paleo-landward (west-northwest) orientation and climbs gradually topographically, parallel to the basinward-sloping outer-shelf fall-in beds (fig. 34).

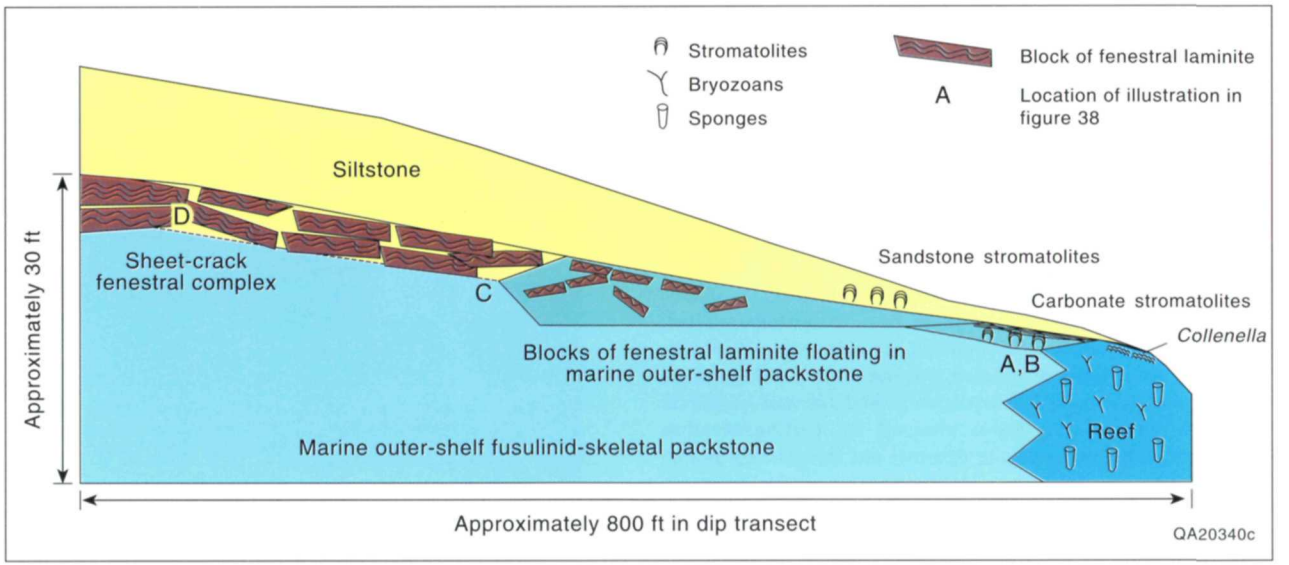

FIGURE 37. Schematic diagram showing facies relations documenting exposure of outer shelf associated with top Yates 4 sequence boundary. Features included from seaward to landward across 244 m (800 ft) of depositional dip transect are carbonate stromatolites, fenestral laminites and breccias, and 0.6- to 6-m-thick (2-to 20-ft) sheet-crack/fenestral complexes. Dramatic basinward thinning of overlying siltstone is also shown (see also fig. 41), with marine-marginal facies displaying sandstone stromatolites.

STOP 25. Outer-Shelf Packstone-Grainstone Cycles

Evidence of low-amplitude (1.5 to 9 m [5 to 30 ft]) high-frequency oscillations of relative sea level is apparent throughout the Permian shelf-top strata (Neese and Schwartz, 1977; Hurley, 1989; Wheeler, 1989; Borer and Harris, 1989, 1991; Kerans and Nance, 1991; Lindsay, 1991; Sonnenfeld, 1991), and recognition of cyclicity as the characteristic depositional pattern of the Yates and Tansill portions of the Permian will be emphasized in Stops 25 to 27.

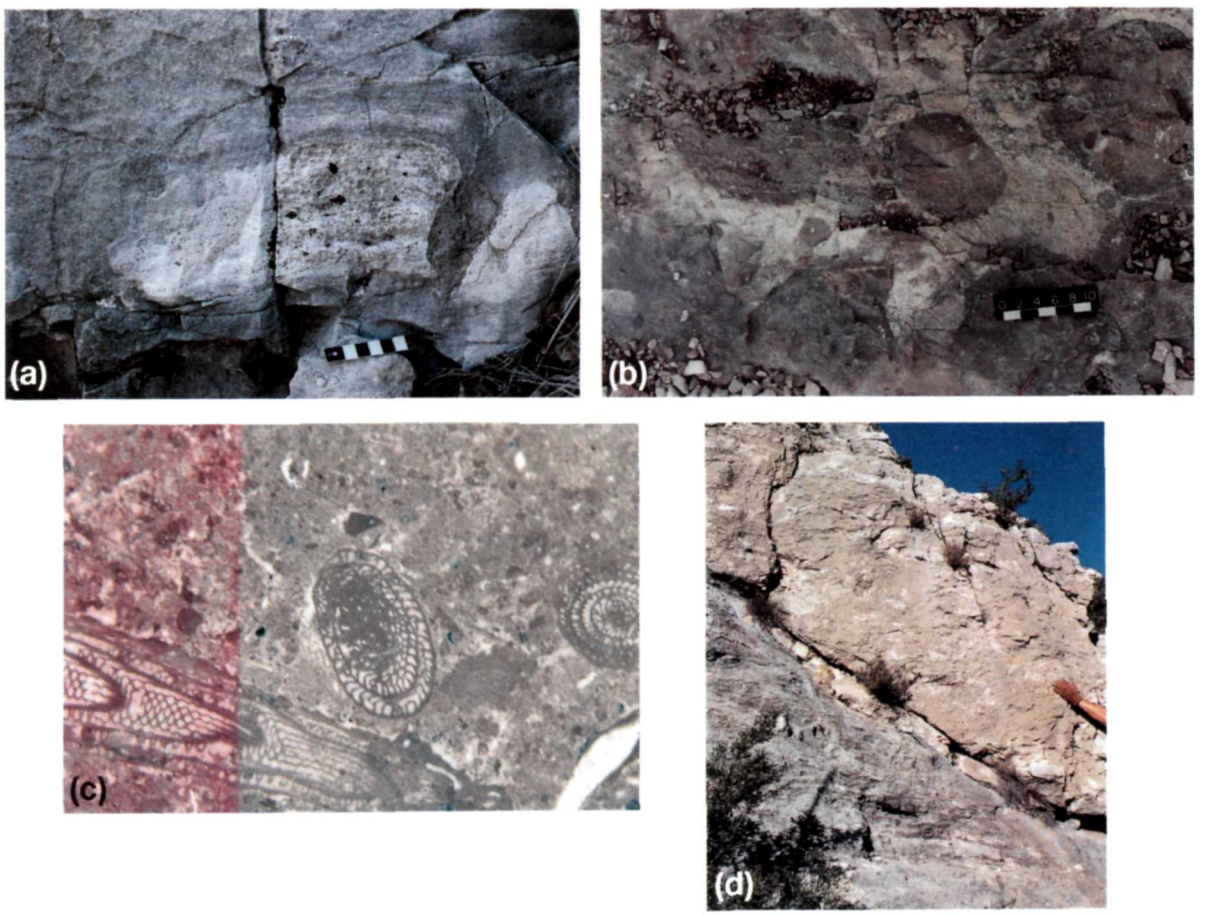

FIGURE 38. Outcrop and thin-section photographs of Stop 24 exposure surface (general location of figures shown in fig. 37): (a) outcrop of small columnar stromatolites with fenestral porosity (scale in cm), (b) plan view of stromatolites along floor of trail. Note that light-gray material is stromatolite and darker skeletal-peloid sediment defines unusually cylindrical intercolumnar areas (scale in cm), (c) photomicrograph of skeletal wackestone with the large benthic fusulinid *Polydiexodina*; blocky spar fills intraskeletal and minor interparticle porosity, (d) outcrop photograph showing thick sheet-crack breccia related to exposure surface with *Polydiexodina* wackestone of figure 38c directly below the breccia (hand for scale).

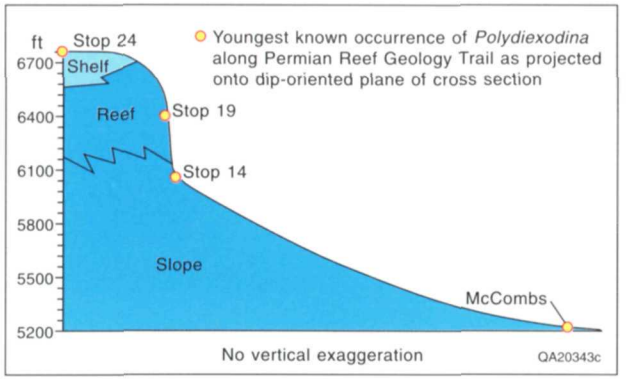

FIGURE 39. Approximate time line connecting youngest known occurrence of the fusulinid *Polydiexodina* along the trail. This uppermost occurrence corresponds to the exposure surface illustrated in figures 37 and 38 and demonstrates a very steep depositional profile for the platform margin at this time.

Outcrops 3 to 9 m (10 to 30 ft) high on the north side of the trail for the next several hundred feet show a layered erosionally resistant to recessively weathered pattern characteristic of upward-coarsening carbonate cycles of the outer shelf (finer grained = recessive, coarser grained = resistant; figs. 34, 35, 40, and 41). These cycles, from above the exposure surface to where the thicker sandstone-capped cycles appear at Stop 26 just above the 6,900-ft marker, are equivalent to the lower portion of the Yates "C" of Newell and others (1953) or Yates–Tansill sequence of this chapter (figs. 4 and 35). In vertical succession, these cycles are composed of basal peloid-algal-skeletal packstones locally displaying large, subvertical peloid-filled burrows (fig. 42a and 42b) that are succeeded by mollusk-algal-peloid packstones and grainstones (fig. 42c). Skeletal components characteristic of the outer-shelf facies are mollusks, crinoids, green algae, the scaphopod *Plagioglypta*, and smaller benthic foraminifers.

A key aspect of Stop 25 is that a single outer-shelf fall-in bed can be traced along the trail seaward to landward up the trail (figs. 34, 40, and 41), thus allowing observations of lateral facies changes within a cycle. As the trail follows this single cycle from the reef toward the shelf crest, an accompanying coarsening of

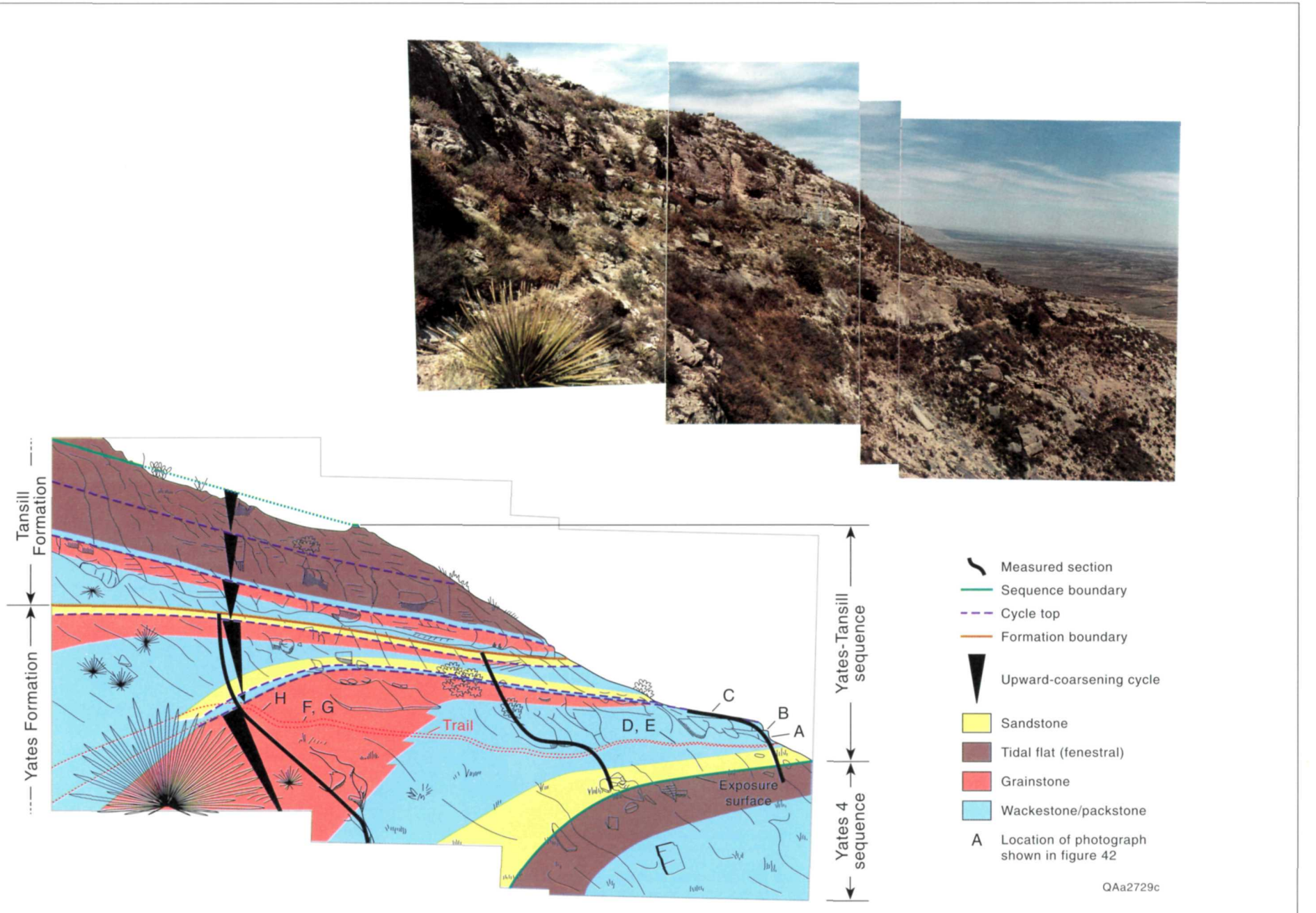

FIGURE 40. Panoramic photomosaic and interpretive sketch of the portion of the trail discussed in Stop 25 looking down the trail into the basin. The fall-in bed cycle that the trail traverses contains sandstone in its base, peloid-skeletal packstone in middle and upper portions in the more basinward exposures, and packstone grading upward into pisolitic-skeletal grainstone in updip portions of Stop 25 along the trail. Other cycles, sequence boundaries, and the location of measured sections from figure 41 are also shown.

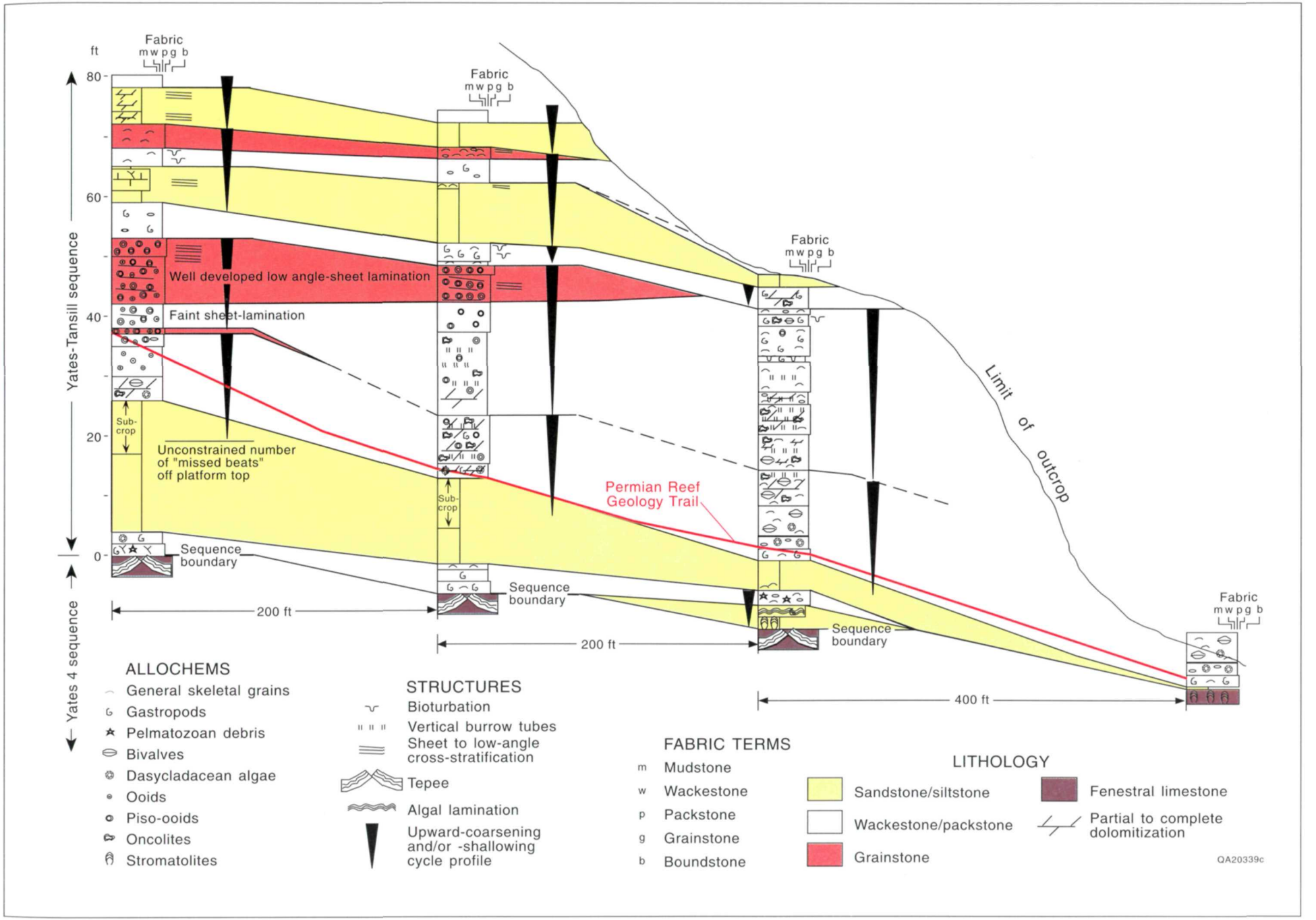

FIGURE 41. Cross section of outer shelf strata in Yates 4 and Yates–Tansill sequences from the area of Stop 25 (see fig. 40 for section location).

grain size reflects an increase in energy of the depositional environment with progressive shoaling (fig. 42a and 42c vs. fig. 42f and 42g, and fig. 43). Bioturbation gives way to cross-stratification in medium-scale, low-angle, tabular-planar to wedge sets (compare fig. 42a and 42h and fig. 43). Grain size and sorting also increase updip (fig. 42i). More of the grains are pisoids interpreted to have been derived from the pisolitic shelf crest by storm surges directed offshore (fig. 42d–g). This transect also displays the basinward-sloping geometry of these outer-shelf strata as the trail climbs vertically some 9 to 12 m (30 to 40 ft) between downdip and updip portions of Stop 25 (fig. 40). All facies changes described above occur in the relatively laterally condensed dip distance of 140 m (450 ft) (fig. 43).

In summary, the topographic sloping character of an individual fall-in bed can be observed as it passes from the shelf toward the reef, as can a distinctive upward-coarsening of fabrics within a cycle from burrowed packstones lacking pisoids to cross-stratified grainstones with increasing amounts of pisoid grains. The shallowing of facies as this cycle is traced from the reef toward the shelf crest, or up a fall-in bed, suggests that at this time the reef was not the crest of the shelf profile (fig. 43). If the marginal mound or fall-in model of the Capitan profile is correct (fig. 4), then a minimum 12 to 15 m (40 to 50 ft) fall of sea level is recorded by the exposure surface observed at Stop 24 that brought peritidal facies into proximity with the reef (assuming shelf crest to reef relief of 12 to 15 m [40 to 50 ft]) (Hurley, 1989; Borer and Harris, 1991).

STOP 26. Mixed Siliciclastic/Carbonate Outer-Shelf Cycles

Where the trail crosses the ledge-forming top of the outer-shelf cycle of Stop 25 just above the 6,900-ft marker (fig. 34), the next 8.5 m (28 ft) of section displays two distinctive sandstone-based skeletal-peloid dolopackstone cycles (figs. 35, 41, and 44a). These two recessive sandstone beds are used to define the top of the Yates Formation (Hayes and Koogle, 1958; Hayes, 1964) and are easily traced laterally in exposures of the shelf strata (figs. 34 and 41). On the basis of stratigraphic position, the sandstones are probably equivalent to the sandstone beds of the Triplet unit of the Walnut Canyon area (Esteban and Pray, 1977; Neese and Schwartz, 1977; Borer and Harris, 1989; Candelaria, 1989; Neese, 1989). The sandstones are best observed in the cliff exposures (figs. 40 and 44a) but are present along the trail as flaggy-bedded, low-relief exposures.

Basal sandstone beds are rich in mollusk and bryozoan fragments (fig. 44b). Moldic pores after feldspar and small carbonate grains occur in the sandstones; authigenic kaolinite and blocky calcite spar are abundant. Parallel lamination is characteristic of the sandstone beds (fig. 44c). Upper carbonates of these cycles are massive dolopackstones containing mollusks, green algae, and peloids.

These sandstone/carbonate cycles are most characteristic of the final stages of platform progradation in the Permian deposits of the Northwest Shelf, wherein siliciclastic-dominated facies tracts of the middle shelf have prograded to a position proximal to the basin margin. In this shelf-margin proximal position, only minor base-level fluctuations are required for siliciclastics to reach and bypass the outer shelf. Newell and others (1953) demonstrate that sandstone-dominated shelf equivalents of the lower Yates (their Yates A) member have prograded to a point only 2.9 km (1.8 mi) shelfward of the mouth of McKittrick Canyon. Borer and Harris (1991), working in the subsurface Yates Formation of the Northwest Shelf and western edge of the Central Basin Platform, demonstrated that this carbonate-to-sandstone facies transition prograded at least 2.4 km (1.5 mi) seaward during Yates deposition. If this observation is applied to the McKittrick Canyon area, the sandstone-dominated middle-shelf facies tract equivalent to the uppermost Yates Formation on the trail possibly occurs less than 0.8 km (0.5 mi) updip from this position at the mouth of McKittrick Canyon.

STOP 27. Shelf-Crest Cycles

Above the second sandstone-based cycle of Stop 26, which marks the top of the Yates Formation, the trail affords partial exposures of three carbonate cycles of the lowermost Tansill Formation that are included here in the Yates–Tansill sequence (fig. 35). The 26 m (85 ft) of Tansill traversed here illustrates evidence of initial upward-increasing subaerial exposure and development of sheet cracks and tepee structures followed by marine transgression (fig. 35). Lower Tansill strata below the Ocitillo siltstone have been correlated biostratigraphically with the Lamar Limestone Member of the Bell Canyon Formation (Tyrell, 1969) that occurs lower on the trail.

Tepee structures in these cycles are well exposed in the cliffs above Stop 26 (fig. 40), but they are not crossed by the trail until near and beyond switchback J (fig. 34). The lower of the three cycles is well exposed in the first good outcrop beyond Stop 26 and shows an upward-coarsening trend from massive, recessively weathered dolopackstones (fig. 44d) through erosionally resistant, low-angle cross-stratified, intraclast-peloidal dolograinstones to fenestral laminites with small tepee structures (figs. 35 and 44e).

FIGURE 42. Outcrop and thin-section photographs of Stop 25 outer-shelf cycle (illustrations located on figs. 40 and 43), (a) outcrop photograph showing vertically burrowed peloid-algal packstone (b) photomicrograph of peloid-algal packstone shown in (a), (c) photomicrograph of peloid-algal packstone with well-preserved *Mizzia* at top of the upward-coarsening outer-shelf cycle in a downdip position with micritic coatings on larger grains, minor cloudy fibrous calcite as first-generation cement, and blocky calcite filling intraskeletal and interparticle porosity, (d) sheet-stratified pisolite packstone in lower portion of outer-shelf cycle in a more shelfward position than in a–c, (e) photomicrograph of (d) showing coarse pisolite-skeletal packstone, skeletal grains include *Mizzia* and mollusks, pisolites have large nuclei and relatively thin cortices, (f) outcrop photograph of pisolite grain-stone in middle of outer-shelf upward-coarsening cycle, (g) photomicrograph of (f), pisolites are similar to those of (e), interparticle porosity filled primarily by isopachous fibrous calcite, (h) outcrop view of low-angle cross-stratified skeletal grainstone at the most landward point of this cycle exposed on the trail, (i) photomicrograph of coated-grain grainstone with well-developed isopachous-fibrous calcite and blocky calcite cement. Note that the grainstone fabric is coarser grained and better sorted than the cycle-capping packstone of (c).

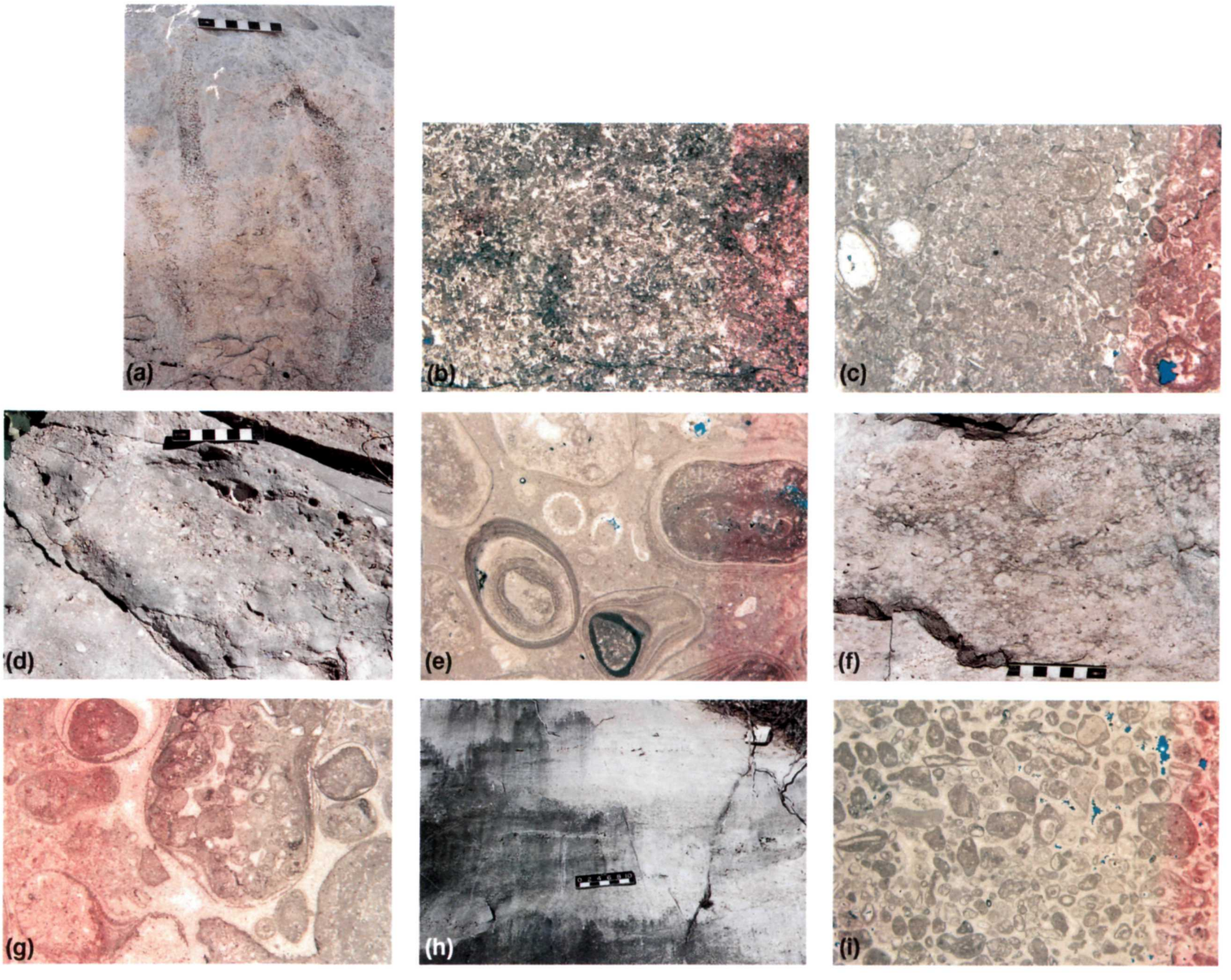
(a)
(b)
(c)
(d)
(e)
(f)
(g)
(h)
(i)

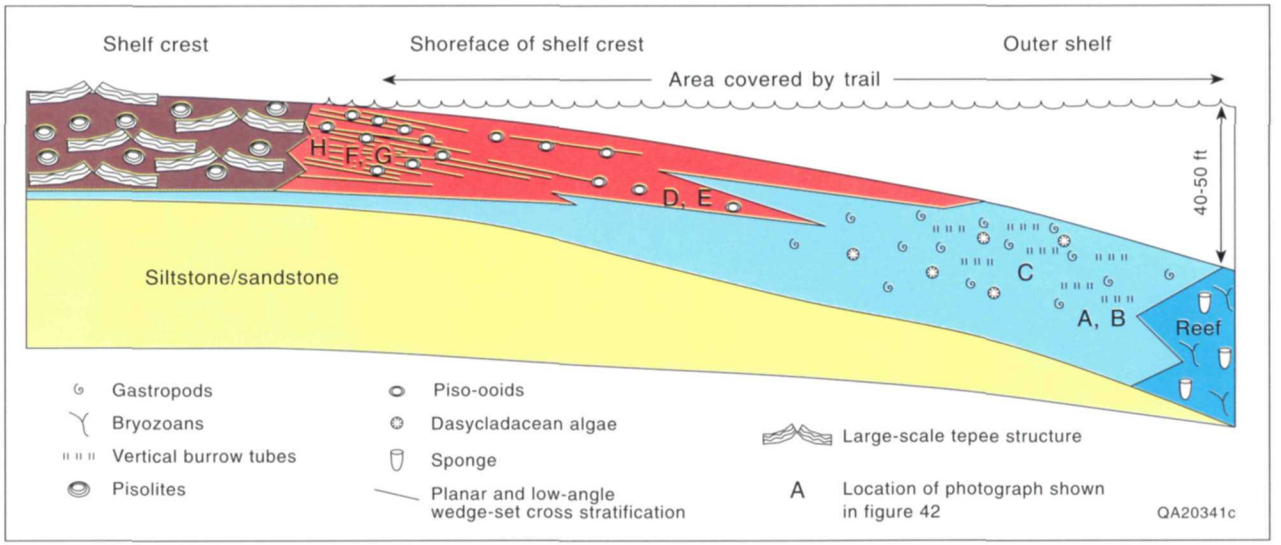

FIGURE 43. Schematic facies patterns seen in outer shelf fall-in beds of Stop 25. Lateral change occurs from massive to vertical burrowed packstone in a more basinward position, changing updip (uptrail) into pisolite-rich packstones and eventually into cross-stratified carbonate grainstone and/or pisolite grainstone. This change reflects a dip-oriented change in sediment source and depositional energy.

From switchback J (fig. 34) to the ridge crest the trail exposes the final 9 m (30 ft) of section containing two shelf-crest cycles dominated by fenestral laminites with tepee structures. Outcrops of the upper of these two cycles near the 7,000-ft marker show tepees with crests with up to 1.5 m (5 ft) of relief. Ponding of the basal packstone of the overlying cycle in low areas between tepee structures resulted in a highly variable thickness of this cycle-base, marine subtidal facies. Skeletal dolowackestone/packstone, with sponges, *Collenia* sp., and belerophont gastropods, occurs locally in tepee-depression areas on the trail (fig. 44f).

A series of 0.2- to 0.3-ft-wide (0.5- to 1-ft) dikes oriented parallel to the shelf-margin also occur in the immediate vicinity of switchback J. One dike is filled with Tansill-equivalent skeletal detritus and laminated quartz silt and is either a neptunian dike or Tansill-age karstic grike (solution-enlarged dike). Two other dikes, one at switchback J and one near the crest of the trail, are filled with lithoclastic breccia in a red, siliciclastic-rich, dolomitic matrix. These features are interpreted to be karstic grikes, but timing of formation, whether Permian or Tertiary, is in question.

STOP 28. Outer-Shelf Dolopackstone

The remaining 6 to 9 m (20 to 30 ft) of section exposed at the top of the trail is mollusk-algal dolopackstone of the Tansill Formation with rare sponges (figs. 34, 35, and 44f). Samples contain abundant large specimens of dasycladacean algae, mollusks, and spicules (fig. 44g). Some grains are micritized, and isopachous fibrous calcite cements and moldic pores occur locally. This dolopackstone is interpreted to mark the gradual return to outer-shelf conditions in successively younger Tansill strata. This transgressive phase of sedimentation in the lower Tansill Formation also appears in both Walnut and Dark Canyons (Neese, 1989; Parsley and Warren, 1989) and marks the base of the Tansill 1 sequence (fig. 35).

Summary

From the crest of the Permian Reef Geology Trail, excellent views are provided along the reef trend to the northeast and down into the basin to the southeast. In the near foreground to the northeast is the southwest-facing wall of Big Canyon, where the near-terminal shelf profile of the Capitan is defined by Tansill/Capitan/Lamar strata. The northward regional dip of the entire platform in the direction of White's City and Carlsbad, where it is finally in the subsurface, is also well demonstrated. The present-day geomorphic top of the platform, which approximately follows the lower Tansill in this view, drops from 2,130 m (7,000 ft) at the trail crest to 1,160 m (3,800 ft) at the farthest visible point of the reef, some 40 km (25 mi) away (average regional dip of ~1°).

The depositional profile of the Lamar toe of slope to basin is viewed by looking basinward across McKittrick Creek and the entrance road to the south. Basinward along the north side of the creek is the Lamar escarpment, which is composed of the Lamar preserved in near-original depositional geometry. Smooth slopes behind the McKittrick Canyon Visitor Center that can be traced upslope on the south wall of the canyon are also of Lamar toe-of-slope deposits. These strata have been truncated about a third of the way up the Capitan slope by present-day erosion.

FIGURE 44. Outcrop and thin-section photographs of Stops 26–28 siliciclastic-carbonate and carbonate cycles: (a) outcrop view of parts of two sandstone-based cycles of the uppermost Yates Formation (equivalent to Triplet unit of Yates in Walnut Canyon; Candelaria, 1989; see fig. 35), (b) photomicrograph of bivalve- and bryozoan-bearing siltstone with abundant moldic porosity after feldspar and mollusks filled with nonferroan blocky calcite spar, (c) cm- to mm-laminated dolomitic siltstone in upper part of cycle shown in (a), (d) characteristic recessively weathered to erosionally resistant profile of upward-coarsening, outer-shelf carbonate cycle in basal Tansill Formation, (e) photomicrograph of peloid grainstone from cross-stratified uppermost interval on cycle shown in (d), (f) gastropod-sponge wackestone locally developed in lows between tepee structures near top of trail marking transgressive surface within the Tansill 1 sequence (see fig. 34), (g) photomicrograph of dasycladacean packstone with abundant moldic porosity at crest of trail.

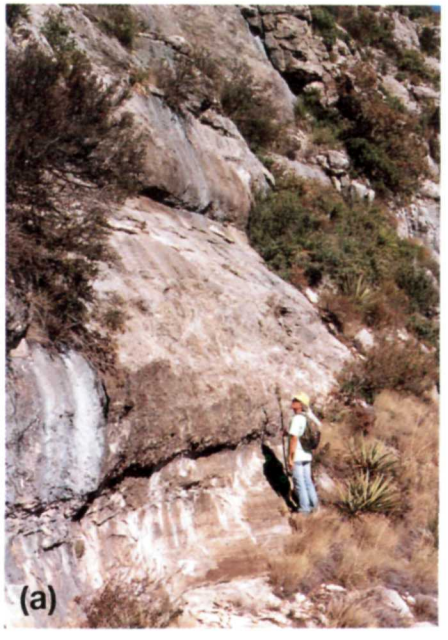
(a)

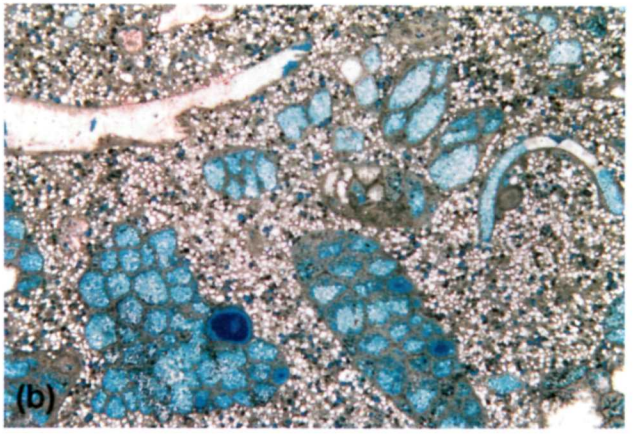
(b)

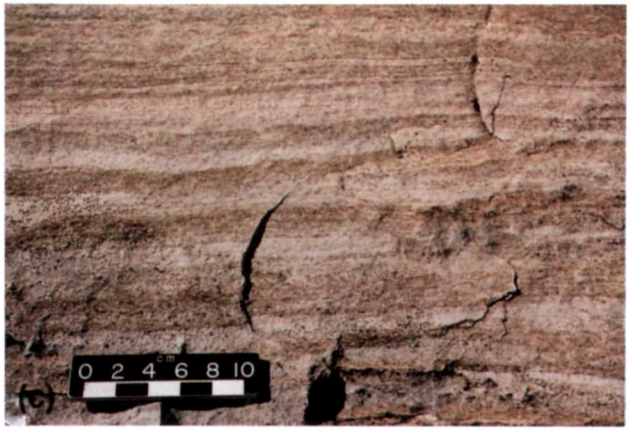
0 2 4 6 8 10
cm
(c)

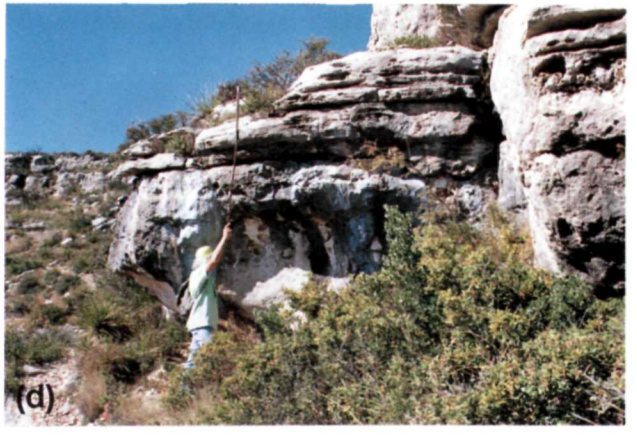
(d)

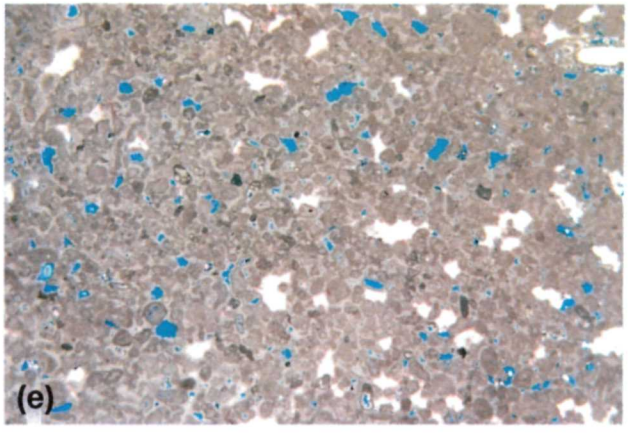
(e)


(f)

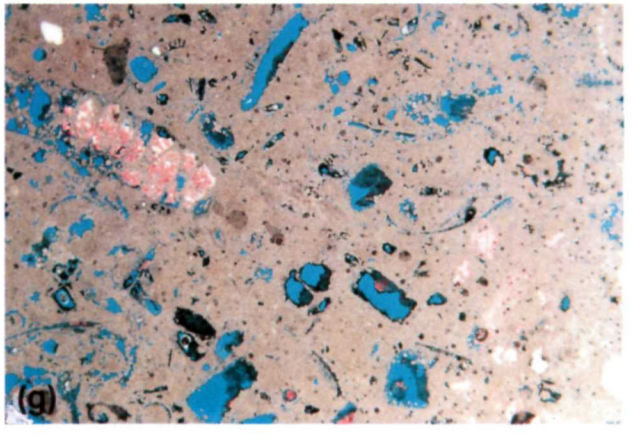
(g)

Geology Loop Trail: Alton Brown and Robert G. Loucks

The Geology Loop Trail description begins at the upper end of the loop, 1 km (0.6 mi) up the Permian Reef Geology Trail from the Visitor Center, and ends at the lower end of the loop (fig. 8 inset). The Geology Loop exposes lateral changes in depositional facies in a toe-of-slope setting thought to be evidence of a slope gully during deposition of the Lamar Limestone Member of the Bell Canyon Formation.

About 110 m (360 ft) north of its uptrail junction, the Geology Loop Trail bends to the north and then descends into a small arroyo ringed with outcrops, thus forming a natural amphitheater (fig. 45).

STOP 29. Margin of Slope Gully

The resistant beds ringing the west side of the arroyo (figs. 8 and 45) are burrowed wackestones correlative with the burrowed wackestone in the upper part of Stop 4. The underlying thin-bedded wackestone, recessively weathered peloidal packstone, and interbedded skeletal packstone and thin-bedded wackestone units at Stop 4 are also present here, but they are poorly exposed.

The top of the burrowed wackestone unit displays a northeasterly dip (~5°) significantly steeper than the regional structural dip (2°). The burrowed unit and individual beds within the unit thin to the northeast. On the northeast end of the low cliff, the thinned burrowed wackestone unit is onlapped from the north by thick-bedded intraclast packstones (fig. 45). These are overlain by poorly exposed skeletal packstones and skeletal-intraclast packstones. These lateral changes are interpreted to mark the southwestern edge of a syndepositional slope gully. Thinning of the burrowed beds is interpreted as syndepositional erosion near the edges of the gully.

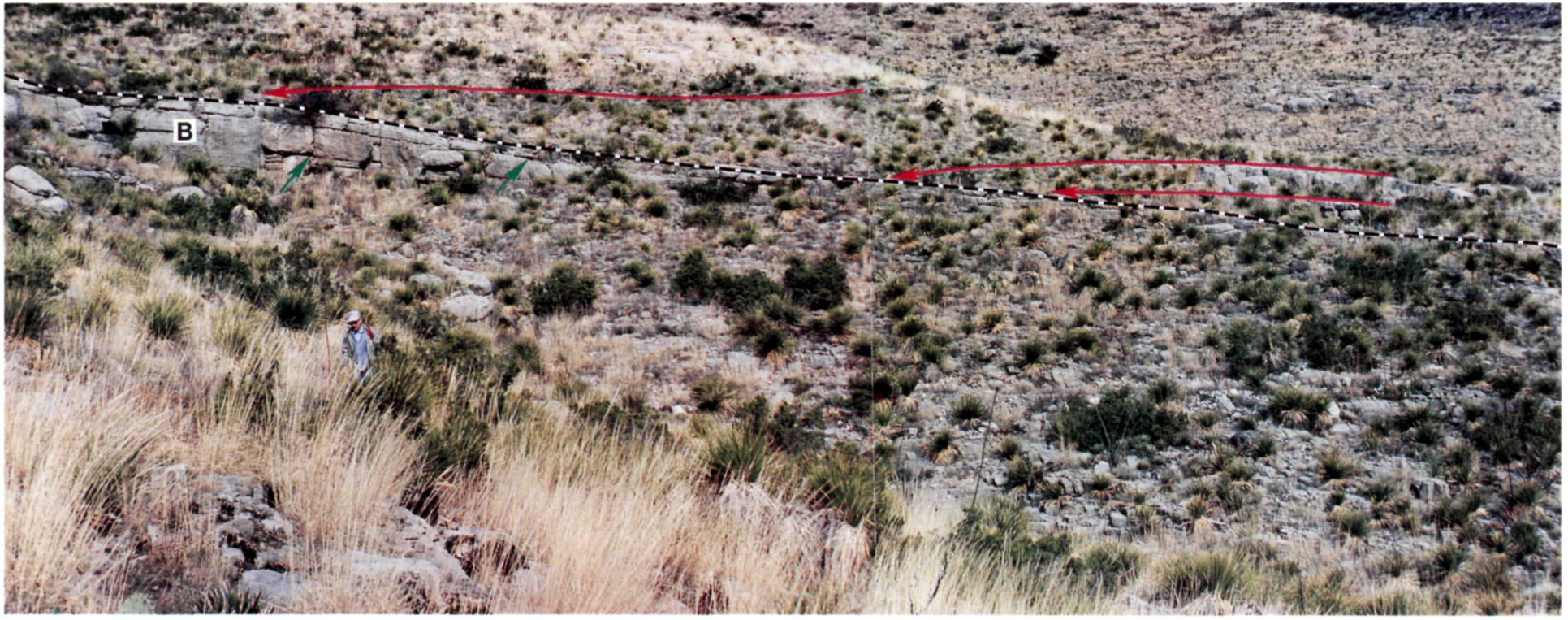

FIGURE 45. Trail photograph of margin of slope gully at Stop 29. The left side of the photograph is the central part of the amphitheater with a thick section of burrowed wackestone (B). The burrowed wackestone thins to the northeast, and the top of the unit (dashed line) has an anomalously steep dip. Individual beds also thin to the northeast (near green arrow). The burrowed wackestone is onlapped by thick-bedded skeletal-intraclast and skeletal packstones (red lines) at red arrows.

Wackestone truncation and packstone onlap mark the actual margin of the gully. Although clearly defined at some stratigraphic intervals such as this, the gully packstones interfinger with marginal wackestone deposits higher and lower in the section.

As the trail descends into the next arroyo, it intersects thin-bedded wackestone correlative to the upper thin-bedded wackestone at Stop 4. A few tens of feet farther down the trail at approximately the same stratigraphic position, these beds are replaced by thick-bedded, skeletal and intraclast packstones deposited by debris flows, marking the edge of the slope gully at a lower stratigraphic position.

STOP 30. Slope Gully Fill

Good exposures of the gully fill crop out in the arroyo where the trail bends sharply to the right (fig. 45). The lithologies seen in these exposures are similar to the grainy facies seen along the Permian Reef Geology Trail at Stops 3, 6, and 7. The two prominent intraclast packstone beds cut by the trail and the thick-bedded, skeletal intraclast packstone on the arroyo floor are interpreted to be debris-flow deposits. The lower part of the northeast wall of the arroyo comprises thin- to medium-bedded, graded packstones to grainstones interpreted to be turbidites. These turbidites are overlain by thin-bedded, sparsely burrowed wackestones, which are in turn overlain by thick-bedded intraclast packstones. Higher in the section, a 0.3-m-thick (1-ft) burrowed wackestone is interbedded with the intraclast packstones. Some channelized beds within the gully fill contain small *Archaeolithoporella* boundstone fragments. The upsection increase in burrowing intensity of the wackestones at Stops 4 and 29 outside the gully are observed in the wackestone beds intercalated with gully packstones. The change in fabrics occurs at approximately the same stratigraphic position in the gully as that outside the gully, indicating that deposition of the gully fill occurred concurrently with deposition of wackestones southwest of the gully.

The schematic cross section connecting Stops 4, 29, and 30 summarizes relationships of the southwestern gully margin (fig. 46). Wackestone and peloidal packstone strata are relatively continuous between Stop 4 and the southwestern end of Stop 29. From Stops 29 through 30, the gully packstones interfinger with and substitute for wackestones occurring at the same stratigraphic position. The gully was characterized by gentle bathymetric relief and penecontemporaneous deposition of grainy units within the gully and muddy units on the margin of the gully.

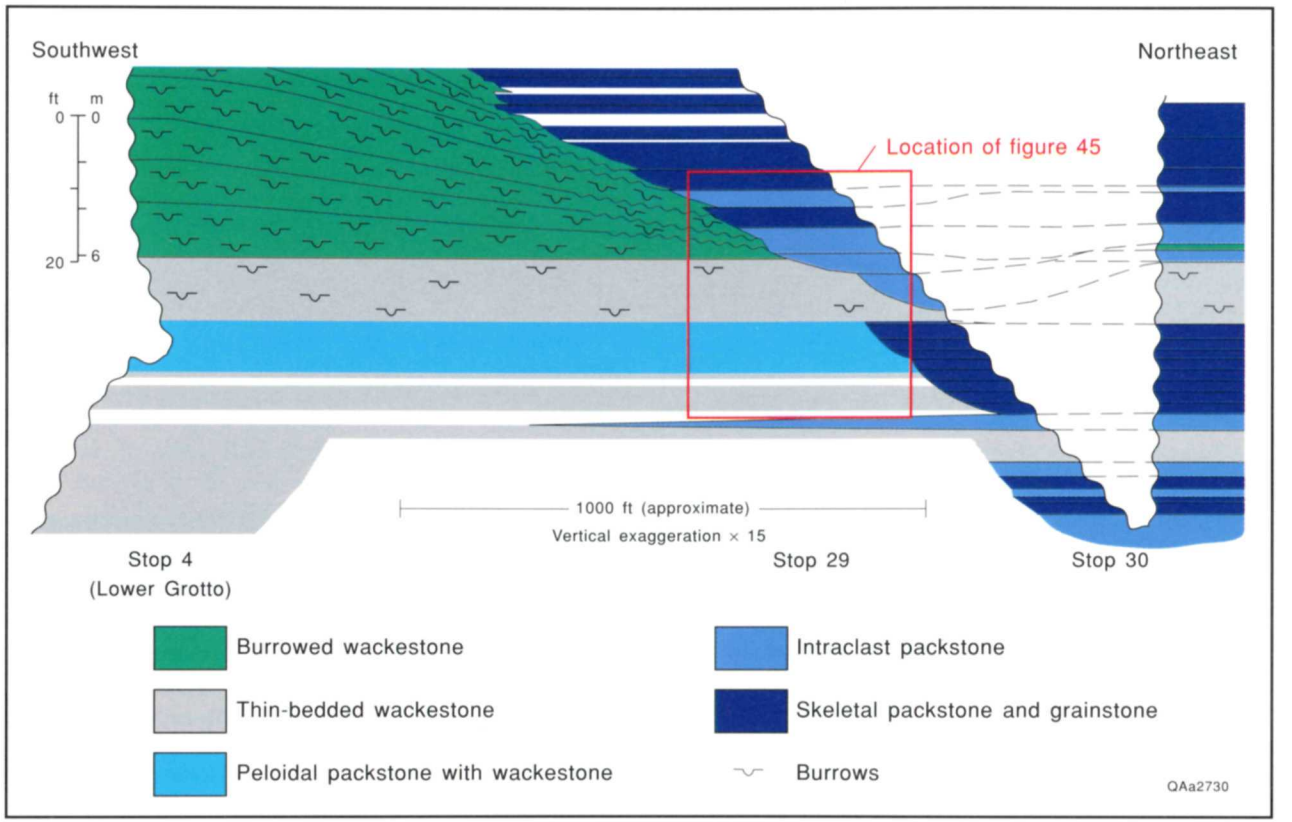

FIGURE 46. Schematic strike cross section between the lower Grotto (Stop 4) and Stop 30. Area of figure 45 is indicated by the inset box. Slope northeast of Stop 30 (section I) is steepened to shorten cross section.

About 69 m (225 ft) down the trail, the updip end of a grainstone- and intraclast packstone-filled channel is exposed at eye level across the arroyo from the trail. To the right of the trail in a small drainage channel, thick-bedded packstones contain excellent silicified brachiopods, mollusks, and bryozoans.

A short distance beyond this point, the limestones grade from grain-rich to mud-rich as the trail obliquely leaves the slope gully. The transition is marked by changes of bedding dip and enhanced slump deformation. The slope gully continues to the east boundary of the park. Where the trail diverges from the arroyo, most of the limestones at trail level are laminated wackestones, which occur along the remainder of the Geology Loop Trail to its lower intersection with the Permian Reef Geology Trail.

Acknowledgments

Larry Henderson (park superintendent), Bob Valen, Brent Wauer, and Roger Reisch, Guadalupe Mountains National Park, supported the project and made all park facilities available to the authors. Elevations for the trail markers were surveyed by Thomas Rohrer (Queen, New Mexico), John Ames, Clifton Neeley, and Don Bebout (Bureau of Economic Geology, The University of Texas at Austin), and the markers were installed by Park Service personnel. The low-altitude, oblique aerial photographs were taken by Jerry Lucia and Charles Kerans, Bureau of Economic Geology, The University of Texas at Austin; Jerry Lucia also aided in preparation of the mosaic photograph of the north wall of McKittrick Canyon. Leslie Melim, Southern Methodist University, provided information on mechanisms of dolomitization in McKittrick Canyon. Keith Rigby confirmed sponge identifications.

Critical reviews that significantly improved the trail guide were provided by Paul Enos, University of Kansas, R. P. Major, H. Seay Nance, and S. C. Ruppel, Bureau of Economic Geology, The University of Texas at Austin, and Jack Babcock, Amoco Production Co. T. F. Hentz was the technical editor, and editing was by Amanda R. Masterson. Word processing was by Susan Lloyd. Illustrations were drafted by Michele Bailey, Joel L. Lardon, Kerza A. Prewitt, Maria Saenz, and Tari Weaver. Margaret L. Evans typeset and created the design.

References

Adams, J. E., and Rhodes, M. L., 1960, Dolomitization by seepage refluxion: American Association of Petroleum Geologists Bulletin, v. 44, p. 1912–1920.

Babcock, J. A., 1974, The role of algae in the formation of the Capitan Limestone (Permian, Guadalupian), Guadalupe Mountains, West Texas–New Mexico: University of Wisconsin, Madison, Ph.D. dissertation, 241 p.

_____ 1977, Calcareous algae, organic boundstones, and the genesis of the upper Capitan Limestone (Permian, Guadalupian), Guadalupe Mountains, West Texas and New Mexico, *in* Hileman, M. E., and Mazzullo, S. J. (eds.), Upper Guadalupian facies, Permian reef complex, Guadalupe Mountains, New Mexico and West Texas: Field Conference Guidebook, PBS/SEPM Publication 77-16, v. 1, p. 3–44.

Babcock, J. A., and Yurewicz, D. A., 1989, The massive facies of the Capitan Limestone, Guadalupe Mountains, Texas and New Mexico, *in* Harris, P. M., and Grover, G. A. (eds.), Subsurface and outcrop examination of the Capitan Shelf Margin, northern Delaware Basin: SEPM Core Workshop No. 13, p. 365–371.

Babcock, L. C., 1976, Life in the Delaware Basin—the paleoecology of the Lamar Limestone, *in* Upper Guadalupian Facies, Permian Reef Complex, Guadalupe Mountains, New Mexico and West Texas 1977 field conference guidebook: Permian Basin Section–SEPM Publication 77-16, p. 357–390.

Bachman, G. O., 1976, Cenozoic deposits of southeastern New Mexico and an outline of the history of evaporite dissolution: USGS Journal of Research, v. 4, p. 135–149.

Borer, J. M., and Harris, P. M., 1989, Depositional facies and cycles in Yates Formation outcrops, Guadalupe Mountains, New Mexico, *in* Harris, P. M., and Grover, G. A. (eds.), Subsurface and outcrop examination of the Capitan Shelf Margin, northern Delaware Basin: SEPM Core Workshop No. 13, p. 305–317.

_____ 1991, Depositional facies and cyclicity in the Yates Formation, Permian Basin—implications for reservoir heterogeneity: American Association of Petroleum Geologists Bulletin, v. 75, p. 726–779.

Candelaria, M. P., 1989, Shallow marine sheet sandstones, Upper Yates Formation, Northwest Shelf, Delaware Basin, New Mexico, *in* Harris, P. M., and Grover, G. A. (eds.), Subsurface and outcrop examination of the Capitan Shelf Margin, northern Delaware Basin: SEPM Core Workshop No. 13, p. 319–324.

Chafetz, H. S., and Butler, J. C., 1980, Petrology of recent pisolites, spherulites, and speleothem deposits from Central Texas: Sedimentology, v. 27, p. 497–518.

Crysdale, B. L., 1986, Fluid inclusion evidence for the origin, diagenesis, and thermal history of sparry calcite cement in the Capitan Limestone, McKittrick Canyon, West Texas: University of Colorado, Master's thesis, 78 p.

Dunham, R. J., 1972, Capitan reef, New Mexico and Texas—facts and questions to aid interpretation and group discussion: Permian Basin Section–SEPM Publication 72–14, 297 p.

Esteban, M., and Pray, L. C., 1977, Origin of the pisolite facies of the shelf-crest, *in* Hileman, M. E., and Mazzullo, S. J. (eds.), Upper Guadalupian facies, Permian Reef Complex, Guadalupe Mountains, New Mexico and West Texas, 1977 field conference guidebook, v. 1: Permian Basin Section–SEPM Publication 77-16, p. 479–486.

Fischer, A. G., and Sarnthein, Michael, 1988, Airborne silts and dune-derived sands in the Permian of the Delaware Basin: Journal of Sedimentary Petrology, v. 58, p. 637–643.

Folk, R. L., Chafetz, H. S., and Tiezzi, P. A., 1985, Bizarre forms of depositional and diagenetic calcite in hot-spring travertines, central Italy, *in* Schneidermann, N., and Harris, P. M. (eds.), Carbonate cements: SEPM Special Publication No. 36, p. 349–369.

Garber, R. A., Grover, G. A., and Harris, P. M., 1989, Geology of the Capitan shelf margin—subsurface data from the northern Delaware Basin, *in* Harris, P. M., and Grover, G. A. (eds.), Subsurface and outcrop examination of the Capitan shelf margin, northern Delaware Basin: SEPM Core Workshop No. 13, p. 3–269.

Ginsburg, R. N., and Lowenstam, H. A., 1958, The influence of marine bottom communities on the depositional environment of sediments: Journal of Geology, v. 66, p. 310–318.

Given, R. K., and Lohmann, K. C., 1985, Derivation of the original isotopic composition of Permian marine cements: Journal of Sedimentary Petrology, v. 55, p. 430–439.

_____ 1986, Isotopic evidence for the early meteoric diagenesis of the reef facies, Permian reef complex of west Texas and New Mexico: Journal of Sedimentary Petrology, v. 56, p. 183–193.

Harms, J. C., 1974, Brushy Canyon Formation, Texas: a deep-water density current deposit: Geological Society of America Bulletin, v. 85, p. 1763–1784.

Hayes, P. T., 1964, Geology of the Guadalupe Mountains: U.S. Geological Survey Professional Paper 446, 69 p.

Hayes, P. T., and Koogle, R. L., 1958, Geology of the Carlsbad Caverns West Quadrangle, New Mexico–Texas: U.S. Geological Survey Geological Quadrangle Map GQ-112.

Hill, C. A., 1987, Geology of Carlsbad Cavern and other caves of the Guadalupe Mountains, New Mexico and Texas: New Mexico Bureau of Mines and Mineral Resources Bulletin 117, 150 p.

Holtz, M. H., 1991, Porosity and permeability characteristics in a mixed carbonate-siliciclastic sequence—an example from the Upper Guadalupian (Permian), West Texas and New Mexico, *in* Candelaria, Magell (ed.), Permian Basin plays—tomorrow's technology today: West Texas Geological Society Publication No. 91-89, p. 123–124.

Hurley, N. F., 1978, Facies mosaic of the Lower Seven Rivers Formation (Permian), North McKittrick Canyon, Guadalupe Mountains, New Mexico: University of Wisconsin, Madison, Master's thesis, 198 p.

_____ 1989, Facies mosaic of the lower Seven Rivers Formation, McKittrick Canyon, New Mexico, *in* Harris, P. M., and Grover, G. A. (eds.), Subsurface and outcrop examination of the Capitan shelf margin, northern Delaware Basin: SEPM Core Workshop No. 13, p. 325–346.

James, N. P., 1983, Reef environments, *in* Scholle, P. A., Bebout, D. G., and Moore, C. H. (eds.), Carbonate depositional environments: American Association of Petroleum Geologists Memoir 33, p. 350–440.

James, N. P., Wray, J. L., and Ginsburg, R. N., 1988, Calcification of encrusting aragonitic algae (Peyssonneliaceae): implications for the origin of late Paleozoic reefs and cements: Journal of Sedimentary Petrology, v. 58, p. 291–303.

Kerans, Charles, and Nance, H. S., 1991, High-frequency cyclicity and regional depositional patterns of the Grayburg Formation, Guadalupe Mountains, New Mexico, *in* Meader-Roberts, Sally, Candelaria, M. P., and Moore, G. E. (eds.), Sequence stratigraphy, facies and reservoir geometries of the San Andres, Grayburg, and Queen Formations, Guadalupe Mountains, New Mexico and Texas, Permian Basin Section–SEPM Publication 91-32, p. 53–69.

King, P. B., 1942, Permian of West Texas and southeastern New Mexico: American Association of Petroleum Geologists Bulletin, v. 26, p. 535–763.

_____ 1948, Geology of the southern Guadalupe Mountains, Texas: U.S. Geological Survey, Professional Paper 215, 183 p.

Kirkland-George, Brenda, 1992, Distinctions between reefs and bioherms based on studies of fossil algae—*Mizzia*, Permian Capitan reef complex (Guadalupe Mountains, Texas and New Mexico) and *Eugonophyllum*, Pennsylvanian Holder Formation (Sacramento Mountains, New Mexico): Louisiana State University, Ph.D. dissertation, 156 p.

Lindsay, R. F., 1991, Grayburg Formation (Permian-Guadalupian) Comparison of reservoir characteristics and sequence stratigraphy in the northwest Central Basin Platform with outcrops in the Guadalupe Mountains, New Mexico, *in* Meader-Roberts, Sally, Candelaria, M. P., and Moore, G. E. (eds.), Sequence stratigraphy, facies and reservoir geometries of the San Andres, Grayburg, and Queen Formations, Guadalupe Mountains, New Mexico and Texas, Permian Basin Section-SEPM Publication 91-32, p. 111–118.

Loucks, R. G., and Folk, R. L., 1976, Fanlike rays of former aragonite in Permian Capitan reef pisolite: Journal of Sedimentary Petrology, v. 46, p. 483–485.

Lowe, D. R., 1983, Sediment gravity flows II. Depositional models with special reference to the deposits of high density turbidity currents: Journal of Sedimentary Petrology, v. 52, p. 279–297.

Mazzullo, S. J., and Cys, J. M., 1978, *Archaeolithoporella*—boundstones and marine aragonite cements, Permian Capitan reef, New Mexico and Texas, USA: Neue Jahrbuch für Geologie und Palaontologie, Monatshafte 1978, p. 600–611.

Melim, L. A., 1991, The origin of dolomite in the Permian (Guadalupian) Capitan Formation, Delaware Basin, west Texas and New Mexico: implications for dolomitization models: Southern Methodist University, Ph.D. dissertation, 200 p.

Melim, L. A., and Scholle, P. A., 1989, Dolomitization model for the forereef facies of the Permian Capitan Formation, Guadalupe Mountains, Texas–New Mexico, *in* Harris, P. M., and Grover, G. A. (eds.), Subsurface and outcrop examination of the Capitan shelf margin, northern Delaware Basin: SEPM Core Workshop No. 13, p. 407–413.

Moore, C. H., 1989, Carbonate diagenesis and porosity: Amsterdam, The Netherlands, Elsevier Science Publishers B.V., 338 p.

Mruk, D. H., 1985, Cementation and dolomitization of the Capitan Limestone (Permian) McKittrick Canyon, west Texas: University of Colorado, Master's thesis, 155 p.

_____ 1989, Diagenesis of the Capitan Limestone, Upper Permian, McKittrick Canyon, west Texas, *in* Harris, P. M., and Grover, G. A. (eds.), Subsurface and outcrop examination of the Capitan shelf

margin, northern Delaware Basin: SEPM Core Workshop No. 13, p. 387–406.

Neese, D. G., 1989, Peritidal facies of the Guadalupian shelf crest, Walnut Canyon, New Mexico, *in* Harris, P. M., and Grover, G. A. (eds.), Subsurface and outcrop examination of the Capitan shelf margin, northern Delaware Basin: SEPM Core Workshop No. 13, p. 295–303.

Neese, D. G., and Schwartz, A. H., 1977, Facies mosaic of the upper Yates and lower Tansill Formations, Walnut and Rattlesnake Canyons, Guadalupe Mountains, New Mexico, *in* Hileman, M. E., and Mazzullo, S. J. (eds.), Upper Guadalupian facies, Permian Reef Complex, Guadalupe Mountains, New Mexico and West Texas, 1977 field conference guidebook, v. 1: Permian Basin Section-SEPM Publication 77-16, p. 437–450.

Newell, N. D., 1955, Depositional fabric in Permian reef limestones: Journal of Geology, v. 63, p. 301–309.

Newell, N. D., Rigby, J. K., Fischer, A. G., Whiteman, A. J., Hickox, J. E., and Bradley, J. S., 1953, The Permian reef complex of the Guadalupe Mountains region, Texas and New Mexico: San Francisco, W. H. Freeman Co., 236 p.

Parsley, M. J., and Warren, J. K., 1989, Characterization of an Upper Guadalupian barrier-island complex from the middle and upper Tansill Formation (Permian), east Dark Canyon, Guadalupe Mountains, New Mexico, *in* Harris, P. M., and Grover, G. A. (eds.), Subsurface and outcrop examination of the Capitan shelf margin, northern Delaware Basin: SEPM Core Workshop No. 13, p. 279–285.

Pray, L. C., 1985, The Capitan-massive and its proximal carbonate, and minor siliciclastics of the Capitan back-reef, Walnut Canyon area, Carlsbad Caverns National Park, New Mexico, *in* Cunningham, B. K., and Hedrick, C. L. (eds.), Permian carbonate/clastic sedimentology, Guadalupe Mountains: analogs for shelf and basin reservoirs; Permian Basin Section-SEPM Publication 85-24, p. 25–41.

Reeckmann, S. A., and Sarg, J. F., 1986, Foreslope deposition on a steep margin reef complex, a record of sea-level fluctuation—Capitan Reef Complex, Guadalupe Mountains, Texas (abs.): 12th International Sedimentological Congress Abstracts, Canberra, Australia, p. 255.

Richardson, G. B., 1904, Report of a reconnaissance in Trans-Pecos Texas north of the Texas and Pacific Railway: University of Texas Mineral Survey Bulletin, no. 9, 119 p.

Ross, C. A., 1983, Late Paleozoic Foraminifera as depth indicators (abs.): American Association of Petroleum Geologists Bulletin, v. 67, p. 542–543.

Scholle, P. A., and Melim, L. A., 1988, Evaporites and dolomites in Permian (Guadalupian) Capitan fore-reef carbonates, Delaware Basin margin, West Texas and New Mexico: Geological Society of America, Abstracts with Program, p. A211.

Sonnenfeld, M. D., 1991, High-frequency cyclicity within shelf-margin and slope strata of the upper San Andres sequence, Last Chance Canyon, *in* Meader-Roberts, Sally, Candelaria, M. P., and Moore, G. E., (eds.), Sequence stratigraphy, facies and reservoir geometries of the San Andres, Grayburg, and Queen Formations, Guadalupe Mountains, New Mexico and Texas: Permian Basin Section–SEPM Publication 91-32, p. 11–51.

Toomey, D. F., and Babcock, J. A., 1983, Field guide to selected localities of Late Proterozoic, Ordovician, Pennsylvanian, and Permian ages, including the Permian reef complex: 3rd International Symposium on Fossil Algae, Colorado School of Mines Professional Contributions No. 11, p. 237–328.

Tucker, M. E., and Wright, V. P., 1990, Carbonate sedimentology: Oxford, Blackwell Scientific, 482 p.

Tyrrell, W. W., Jr., 1962, Petrology and stratigraphy of near-reef Tansill–Lamar strata, Guadalupe Mountains, Texas and New Mexico, *in* Permian of the central Guadalupe Mountains, Eddy County, New Mexico, field trip guidebook and geological discussions: West Texas Geological Society Publication No. 62-48, p. 59–75.

_____ 1969, Criteria useful in interpreting environments of unlike but time-equivalent carbonate units (Tansill-Capitan-Lamar), Capitan Reef Complex, West Texas and New Mexico, *in* Friedman, G. M. (ed.), Depositional environments in carbonate rocks: SEPM-Special Publication 14, p. 80–97.

Ward, R. F., Kendall, C. G. St. C., and Harris, P. M., 1986, Upper Permian (Guadalupian) facies and their association with hydrocarbons—Permian Basin, West Texas and New Mexico: American Association of Petroleum Geologists Bulletin, v. 70, p. 239–262.

Wheeler, C., 1989, Stratigraphy and sedimentology of the Shattuck Member (Queen Formation) and lowermost Seven Rivers Formation (Guadalupian), North McKittrick and Dog Canyons, Guadalupe Mountains, New Mexico and west Texas, *in* Harris, P. M., and Grover, G. A. (eds.), Subsurface and outcrop examination of the Capitan shelf margin, northern Delaware Basin: SEPM Core Workshop No. 13, p. 353–364.

Yurewicz, D. A., 1977, Origin of the massive facies of the lower and middle Capitan Limestone (Permian), Guadalupe Mountains, New Mexico and West Texas, *in* Hileman, M. E., and Mazzullo, S. J. (eds.), Upper Guadalupian facies, Permian reef complex, Guadalupe Mountains, New Mexico and West Texas: Field Conference Guidebook, Permian Basin Section–SEPM Publication 77-16, v. 1, p. 45–92.

Zempolich, W. G., Wilkenson, B. H., and Lohmann, K. C., 1988, Diagenesis of Late Proterozoic carbonates—the Beck Spring Dolomite of eastern California: Journal of Sedimentology, v. 58, p. 656–672.

The Bureau of Economic Geology, established in 1909, is a research entity of The University of Texas at Austin and also functions as the state geological survey. The Bureau conducts studies of energy and mineral resources, coastal and environmental concerns, geological mapping, and ground water, among other topics. Results of these projects are detailed in a publication series that includes technical reports, guidebooks, geologic maps, and handbooks. For a complete list of Bureau publications, please contact:

Publication Sales Office
Bureau of Economic Geology
The University of Texas at Austin
University Station, Box X
Austin, Texas 78713-7508

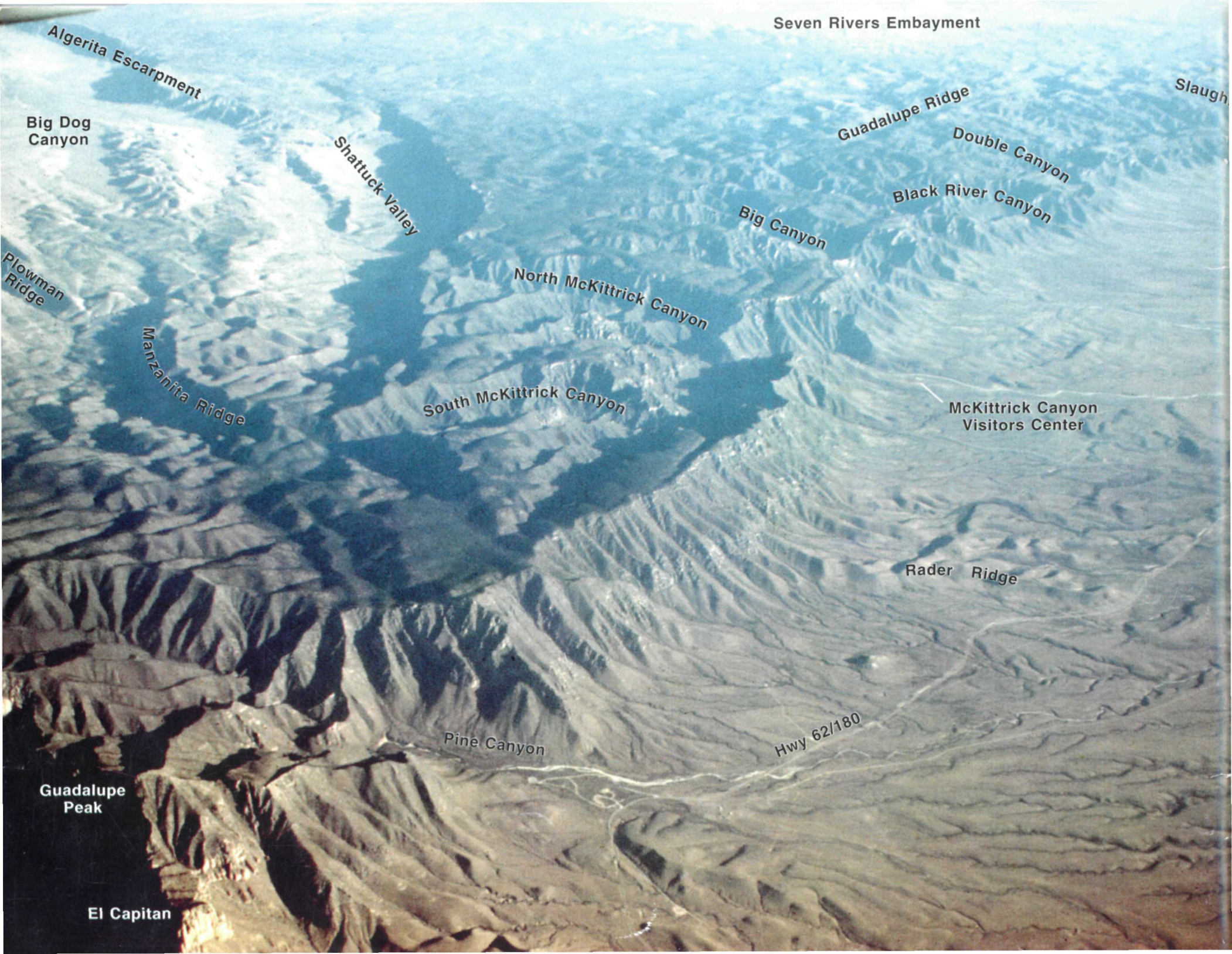
Seven Rivers Embayment
Algerita Escarpment
Slaugh
Guadalupe Ridge
Big Dog Canyon
Double Canyon
Shattuck Valley
Black River Canyon
Big Canyon
Plowman Ridge
North McKittrick Canyon
Manzanita Ridge
South McKittrick Canyon
McKittrick Canyon Visitors Center
Rader Ridge
Pine Canyon
Hwy 62/180
Guadalupe Peak
El Capitan